NATIONAL UNIVERSITY OF RWANDA
Faculty of Sciences
Department of Physics

CONTRIBUTION TO THE CHARACTERIZATION OF NATURAL AND ARTIFICIAL PHOTOSYNTHETIC SYSTEMS

Silas MURERAMANZI

Ph. D. Thesis

March 1987

NATIONAL UNIVERSITY OF RWANDA
Faculty of Sciences
Department of Physics

CONTRIBUTION TO THE CHARACTERIZATION OF NATURAL AND ARTIFICIAL PHOTOSYNTHETIC SYSTEMS

Silas MURERAMANZI

Ph. D. Thesis

March 1987


3276

ACKNOWLEDGEMENTS

This work was accomplished partially in the Laboratory of Professor Dr S.P. Stoylov of the University of Sofia, partially in the laboratory of Professor Dr Melvin Calvin of the University of California at Berkeley and finally in the "Centre de Recherche et de Formation Permanente (CRAFOP)". Thanks to the financial support of UNESCO by the intermediary of the "Project PNUD - UNESCO RWA/80/008 and to the assistance of the National University of Rwanda-Campus of Ruhengeri". Financial support from this organization as well as from the "Ministère de l'Enseignement Supérieur et de la Recherche Scientifique au Rwanda" are gratefully acknowledged.

I would especially like to thank Professor Dr S.P. Stoylov who kindly accepted to assure the direction of this thesis. I have benefitted from his long experience in the field of electrooptical researches. Thanks to his hospitality during my sojourn at Sofia, to his judicious advice, to his numerous suggestions and rigorous observations, this work could be conceived and realized. I am taking this opportunity to thank once more all the collaborators of Professor Dr S.P. Stoylov who helped me in my electrooptical experiments. I am also indebted to Professor Dr S.P. Stoylov and to his colleague Professor Dr Lajos KESZTHELYI, Director of the Institute of Biophysics at Szeged, for helping me find a University where I may defend my thesis. I express my profound respect and gratitude to them.

I wish to express my gratitude to Professor Dr F. KEVEI, Vice-Dean of the Faculty of Sciences of Attila Joszef University for kindly answering favorably to my first letter requesting the possibility to defend my thesis in this faculty and informing me about the procedure that I have to follow in order to apply for defending my thesis in this Faculty.

I am taking this opportunity to thank his Excellency the Secretary of Education of Hungary for giving me the permission to defend my thesis in the Faculty of Sciences of Attila Joszef University.

My thanks also go to Professor Dr Melvin Calvin who accepted me with great kindness in his laboratory. He has initiated me to researches in the domain of "Artificial Photosynthesis".
I would also like to thank some of his collaborators especially Dr John OTVOS and Dr Roland WOHLGEMUTH who helped me in some experiments with their wealth of knowledge.

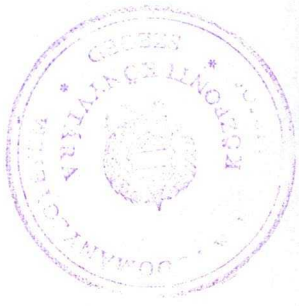

I have benefitted from discussions with Professor H.T. TIEN of Michigan State University (East Lansing). I also thank him for accepting me in his laboratory from July, 1984 - November, 1984.

I am also thankful to the authorities of the Faculty of Science of the National University of Rwanda for authorizing the typewriting of my thesis in the Faculty Secretary's office. My thanks are due to the typists of this Faculty especially to Mister LUKUSA Nkongo and Mrs NDENGEJEHO-BONGWA Béatrice for excellent secretarial assistance.

I also thank Mrs Gladys Magnani for kindly accepting to read the English version of my thesis and indicating where corrections are required.

Finally, I want to express my gratitude to all other persons who have contributed, closely or at a distance, to the realization of this work.

C O N T E N T S

List of Symbols and Abbreviations

A	An electron acceptor molecule.
A_o	Absorbance of a sample solution in the absence of an electric field.
$A_{\parallel}, A_{\perp}$	Absorbance of a sample solution for light polarized parallel and perpendicular to the applied electric field, respectively.
a	Either the long semi-axis of an ellipsoid-like particle or the half-length for a particle of cylindrical shape.
a_i	Area.
B_a	Internal field function.
b	Either the short semi-axis of an ellipsoid-like particle or the radius of a particle of cylindrical shape.
C	Either a constant of proportionality or the overall concentration of surfactants.
CMC	Critical micelle concentration.
C_M	Molar concentration of micelles.
c	Molar concentration of a solute.
D	Either the rotational diffusion coefficient or an elecron donor molecule.
E	Electric field strength.
	Maximum amplitude of an alternating electric field.
F	A function which reflects the degree of orientation.
f	Angular distribution function.
$G =$	$\frac{p^2}{3k^2T^2} + \frac{\gamma}{3kT}$
5-HA	5-hexenoic acid.
$h =$	$\frac{4\pi}{\lambda} \sin(\frac{\theta'}{2})$
I	Light intensity transmitted by a sample solution in the absence of an electric field.
I_E	Light intensity transmitted by a sample solution in the presence of an electric field of strength E.
I_o	Either scattered light intensity in the absence of an electric field or incident light intensity impinging on a sample solution
$I_{\parallel}, I_{\perp}$	Intensity transmitted by a sample solution in the presence of an electric field when the incident light is polarized parallel and perpendicular to the electric field, respectively.
$i(\theta,\phi)$	Scattered light intensity as a function of the orientation of particle.
$K =$	$\frac{2\pi\ell}{\lambda} \sin(\frac{\theta'}{2})$
k	Either the Boltzamann constant or a constant of proportionality.
k_d, k_f	Rate constant for micelle dissociation and formation, respectively.
ℓ	Length of a rod-like particle.

M	Single surfactant molecule.
M_n	Micelle constituted by n surfactant molecules.
$\bar{M}_w$	Weight-average molecular weight.
$MnTP_yP\text{-}C_{16}$	Bromo-aquo-(5-[1'-hexadecylpyridinium-4'-yl]-10,15,20,-tris [4'-pyridyl]-21H,23H-porphine)-manganese perchlorate.
MV^{2+}	1,1'-Dimethyl-4,4'-bipyridinium dichloride (methyl viologen).
N	Either number of scattering elements in a particle or number of particles per unit volume.
N_0, N_1, N_2	Number of moles of photons.
n_m	Refractive index of the solvent which, for low concentrations, coincides with that of the solution.
n_p	Refractive index of the particle.
$\Delta n = n_{\parallel} - n_{\perp}$	Difference in the refractive index for light polarized parallel and perpendicular to an applied electric field.
OD	Optical density.
$P = \frac{\beta^2}{E^2} = (\frac{p}{kT})^2$	Contribution of permanent dipole moments to the degree of orientation.
PVS°	N,N'-bis(sulfonato-n-propyl)-4,4'bipyridyl(propyl viologen sulfonate)
p_a, p_b	Permanent dipole moment along and across the symmetry axis, respectively.
$p = p_a$	Permanent dipole moment when $p_a \gg p_b$.
$Q = \frac{2\chi}{kT} - \frac{\gamma_a - \gamma_b}{kT}$	Contribution of induced dipole moments to the degree of orientation.
$Ru(bpy)_3^{2+}$	Tris(2,2'-bipyridinium)ruthenium(II) chloride hexahydrate.
S	Sensitizer molecule.
S	As index designates the saturation value of an electro-optic effect.
SDS	Sodium dodecyl sulfate.
$\vec{s}$	Wave vector in the direction of the scattered light beam.
$\vec{s}_0$	Wave vector in the direction of the incident light beam.
T	Either absolute temperature or transmittance of an isotropic solution.
$T_{\parallel}, T_{\perp}$	Transmittance of a sample solution in the presence of an electric field when the incident light is polarized parallel or perpendicular to the electric field, respectively.
TEA	Tris(2-hydroxyethyl)amine or Triethanolamine.
t	Time.
U	Potential energy of a particle in an electric field.
V	As index designates vertically polarized scattered light intensity.

v	As index designates vertically polarized incident light.
w	As index designates the weight-average.
$ZnTP_yP\text{-}C_{16}$	(5-[1'-hexadecylpyridinium-4'-yl]-10,15,20-tris[4'-pyridyl]-21H, 23H-porphine)-zinc perchlorate.
z	As index designates the z-average.
α	Electro-optic effect.
α_∞	Electro-optic effect for intinitely high electric field strengths, when all particles are completely oriented.
α_o	Electro-optic effect at the moment at which the electric field is switched off.
γ_a, γ_b	Electric polarizability along and across the symmetry axis, respectively.
$\gamma_a = \gamma$	Electric polarizability when $\gamma_a \gg \gamma_b$.
Δ	Difference in the values of magnitude; Laplacian operator.
δ	Optical anisotropy.
Ω	Angle between the direction of the applied electric field and the bisector of the viewing angle.
$\varepsilon_a, \varepsilon_b$	Molar extinction coefficients along and across the symmetry axis of the particle, respectively.
ε_o	Molar extinction coefficient of a solution in the absence of an electric field.
	Average molar extinction coefficient.
$\varepsilon_\parallel, \varepsilon_\perp$	Molar extinction coefficients of a solution in the presence of an electric field for light polarized parallel and perpendicular to the applied electric field, respectively.
η	Coefficient of viscosity.
θ	Angle between the particle symmetry axis and the applied electric field.
θ'	Angle between the incident and scattered beams.
ν	Either the frequency of an applied electric field or the frequency of a photon which is absorbed by a sensitizer.
λ	Wavelength.
τ	Relaxation time.
ϕ	Phase angle between an electro-optic effect and the applied electric field.
ϕ_i, ϕ_p	Phase angle between an electro-optic effect and the applied electric field for particles without permanent dipole moment and without electric polarizability, respectively.
ψ	Either a wave-function or the angle between the direction of the transition dipole moment and the particle's symmetry axis.
ω	Angular frequency.
$\underset{\sim}{\vec{\mu}}$	Dipole moment operator.

Is it important (page number 129, only)?

CHAPTER I

MAIN INTRODUCTION

1.1. Position of the problem

The impending shortage of our fossil fuels that coal, petroleum and natural gas represent, their increasing costs and the disastrous increase in the CO_2 level in the atmosphere resulting from the burning of these fuels, preoccupy not only many governments and industries but also many researchers all over the world /1-5/. Are these relevant references to this topics?

why is the CO_2 increase disastrous? It can have many advantages (e.g. heat trap)

Finding other renewable alternative sources of energy which do not depend on the exhaustible products of past photosynthesis, i.e., fossil fuels, is a crucial problem that many scientists are facing in order to fulfill the energy needs of humanity. Solar energy is potentially one of the most important renewable sources of energy, especially for countries like Rwanda for which geographical and atmospheric conditions are favorable. At the present time, two methods for the collection of sunlight energy have been developed and improved by physicists and engineers.

Even today (after 15 years of oil-shock) is the problem to find new energy sources so important?

Other energy sources? (even not mentioned)

- Sunlight Energy Can be Collected as Heat on a Blackened Surface

This heat can be used directly for residential and commercial heating or it can be transformed into electricity via a thermal engine. This conventional method for the collection of sunlight energy presents two major deficiencies: first, it implies the degradation of the sunlight energy from high-quality quanta of 125-335 kJ/mole (30-80kcal/mole) into low-quality thermal quanta of 2.5-4.2kJ/mole (0.6-1.0 kcal/mole); and second, the efficiency of the conversion of thermal energy into electricity is limited by the theoretical efficiency (η) of a reversible Carnot cycle,

?

?

$$\eta \overset{\text{invers.}}{\leq} \frac{T - T'}{T}$$

1) It refers to mechanical conversion

2) η can be large (25%) 0→100 ~100% 0→6000

where T and T' are, respectively, the upper temperature and lower temperature at which the thermal engine can function.

- Sunlight Energy Conversion Into Electricity by Means of Solid State Semiconductor Photovoltaic Cells

Even if the efficiency of sunlight conversion into electricity reaches values as high as 22% /4/ for a solid state silicon solar cell, on large scale, the use of solid state photovoltaic cell

Order of references?
alphabetical - no
occurance - no

poses practical problems. First, the requirement of single-crystal silicon of high purity makes the cost of photovoltaic cells high; second, the small area involved requires a focusing collector and this contributes to increasing the cost of the system; third, the electric power delivered by these devices cannot exceed 2KW /3/; and fourth, while converting sunlight energy to electricity via photovoltaic cells, the major problem is storage.
Two major drawbacks have delayed the utilization of solar energy on a large scale /2,3/: first, solar energy is diffuse and this requires large areas of collectors which, consequently, are very expensive; second, although solar energy is an immense resource, it is intermittent. This drawback requires some form of storage system so that the energy can be made available when it is needed. If the sunlight energy could be used to generate an easily storable fuel (the term fuel is used in a broad sense, i.e., a reduced chemical compound produced in an endergonic chemical reaction which upon reaction with oxygen can release the stored energy), this problem would be solved/6/.

In the past decade or so, many researchers /1,2,4-12,15,17, 20/ have tried to find the best way to store solar energy by means of photochemical reactions: the aim of this research is to use the sunlight energy as a driving force for an endergonic chemical reaction where the end product would be a chemical fuel and/or electrical energy.
One part of the work presented in this thesis deals with sunlight energy conversion and storage by means of dye-sensitized photochemical reactions. ... and the rest?

Since photosynthesis by green plants, algae and bacteria is the only known process which can photochemically convert and store solar energy, it is very probable that an artificial system that will accomplish an analog process will be modelled on the natural photosynthesis process /2,4,7,17/. Artificial photosynthesis based upon Nature's way for sunlight energy capture and conversion into some stable chemical form is a goal pursued by many researchers all over the world.
The ideal would be to simulate the natural process of sunlight ?
energy conversion into chemical energy in order to accomplish the photodecomposition of water into oxygen and renewable hydrogen fuel, to reduce the carbon dioxide to useful fuels such as formic acid, formaldehyde, methanol and methane, or to reduce nitrogen to ammonia.

Not severe argument!

easy to realize?

If a solution containing appropriate chemicals could perform a role similar to that of the photosynthetic chloroplasts, i.e. converting sunlight energy into chemical energy and storing it in some stable form, some problems associated with solid state photovoltaic cells (solid-solid junction which is difficult to realize, focusing, etc.) will be alleviated since solutions can be spread into a larger area and costs may not be as high. It is necessary to understand the essential parts of the quantum conversion process in natural photosynthesis in order to mimic that process by using synthetic chemical compounds.

1.2. QUANTUM CONVERSION IN GREEN PLANTS AND ALGAE

The overall stiochiometric reaction of green plants photosynthesis and algae,

$$CO_2(g) + H_2O\ (\ell) \xrightarrow{8h\nu / Chl} \frac{1}{6} C_6H_{12}O_6(S) + O_2(g) \qquad (1.1)$$

(where $C_6H_{12}O_6$ is a D - glucose), can be separated into two major steps: a photophysico-chemical step in which visible light ($400\ nm \leq \lambda \leq 780\ nm$) is captured and transformed into stored biochemical energy, and a chemical step, in which the stored energy is utilized in a sequence of enzymatic dark reactions. We want to emphasize and describe briefly the mechanisms of the photophysico-chemical step because it involves light energy conversion into electrical/chemical energy and it is possible to mimic some aspects of that process /2/.

the limits are not correct

1.2.1. The Primary Photophysico-chemical Reactions of Photosynthesis

The primary photophysico-chemical reactions is a process which takes place on a complex structure consisting of the thylakoid membranes in the grana stacks and stroma lamellae within the chloroplast /11/ and which converts light energy into a reducing power (nicotinamide adenine dinucleotide diphosphate, NADPH) and chemical energy /11,14/. The details of the process are summarized in the so called "Z-scheme" (Fig.1.1) which has been postulated for the first time by Hill and Bendall in 1960. Three essential points merit to be emphasized since they are an important guide for the construction of an artificial photosynthetic device.

1.2.1.1. Light harvesting. An antenna of several light harvesting pigment molecules, of which chlorophyll is the principal component, gather light quanta and channel this excitation energy via excited singlet state to one of two photoactive centers of the electron transport chain, called photosystem I (PSI) and photosystem II(PSII) /15/. The photoactive compounds of PSI and PSII are the pigments P_{700} and P_{680} which have an absorption band at 700 nm and 680 nm, respectively. The two photosystems operate in series. Observation of the photosynthetic activity of chlorophyll molecules incorporated in models systems led Showell and Fong /19/ to the following conclusions: the dimers of chlorophyll a, $(\text{Chl a. } H_2O)_2$ and $(\text{Chl a. } 2H_2O)_2$ display, respectively, photophysico-chemical properties analogs to those attributed to the light-driven reactions of the photoactive reaction centers P_{700} and P_{680}.

P_{680} is also a dimer? (P_{700} O.K) The analogy is not well supported

1.2.1.2. Charge separation and photoinduced electron transfer reactions. As soon as the reaction-centers trap P_{680} and P_{700} have absorbed photons of suitable wavelength, they are electronically excited to the singlet state . Each of the excited reaction-center traps P^*_{680} and P^*_{700}, transfers an electron to a closely associated reaction partner within 20 nsec /16/. P^*_{680} transfers an electron to a plastoquinone molecule, Q_1 (the primary electron acceptor of PSII):

the limit is too loose old reference

?

$$P^*_{680} + Q_1 \longrightarrow P^+_{680} + Q_1^- \qquad (1.2)$$

not true

P^+_{680} is reduced by unknown reactions within the enzyme system S, which is probably a manganese-containing complex (Eq. 1.3). After four successive photoacts the four positive holes generated in the S enzyme oxidize water to oxygen:

P^+ is reduced by Z which is not part of S!

Z is a one-electron component

?

$$4P^+_{680} + Z \longrightarrow 4P_{680} + Z^{4+} \qquad (1.3)$$

Z and S are different species (see Z scheme!)

?

$$Z^{4+} + 2H_2O \longrightarrow Z + O_2 + 4H^+$$

The electron accepted by Q_1 flows down a potential gradient through a plastoquinone pool, plastocyanine, cytochrome f, etc. The electron flow is coupled to a proton gradient across the membrane which is used to generate a high energy phosphate, adenoside triphosphate (ATP), from adenoside diphosphate (ADP) and an orthophosphate via a chemiosmotic mechanism /17,22/. The electron removed from water will reach the hole left behind by the photoinduced oxidation of P^*_{700}. The electron released by this excited pigment is accepted by A_1 (probably chlorophyll molecule a)

at a reduction level higher than that of a molecular hydrogen. This electron falls back through a series of electron transfer agents, including an iron/sulfur protein known as ferrodoxin, to flavoprotein, and finally to $NADP^+$ to form NADPH, which together with the light-generated ATP, will drive the reduction of CO_2 into carbohydrate in the reduction cycle of photosynthesis. It is known /12,13a/ that in anaerobic conditions (i.e. oxygen is excluded or minimized and carbon dioxide withheld), some plants synthetize an enzyme called hydrogenase which can use NADPH, ferrodoxin (or both), to generate molecular hydrogen.

1.2.1.3. Role of the thylakoid membrane.

Kinetics and thermodynamic limitations on the photophysico-chemical conversion and storage of solar energy forced green plant photosynthesis to use two complementary photochemical reactions operating in series so that two quanta have to be absorbed for every electron transferred from water to $NADP^+$ /2,17,22/. The fact that two quanta have to be absorbed for each electron transferred and that the thylakoid membrane has two sides suggests that the excited electron passes from one side to the other and the ability of the plant to perform the photochemical steps resides in the fact that PSI and PSII particles are probably located on opposite sides of the membrane which therefore serves to keep spatially separate the reduced and oxidized species of the electron transfer process /10a,26/. The electron is moved from one side to the other, across two phase boundaries: a water-to-membrane boundary and membrane-to-water phase boundary on the outer side of the thylakoid membrane. In summary, not only the thylakoid membrane assumes the role of host for the reactants, but also the unique arrangement of reactants assures a rapid and efficient electron transfer, and is such that the thermal back electron transfer is prevented. Being spatially separated, the reduced species and oxidized species will represent a potential chemical energy (via their redox potential).

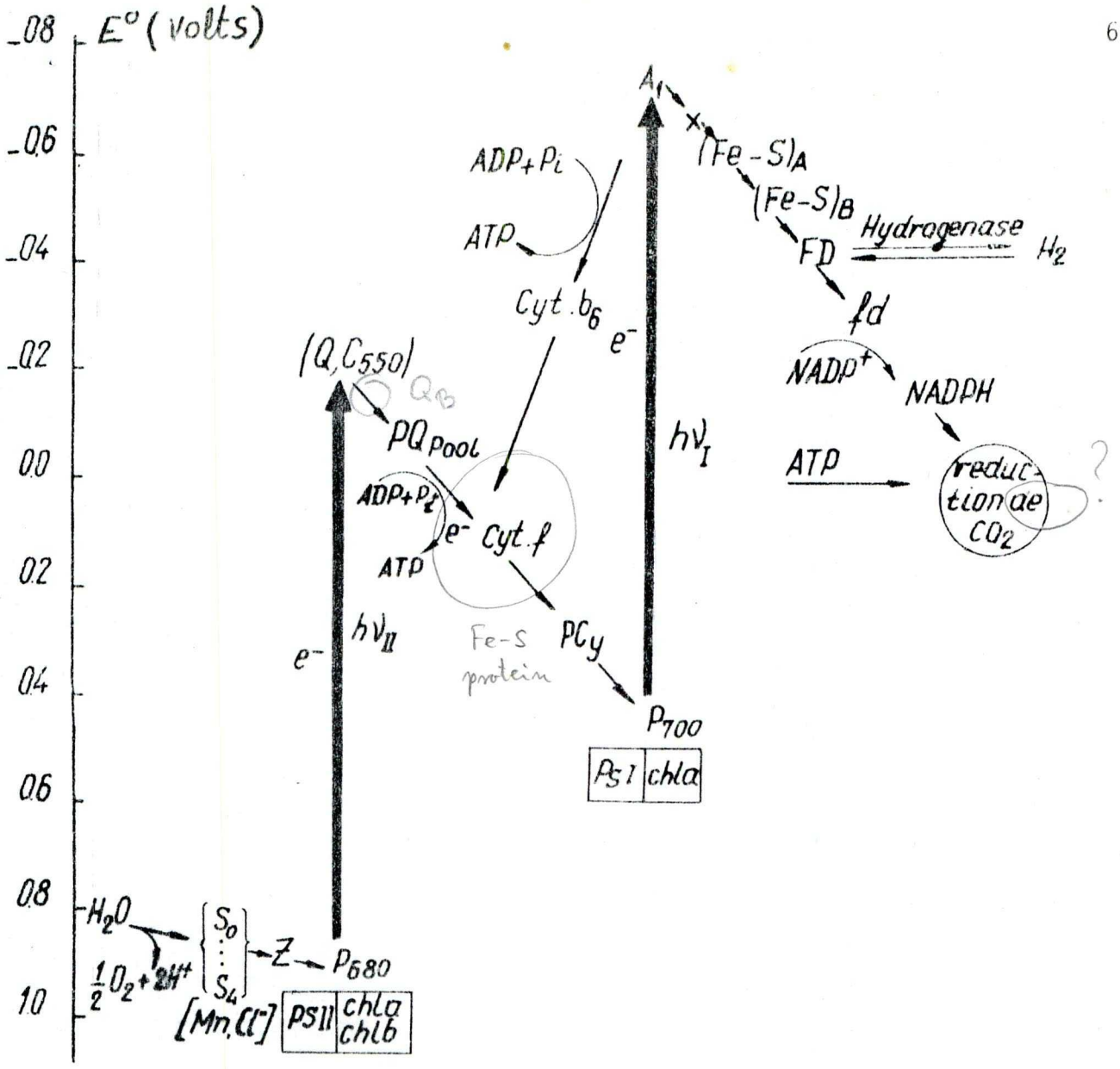

Fig.1.1 The "Z-Scheme" of the photosynthetic electron-transport chain in green plants and algae. The scheme shows two photochemical reactions operating in series to drive an electron from water to nicotinamide adenine dinucleotide phosphate ($NADP^+$). Photosystem I (PS-I) utilizes chlorophyll a (Chla) and Photosystem II (PS-II) utilizes chlorophyll a (Chla) and chlorophyll b (Chlb). A pool of plastoquinone (PQ pool) which lies in the photosynthetic electron-transport chain is the essential link for electron flow from PS-II to PS-I.

Symbols: Z represents the oxygen-generating enzyme system;
Q is a plastoquinone molecule or the first stable electron acceptor of PS-II;
Cyt-f means cytochrome f;
PCy means plastocyanine;
A_1 is the first electron acceptor of PS-I which is probably a Chla molecule.
(See other details and abbreviations in the text).

1.3. Characterization of natural photosynthetic systems by electro-optic methods

In order to construct in vitro and/or artificial photosynthetic systems which seek to mimic some aspects of the photophysico-chemical reactions of natural photosynthesis, it is necessary to have sufficient information on the structure and mechanism of green-plant chloroplasts, especially on the orientation of specific pigments within the chloroplast membrane. (e.g., photoactive pigments of PSI and PSII are these specific pigments). In order to explain how the photoproducts of the photoinduced electron-transfer process of natural photosynthesis are kept spatially separated, many researchers /2,8a/ have postulated that PSI and PSII particles are probably located on the opposite sides of the thylakoid membrane, but the mutual orientation of these reaction centers are still unknown.
A detailed knowledge of the degree of mutual orientation of pigments on a local level (within a given photosynthetic unit or in its immediate neighbors) is necessary for the understanding of the mechanism of the transfer of excitation light energy among the pigments of the chloroplast /24/.

The particles of a colloidal suspension respond to an applied electric field by orientation or deformation, and this produces optical anisotropies on a macroscopic scale /25/. The modification of optical properties of a colloidal suspension when an electric field is applied or changed across the suspension is called an electro-optic phenomena. The magnitudes and speeds of electro-optic effects are related to the molecular charge distribution, directional polarizabilities, and reorientational or disorientational rates /25,53/.

It is obvious to expect that electro-optic phenomena which provide information on particle's electric parameters (electric polarizabilities and permanent dipole moments), on their optical anisotropy, on the direction of the transition dipole moments of specific chromophores within these particles, on their geometrical and mechanical parameters, could contribute to a better understanding of the structure of natural photosynthetic membranes. In fact, the evaluation of data from electro-optic measurements could give, in principle, information on the interfacial charge of chloroplast membranes, on the asymmetry and dynamics of these charges, on the orientation of specific pigments in (or on) the chloroplast membrane and it is quite reasonable to expect that all these properties determine one of the fundamental roles of the thylakoid membrane, i.e. to keep spatially separated the reduced species and oxidized species of the photochemical step of the natural photosynthesis.

However, given that a suspension of chloroplasts is very polydisperse, electro-optical measurements carried out only on such a suspension, would be difficult to interpret.
The fragmentation of chloroplasts either by chemical methods (treating the chloroplast suspension with a detergent such as the digitonin), or by physical methods (ultrasonic treatment), followed by a separation into more or less homogeneous fractions (sub-chloroplast fragments) by differential centrifugation, provides samples for which the electro-optical measurements can be interpreted more or less easily.

In chapter II, we present briefly the fundamental principles of the theory and experimental methods for two electro-optic methods, - the electric linear dichroism and the electric field light scattering. We have used these two electro-optic methods in order to determine the electric and hydrodynamic properties of chloroplasts and sub-chloroplast fragments. The orientation of whole chloroplasts and that of large chloroplast fragments in an electric field is due to the interfacial polarization. The mean values obtained for the interfacial electric polarizability and its relaxation time are, respectively, in the order of 10^{-12} cm^3 and 6×10^{-5} s. The experimental results provided us some information on the structure of the photosynthetic membranes; the discussion of these results elucidate this information.

1.4. Artificial photosynthetic systems

The complexity and the very high organization of natural systems do not allow us to understand the natural photosynthetic process by carrying out experiments on a suspension of whole chloroplasts. Relatively simple model systems for photosynthesis have to be used. A first approach involves the utilization of in vitro models for photosynthesis which consist /1,26/ of biological pigments, lipids, proteins, enzymes, etc... extracted from plants, or from algae, or from photosynthetic bacteria and placed in an appropriate environment (e.g., ultrathin membranes, liquid solutions, etc.) so that the whole system can mimic some aspects of the photophysico-chemical mechanisms of the thylakoid membrane. A closed vesicle of spherical configuration is a suitable model for the thylakoid membrane: it has two aqueous phases separated by a lipid bilayer. Many investigations have been made /14/ on vesicles which contain biological pigments

(e.g., chlorophylls), proteins or other purified components of the chloroplast. Even if in vitro photosynthetic systems are extensively used /2,8a,26/, they have two major deficiencies. First, the quantum efficiencies obtained so far are very low. Second, in vitro photosynthetic systems are unstable : in fact isolated biological pigments, enzymes, etc... are not stable when they are placed in an unnatural environment where they have to be maintained under specific conditions (e.g. anaerobic conditions), or must be exposed to large areas in order to absorb an appreciable fraction of incident light.

A second approach involves the utilization of artificial photosynthetic systems which are constituted of synthetic chemical compounds and seek to imitate parts of the photochemical reactions of the natural photosynthesis.

Artificial photosynthetic systems consisting of homogeneous or heterogeneous aqueous solutions containing an appropriate amount of a dye or photosensitizer, electron donors and electron acceptors and catalysts have been used in our work. Artificial photosynthetic systems have two purposes /1,4,7,8a/:

(i) using a relatively simple system where interactions are limited or can easily be controlled and which is not as sophisticated as a living system, it is possible to check the proposed photophysico-chemical mechanisms of the thylakoid membrane; such studies may confirm or refute hypotheses about the structure and mechanism of the natural photosynthetic process.

(ii) artificial photosynthetic systems attempt to mimick our current knowledge on the natural process in order to design a purely photochemical system for the conversion of sunlight energy into chemical energy.

In the field of artificial photosynthesis, we have been interested in converting sunlight energy into chemical energy via photo-induced electronic excitation of dye molecules (photo-sensitizers) in a solution containing also electron donors and acceptors and, eventually, catalysts. The electronic excitation of a dye molecule by visible light is followed by photo-induced electron transfer reactions which may ensure to store light energy.

In the past decade or so, many researchers/9,27-32/ have been interested especially in the decomposition of water into hydrogen and oxygen upon illumination with visible light, in the presence of suitable catalysts (equation 1.4.). This interest is quite understandable because the raw materials (water and sunlight) are readily available and hydrogen is an almost ideal fuel which has the highest energy-density (of any non-nuclear fuel) and is non-polluting.

$$2H_2O \xrightarrow[\text{catalysts}]{h\nu} 2H_2 + O_2 \qquad (1.4)$$

However, a direct photolysis of water is not possible because water is transparent to solar radiation in the ultra-violet and visible region; the reaction has to be sensitized by dyes (photo-sensitizers, designated by the letter "S", in the text). For such a dye-sensitized photo-decomposition of water, the photo-chemical step (Equation 1.5.) is followed by two continuous reactions which constitute the catalytic step (Equation 1.6. and 1.7).

$$S + A \xrightarrow{h\nu} S^* + A \longrightarrow S^+ + A^- \qquad (1.5)$$

$$(S^+ + A^- \longrightarrow S + A) \qquad (1.5')$$

$$2A^- + 2H_2O \xrightarrow{\text{cat.1}} 2A + 2OH^- + H_2 \qquad (1.6)$$

$$4S^+ + 2H_2O \xrightarrow{\text{cat.2}} 4S + 4H^+ + O_2 \qquad (1.7)$$

S^* represents an excited state of the photosensitizer; A and D are respectively an electron acceptor and an electron donor. Cat.1 and Cat.2 represent the catalysts for the reduction and oxidation of water, respectively. The light energy initially stored in the excited photosensitizer is transformed into the redox gradient of the oxidized species (S^+), and reduced species (A^-). The photosensitizer S and the electron acceptor has to fulfil the following requirements : the redox potential of the A/A^- couple must be below that of the H^+/H_2 couple; the redox potential of the S^+/S couple must be above that of the O_2/H_2O couple.

The charge-storage catalysts which have to mediate the two-electron transfer process of the dye-sensitized reduction of water to hydrogen (Equation 1.6) are well known /36-39/. In 1949, H. Gaffron and J. Rubin performed experiments which show that under anaerobic conditions certain green algae synthetize an enzyme called hydrogenase which can use nicotinamide adenine dinucleotide diphosphaste (NADPH), ferrodoxin or both to generate molecular hydrogen. The structure of hydrogenase-enzyme is well known /4,22/: it is a multi iron-sulfur protein, probably a 4Fe-4S complex in a protein. In 1961, Arnon, Mitsui and Paneque /34/ showed that an in vitro photosynthetic system composed of isolated chloroplasts, ferrodoxin and hydrogenase (CFH systems) could evolve hydrogen upon illumination with visible light, in a reaction of photosystem I, using cysteine as an electron donor. In 1973, Benemann et al /35/ demonstrated that no photoproduction of hydrogen was observed in the CFH system if an inhibitor of photosystem II (3-(3,4 dichlorophenyl)1,1-dimethylurea, DCMU) was applied; they concluded that an active photosystem II was required and that water was the electron donor, although no oxygen was observed. Greenbaum /13c/ showed that the CFH system and anaerobically adapted chlamyadomonas algae were capable of performing an artificial photodecomposition of water into hydrogen and oxygen. However, the absolute rate of oxygen obtained was about 100 times smaller than the absolute rate of oxygen production in normal photosynthesis. This small rate of oxygen production was attributed to fewer functional photosynthetic units relatively to that in natural photosynthesis.
In artificial photosynthetic systems, synthetic model compounds for hydrogenase have been synthesized and used /10a/. On the other hand, other synthetic catalysts such as colloidal platinum, colloidal silver and gold sols have been used as catalysts in the dye-sensitized reduction of water to hydrogen /36-39/. The dye-sensitized oxidation of water to oxygen (Equation 1.7) is less efficient than the dye-sensitized reduction of water/40/.

Although the dye-sensitized oxidation of water was found to be catalysed by transition metal oxides such as RuO_2/27,41/, IrO_2/42/, PtO_2/27/ and CoO/9/, the quantum efficiencies for the photoproduction of O_2 were very low. Then, a limiting factor for this approach of the production of renewable hydrogen fuel by the dye-sensitized decomposition of water to H_2 and O_2 is the achievement of the dye-sensitized oxidation of water.

This difficulty is understandable. In fact, in the photoinduced redox reactions, only one electron is transferred from the excited sensitizer to the electron acceptor for each photoact; then a suitable charge-storage catalyst which has to mediate the four-electron transfer process is necessary in order to oxidize two molecules of water into one molecule of oxygen without the production of free hydroxyl radical intermediates which would undergo destructive side reactions.
Many researchers /8a,22/ have suggested that polynuclear manganese complexes would be the probable catalysts for the dye-sensitized photooxidation of water. In fact, since manganese has many states of oxidation, in principle, manganese complexes (for example a binuclear complex of manganese-IV) are able to remove four electrons from two molecules of water and, consequently, oxidize them to oxygen without the production of free oxygen atoms, or hydroxyl radicals, or other intermediates which would destroy the system /17,24/. Many laboratories /8,22,43/ have tried to synthesize polynuclear manganese complexes which would catalyse the dye-sensitized oxidation of water. Oxygen-bridged binuclear complexes of manganese have been synthesized and used, but the quantum efficiencies for oxygen photoproduction were very low.

In homogeneous solutions, the rapid thermal back reaction between S^+ and A^- to give S + A (Eq.1.5') does not allow this type of solar energy conversion and storage. Supramolecular assemblies or interfacial systems, the purpose of which are not only to organize the reactants of an artificial photosynthetic system but also to separate the desired photoproducts, are necessary. In our experiments, interfacial systems consisting of negatively charged inferfaces of sodium dodecyl sulfate (SDS) in an aqueous micellar solution, have been used. Micelles are very useful in artificial photosynthetic systems because on one hand, the hydrophobic core in the micelle permits the solubilization of organic reactants, and on the other hand, through electrostatic interactions, ions can be concentrated near the micellar inferface or repelled away into the bulk solution. Then, micelles can be used to control the rates of the photoinduced electron transfer reactions as well as the rates of the thermal back reactions by means of hydrophobic, hydrophilic or electrostatic interactions.

In Chapter III, we describe the artificial photosynthetic systems that we have used for the photochemical conversion and storage of sunlight energy. In the first part of Chapter III, a concrete experiment in which an "homogeneous photochemical sacrificial system" is used to achieve the dye-sensitized reduction of water to hydrogen with a quantum efficiency as high as 32 % is presented.
So far, the photochemical oxidation of water to oxygen is not yet achieved with a satisfying quantum efficiency. However, in order to achieve the practical goal of photolysis of water to hydrogen and oxygen by solar energy, it is necessary to simulate the light driven reactions of PSII in which water is oxidized to oxygen. As a manganese-containing complex plays a crucial role in these photochemical reactions, in order to simulate natural photosynthesis in an efficient manner it is necessary to synthesize polynuclear complexes of manganese analogous to those used in the photochemical reactions of PSII.

In the last part of the third chapter, we have investigated the possibility of photochemically oxiziding a Mn(III)-tetrapyridyl porphyrin derivative ($MnTP_yP\text{-}C_{16}$) using a Zn-tetrapyridyl porphyrin derivative ($ZnTP_yP\text{-}C_{16}$) as a sensitizer and propyl viologen sulfonate as the first electron acceptor. The experiments were carried out in aqueous micellar solutions of sodium dodecyl sulfate(SDS). The micelles permitted the solubilization and organization of reactants and, more or less, prevented the thermal back electron transfer between the photoproducts. Following the illumination of these heterogeneous photochemical systems and subsequent photoinduced electron transfer from the excited sensitizer to the first electron acceptor (PVS°), the latter was reduced in the aqueous phase. The sensitizer was regenerated in the following manner: the electron donor ($MnTP_yP\text{-}C_{16}$) transfered an electron to the oxidized sensitizer, and then the former was oxidized to $Mn^{IV}TP_yP\text{-}C_{16}$. The rates of formation of PVS^- and $Mn^{IV}TP_y\text{-}C_{16}$ were measured spectrophotometrically.
If in the aqueous micellar solution of sodium dodecyl sulfate containing appropriate amounts of $ZnTP_yP\text{-}C_{16}$, $Mn^{III}TP_yP\text{-}C_{16}$ and PVS°, we added an appropriate amount of an olefin (5-hexenoic acid, 5-HA), the photoproducts detected were PVS^- and $Mn^{II}TP_yP\text{-}C_{16}$. This observation is an agreement with a model according to which, upon illumination of the photochemical system, we have dye-sensitized the photoinduced electron transfer across the interface of the SDS micelle, from the two coupled electron donors ($MnTP_yP\text{-}C_{16}$ and 5-HA) dissolved in the micelle to the electron acceptor (PVS°) outside the micelle using $ZnTP_yP\text{-}C_{16}$ as a sensitizer.
The above dye-sensitized photochemical reactions cannot take place in homogeneous

solutions with Mn(III)-tetrapyridyl porphyrin and Zn-tetrapyridyl porphyrin.

From the results of these experiments we can make the following conclusions:

(a) The organization of a photosensitizer, of an electron donor and an electron acceptor on the interface between the aqueous phase and the organic phase of a micelle allow it to achieve photochemical reactions which otherwise could not happen in homogeneous solutions;

(b) We have simulated the main feature of the natural photosynthesis photochemical reaction, i.e. an irreversible photo-induced electron transfer across a membrane or water-to-organic phase boundary.

What is the difference between a) and b)?
Are these new conclusions? They seem to me pretty old (20-30 years old)

too general !

CHAPTER II

CHARACTERIZATION OF NATURAL PHOTOSYNTETIC SYSTEMS BY ELECTRO-OPTIC METHODS

2.1. Introduction

One of the more intriguing problems facing all biologists, biophysicists and chemisty researchers who are interested in the natural photosynthesis process is to get a better understanding of the structure of the photosynthetic membranes. By accumulating enough information on that structure, it would be possible, on one hand, to confirm or to refute the proposed hypotheses about the structure and mechanisms for the natural photosynthesis process, and on the other hand, to construct artificial photosynthetic systems capable of capturing and storage of sunlight energy /14,26/. There are some systematic studies of the interfacial charge of photosynthetic membranes which have shown its importance in the photosynthetic process /68/. This interfacial charge, which is part of the membrane electric double layer, may assume a crucial role in the spatial separation, by the thylakoid membrane, of oxidized species and reduced species of the primary photochemical step of natural photosynthesis.

A detailed knowledge of the orientation of chlorophyll, caroten and other pigment molecules embedded within the chloroplast membrane and their relative orientation at the local level, in a given photosynthetic unit or in its immediate neighbors, are necessary in order to understand the mechanisms by which the excitation light energy is transferred between the pigments of the chloroplast membrane and the structure of the latter /2,24a,45/.

Finally, investigations on the optical anisotropy of photosynthetic membranes may provide information not only on the overall orientation of chlorophyll and other pigment molecules relative to the membrane plane but also on their mutual orientation on a local level.

The orientation of the particles of a colloidal suspension in an applied electric field induces an optical anisotropy on a macroscopic scale and the optical properties of the suspension are modified /25a,46,47,51/. The electrically induced changes in the optical properties of a colloidal suspension is called an electro-optic phenomena/51/.

It is obvious that the electro-optic phenomena may provide us information on the structure of photosynthetic membranes. In fact, electro-optical investigations of a suspension of chloroplasts and that of sub-chloroplast fragments are susceptible to provide us information on their electrical properties (electric polarizabilities and permanent dipole moments), on their geometrical properties, on their optical anisotropy and on the orientation of some specific pigments within the photosynthetic membranes.

The electric linear dichroism method, for example, permits us to determine not only the electrical properties of particles but also the orientation of transition dipole moments of their chromophores /46,48/.

2.2. Basic principles of the theory of electro-optic methods

2.2.1. Generalities

An electro-optic phenomena is the modification of optical properties of a suspension submitted to an external applied electric field. Particles of a colloidal suspension respond to an applied electric field either by orientation or deformation and this induces an optical anisotropy on a macroscopic scale. The electro-optic phenomena which is observed is a consequence of that anisotropy

The model of the interaction of electric dipole moments with an electric field permits us to understand the origins of that anisotropy. To the electrical point of view, the particles of a colloidal suspension can be classified in two categories:

(a) Particles in which (or on which), in the absence of an external electric field, the charge distribution is asymmetric; they are characterized by a permanent dipole moment, $\vec{p}$. The electric dipole moments which, in the absence of the electric field and on account of the thermal motion were initially randomly distributed, will tend to orient themselves in the direction of the applied electric field in order to achieve a minimum potential energy ($U_1 = - \vec{p} \cdot \vec{E}$).

(b) Particles in which (or on which), in the absence of an external electric field, the charge distribution is symmetric. In this case, an applied electric field can induce a distortion of the charge distribution within the particles. Each particle will be characterized by an induced electric dipole moment, $\vec{p}_{ind}$. For a linear and isotropic material, $\vec{p}_{ind}$ is proportional to the local electric field intensity, $\vec{E}_{loc}$, the factor of proportionality being the particle's electric polarizability, γ :

$$\vec{p}_{ind} = \gamma \vec{E}_{loc} \qquad (2.1)$$

The local electric field intensity, $\vec{E}_{loc}$, is the average electric field intensity acting on a particular particle of the colloidal suspension : $\vec{E}_{loc}$ is equal to the macroscopic electric field intensity in the colloidal suspension plus the electric field intensity resulting from the polarization effects in the vicinity of the particle of interest. The electric polarizability, γ, is the sum of the electronic, atomic, dipolar, interfacial, etc...contributions:

$$\gamma = \gamma_e + \gamma_{at} + \gamma_{dip} + \gamma_{int} + \cdots \qquad (2.2)$$

The electronic polarizability, γ_e, which is due to the oscillations of electrons occurs at optical frequencies: it is then equal to the optical polarizability, γ°.

The atomic polarizability, γ_{at}, which is related to a possible relative displacement of different nuclei within a molecule under the effect of the local electric field, contributes to frequencies lower or equal to infrared frequencies.

The dipolar polarizability, γ_{dip}, is associated with the orientation of molecular dipoles.

The interfacial polarizability, γ_{int}, manifests itself especially for solutions of charged polyelectrolytes; it is due to the electric field induced movement of counterions on the polyelectrolyte's surface (counterion atmosphere polarization). The interfacial polarizability contributes at low frequencies.

The potential energy of an induced dipole moment in an electric field of intensity E is given by the expression /47/:

$$U_2 = - \frac{\gamma E^2}{2} \cos^2\theta \qquad (2.3)$$

Where θ is the angle between the direction of $\vec{p}_{ind}$ and that of $\vec{E}$.

Then, the response of particles to an applied electric field is a preferential orientation in the direction of the field and this will affect the optical properties of the suspension.

When, under the influence of the applied electric field, one observes a difference between the refractive indexes $n_{\parallel}$ and $n_{\perp}$ associated, respectively, to the components $\vec{E}_{\parallel}$ and $\vec{E}_{\perp}$ of the electric vector of the incident light vibrating, respectively, along the direction of the applied electric field and perpendicular to it, one has an electro-optic effect of double refraction or electric birefringence. The electric birefringence is defined by /25a,46/:

$$\Delta n = n_{\parallel} - n_{\perp} \qquad (2.4)$$

If, on account of the optical anisotropy induced by an electric field applied to a medium, the absorption of light by the latter depends on its polarization, the electro-optic effect is called electric linear dichroism. Sometimes, by analogy with the electric birefringence, the electric linear dichroism is defined by /25a,46,47/:

$$\Delta A = A_{\parallel} - A_{\perp} \qquad (2.5)$$

Where $A_{\parallel}$ and $A_{\perp}$ are the absorbances of the medium for incident light polarized along and perpendicular to the applied electric field, respectively.

The electric field induced optical anisotropy also affects the intensity of the scattered light. In the case where an external electric field induces only the orientation of the particles of a colloidal suspension leading to a change of the intensity of the scattered light, the electro-optic effect is defined as the relative change in the scattered light intensity /45,50/:

$$\alpha = \frac{I_E - I_0}{I_0} = \frac{\Delta I}{I_0} \qquad (2.6)$$

Where I_E is the intensity of the scattered light when an electric field of strength E is applied on the colloidal suspension and I_0 is the intensity of the scattered light in the absence of the electric field.

2.2.2. Theory of steady-state electro-optic phenomena

Generally, the electro-optic phenomena have several origins: orientation, aggregation, deformation and permeation. However, the basic principles of the theory that we present in this work deal with orientational electro-optic effects; it is for this type of electro-optic effect that the theory is most elaborated and more than 90 % of existing electro-optical data are interpreted as orientational effects /51/. The theory of electro-optic phenomena which has been developed in terms of electric birefringence can be extended to electric linear dichroism/46/. The theory of electric field light scattering, in which much more attention is paid to particles whose dimensions are comparable and even greater than the wavelength of incident light, has been developed independently/47/.

The electro-optic effect depends on the electrical, optical, geometrical and mechanic properties of the particles. It also depends on the degree of orientation which is determined by the ratio $\frac{U}{KT}$, where U is the potential energy of the electric dipole moments in the applied electric field, k is the Boltzmann constant, and T the absolute température.
At low degrees of orientation ($U \gg T$), the electro-optic effect varies linearly with the square of the applied electric field (Kerr's law). At high degrees of orientation ($U \gg T$), the thermal motion effect is negligible compared to the electric field induced orientational effect: one assumes that all particles are fully oriented.

Generally, the basic expression for the theory of orientationnal electro-optical phenomena is given by /47/:

$$\alpha = \alpha_\infty F(p,\gamma,E,T) \qquad (2.7)$$

Where α_∞ is the electro-optic effect for infinitely high electric fields for which it can be assumed that all particles are fully oriented; α_∞ is a specific function only depending on optical, geometrical or mechanic parameters of the particles. $F(p,\gamma,E,T)$ is a function of the particle's dipole moment, p, its electric polarizability, γ, the applied electric field strength, E, and the absolute temperature, T, and is called the orientation fuction, a function which reflects the degree of orientation of the particles at the field strength E.

The theoretical expression for the birefringence of a dilute solution of rigid axially symmetric macromolecules has been derived by Peterlin and Stuart/54/, O'Konski et at/52°/. For simplification, they have made the following hypotheses :

(a) The macromolecules* have a large electric polarizability (γ_a) along the symmetry axis a, and two small electric polarizability in the transverse direction, which are equal ($\gamma_b = \gamma_c$);

(b) The main component of the permanent dipole moment lies along the symmetry axis of the macromolecule.

(c) The orientational electro-optic effect, which is due to the interaction between the electric moments of the macromolecules (permanent dipole moment and the applied electric field, can be separated into an electro-optic effect, $\alpha(\gamma)$, due to induced dipole moment alone, and an electro-optic effect $\alpha(p)$, due to the permanent dipole moment only:

$$\alpha(\gamma,p) = \alpha(\gamma) + \alpha(p)$$

(d) When the macromolecule is fully oriented, its symmetry axis is parallel to the direction of the applied electric field.
By using all the assumptions cited above, Peterlin and Stuart, O'Konski et al. have derived the following expression for the orientation function:

$$F(p,\gamma,E,T) = \int_0^{\pi} f(\theta) \frac{3\cos^2\theta-1}{2} 2\pi\sin\theta d\theta \qquad (2.8)$$

θ is the angle between the macromolecule's symmetry axis and the direction of the applied electric field; $f(\theta)$ is the angular distribution function or the probability per unit solid angle of finding a macromolecule at angle θ with respect to the direction of the applied electric field.

When alternating simusoidal electric fields are applied, the angular distribution function also depends on the angular frequency of the applied electric field, ω, and on the time, t. The form of $f(\theta,\omega,t)$ can be found as a solution of the general differential equation of the brownian motion /47/:

$$\Delta f + \frac{1}{kT} (\text{div} f)(\vec{\text{grad}}\ U) = \frac{1}{D} \frac{\partial f}{\partial t} \qquad (2.9)$$

Where D is the rotational diffusion constant.

Let us consider the case of static electro-optic phenomena. After an electric field, E, has been applied to a system for a sufficiently long time so that we can assume that the system has come to a steady-state orientation distribution, we may calculate from the Boltzman distribution function the relative populations of molecules at various orientations /54/. Then the distribution function is proportional to $e^{-U/kT}$:

---

* This theory which has be developed for a solution of macromolecules is mostly applicable to particles of a colloidal suspension.

$$f(\theta) = C\, e^{-U/kT}$$

U is the potential energy of the macromolecule in the applied electric field.

The constant C must be chosen so that the probability in the entire solid angle is equal to one:

$$\int_0^{\pi} f(\theta)2\pi\sin\theta d\theta = 1 \Rightarrow C = \left(\int_0^{\pi} e^{-U/kT}2\pi\sin\theta d\theta\right)^{-1}$$

Then,

$$f(\theta) = \frac{e^{-U/kT}}{\int_0^{\pi} e^{-U/kT}\, 2\pi\sin\theta d\theta} \qquad (2.10)$$

The potential energy of the macromolecule in the applied electric field is given by the expression /25a,47/:

$$U = U_1(p) + U_2(\gamma) = - pB_a E\cos\theta - \frac{1}{2}(\gamma_a - \gamma_b)E^2\cos^2\theta \qquad (2.11)$$

Where the permanent dipole moment, p, is assumed to lie along the symmetry axis of the macromolecule, designated by the subscript a ($p_a = p$; $p_b = p_c = o$); B_a is the internal field function which takes into account the difference of the actual electric field interacting with the permanent dipole moment p from that applied on the solution due to the polarization of the adjacent solvent. B_a is almost equal to unity for very elongated and thin particles /46/.

In order to interprete data related to the field strength dependence of electric linear dichroism and electric birefringence, it is necessay to know the explicit form of $F(p,\gamma,E,T)$. For elongated particles with cylindrical symmetry, the orientation function is defined in the following way /54,55/:

$$F = \frac{3}{2}(\cos^2\theta)_{av} - \frac{1}{2}$$

By the use of Equations (2.10) and (2.11), we may write:

$$F = \frac{3}{2}\,\frac{\int_0^{\pi} \cos^2\theta\, e^{-U(\theta)/kT}2\pi\sin\theta d\theta}{\int_0^{\pi} e^{-U(\theta)/kT}\, 2\pi\sin\theta d\theta} - \frac{1}{2}$$

$$F(\beta, \chi) = \frac{3}{2}\,\frac{\int_{-1}^{+1} u^2 e^{(\beta u + \chi u^2)}\, du}{\int_{-1}^{+1} e^{\beta u + \chi u^2} du} - \frac{1}{2} \qquad (2.12)$$

Where other symbols have been introduced:

$$\beta = pE/kT$$

$$u = \cos\theta$$

$$\chi = \frac{\gamma_a - \gamma_b}{2kT} E^2$$

At very low electric fields, $(\beta u + \chi u^2) \ll 1$, $e^{(\beta u + \chi u^2)} = 1 + \beta u + \chi u^2 + \frac{\beta^2 u^2}{2}$.

So that after we have solved the integrals of the numerator and denominator of the equation (2.12) we find:

$$F(\beta,\chi) = \frac{3/2\ (\frac{2}{3} + \frac{2}{5}\chi + \frac{\beta^2}{5})}{2(1 + \frac{\chi}{3} + \frac{\beta^2}{6})} - \frac{1}{2} = \frac{3}{4}(\frac{2}{3} + \frac{2}{5}\chi + \frac{\beta^2}{5})(1 - \frac{\chi}{3} - \frac{\beta^2}{6}) - \frac{1}{2}$$

and finally,

$$F(\beta,\chi) = \frac{\beta^2 + 2x}{15} = [\frac{p^2}{kT} + (\gamma_a - \gamma_b)]\frac{E^2}{15kT} \qquad (2.13a)$$

The equation (2.13a) is in agreement with the Kerr law. In particular, if only permanent dipole moments are involved in the mechanism of orientation ($\chi = o$),

$$F(\beta) = \frac{p^2E^2}{15k^2T^2} \qquad (2.13b)$$

Whereas, if only induced dipole moments are involved ($\beta = o$),

$$F(\chi) = \frac{(\gamma_a - \gamma_b)}{15kT} E^2 \qquad (2.13c)$$

By using the general expression (Eq.2.12), one shows that for $\chi = o$ (only permanent dipole moment orientation):

$$F(\beta) = F(p,E,T) = 1 - 3\frac{\coth(pE/kT) - (kT/pE)}{(pE/kT)} \qquad (2.14)$$

Whereas , for only induced dipole moment orientation (i.e, $\beta = o$) one has /46,55/:

$$F(\chi) = F(\gamma,E,T) = \frac{3}{4}\{\frac{e^{\chi}/\sqrt{\chi}}{\int_o^{\sqrt{\chi}} e^{x^2}dx} - \frac{1}{\chi}\} - \frac{1}{2} \qquad (2.15)$$

One may use the general equations (2.14) and (2.15) in order to find the corresponding equations at very high electric fields /47,55/.

2.3. Electric linear dichroism

2.3.1. Basic definitions

A medium which is submitted to an electric field may absorb an incident light to different extents depending on whether the direction of polarization of that light is parallel to the applied electric field or perpendicular to it. This property is called electric linear dichroism. The latter is defined by equation (2.5).

Most electro-optical instruments which are used for the measurement of the electric linear dichroism, permit us to measure either $A_{\parallel}$ or $A_{\perp}$; then it is more convenient to define the specific parallel and perpendicular electric dichroism /47,48/:

$$\frac{\Delta A_{\parallel}}{A_0} = \frac{A_{\parallel} - A_0}{A_0}$$
$$\frac{\Delta A_{\perp}}{A_0} = \frac{A_{\perp} - A_0}{A_0} \qquad (2.16)$$

$A_{\parallel}$ and $A_{\perp}$ have previously been defined (see, page 17);
A_0 is the absorbance of the sample in the absence of the electric field.
The specific electric linear dichroisms are dimensionless and concentration-independent quantities. They can be expressed in terms of the molar extinction coefficients of the solute /48/:

$$\frac{\Delta A_{\parallel}}{A_0} = \frac{\varepsilon_{\parallel} - \varepsilon_0}{\varepsilon_0}$$
$$\frac{\Delta A_{\perp}}{A_0} = \frac{\varepsilon_{\perp} - \varepsilon_0}{\varepsilon_0} \qquad (2.17)$$

Where, according to the Beer-Lambert law, $A_0 = \varepsilon_0 Cl$, $A_{\parallel} = \varepsilon_{\parallel} Cl$, $A_{\perp} = \varepsilon_{\perp} Cl$.
C is the molar concentration; l is the optical pathlength; ε_0 is the molar extinction coefficient of the solution in the absence of the electric field; $\varepsilon_{\parallel}$ and $\varepsilon_{\perp}$ are the molar extinction coefficients of the solution in the presence of an electric field for incident light polarized parallel and perpendicular to the electric field, respectively.
Assuming that the two directions of space which are perpendicular to the applied electric field are equivalent (axial symmetry with respect to the direction of the applied electric field) and that the optical absorbance is proportional to the square of the transition dipole moment, Frederick and Houssier /46/ have established a relation between the absorbance of the isotropic solution, A_0, and the absorbances in the presence of an electric field, $A_{\parallel}$ and $A_{\perp}$:

Originally attributed to Jablonski

$$A_0 = \frac{A_{\parallel} + 2A_{\perp}}{3} \qquad (2.18)$$

From equations (2.16) and (2.18), one easily shows that :

$$\frac{\Delta A}{A_0} = 1.5 \frac{\Delta A_{\parallel}}{A_0} = -3 \frac{\Delta A_{\perp}}{A_0} \qquad (2.19)$$

2.3.2. Relation of electric linear dichroism to orientation function

The theory of the orientation of particles in electric fields has been developed mainly in terms of birefringence /46/. As long as the electric linear dichroism is due to the preferential orientation of the electric moments of the particles in the direction of the applied electric field (without field-induced changes in the frequency or overall intensity of the transition), the electric linear dichroism is related to the orientation distribution function in the same manner as electric birefringence /48,51/. Electric birefringence expressions can be applied to electric linear dichroism by simply replacing optical polarizabilities by molar extinction coefficients /46,53/. By using a model which assumes that the principal axes of electrical and optical polarizabilities coincide, Holcomb and Tinoco /25a/ have established a relationship between the electric linear dichroism and the orientation function. According to this relationship, for axially symmetric particles, one has the following expression /47,48/:

$$\left(\frac{\Delta A}{A_o}\right) = \left(\frac{\Delta A}{A_o}\right)_S F(p,\gamma,E,T) \qquad (2.20)$$

Where $F(p,\gamma,E,T)$ is the orientation function given by equation (2.8) (page 10); the electric linear dichroism saturation expression is given by /47/ :

$$\left(\frac{\Delta A}{A_o}\right)_S = \frac{\varepsilon_{ab}}{\bar{\varepsilon}} \qquad (2.21)$$

In equation (2.21), ε_{ab} is the optical asymmetry defined as: $\varepsilon_{ab} = \varepsilon_a - \varepsilon_b$ where ε_a and ε_b are, respectively, the molar extinction coefficient for light polarized along the particle's symmetry axis and perpendicular to it and $\bar{\varepsilon}$ is the average molar extinction coefficient, $\bar{\varepsilon} = \frac{\varepsilon_a + 2\varepsilon_b}{3}$.

One may use the electric linear dichroism data in order to determine the mechanism of orientation. In fact, for low electric fields, the electric linear dichroism is proportional to the square of the electric field in agreement with the Kerr law. According to equation (2.13a), page 21 , we may write:

$$\lim_{E\to o}\left(\frac{\Delta A}{E^2}\right) = \lim_{E\to o}\frac{\Delta A_S\, F(\beta,\chi)}{E^2} = \frac{\Delta A_S}{15}(P + Q) \qquad (2.22)$$

Where $P = \frac{\beta^2}{E^2} = \left(\frac{p}{kT}\right)^2$ and $Q = \frac{2\chi}{E^2} = \frac{\gamma_a - \gamma_b}{kT}$

P and Q represent, respectively, the contributions of permanent dipole moments and induced dipole moments to the degree of orientation. Frederico and Houssier /46/

have discussed techniques which permit us to estimate the relative contributions of permanent dipole and induced dipole moments on the mechanism of orientation. These techniques include a detailed analysis of the buildup curve and decay curve of the orientational electro-optic phenomena when a square electric pulse is first applied and then removed (see next section: 2.3.3.).

$$\text{Besides, } \frac{\Delta A/E^2}{(\Delta A/E^2)_{E\to 0}} = \frac{\Delta A_S\, F(\beta,\chi)/E^2}{(\Delta A_S/15)(P+Q)} = \frac{15\, F(\beta,\chi)}{\beta^2 + 2\chi} \qquad (2.23)$$

The analysis of the curve obtained by plotting $\frac{(\Delta A/E^2)}{(\Delta A/E^2)_{E\to 0}}$ as a function of $\log E^2$ gives information on the mechanism of orientation /45,46/.

2.3.3. Transient electro-optic phenomena

2.3.3.1. Relaxation time and rotational diffusion coefficients

When an electric field is applied or changed across a solution or colloidal suspension, the orientation distribution function depends not only on the angle θ between the applied electric field and the symmetry axis of the particle under consideration, but also on the time, t : $f = f(\theta,t)$ /25a,47/.
The function $f(\theta,t)$ must satisfy the partial differential equation of the Brownian diffusion process, (Eq.2.9). Due to the frictional and inertial effects between the particles and the surrounding medium, the orientational electro-optic effect doesn't change instantaneously; one observes a transient phenomena.
For example, when the particles of a colloidal suspension have been oriented by an electric field and the latter is suddenly removed, the particles return to the random orientation state and the electro-optic effect decreases and falls asympotically to zero. For, a monodisperse suspension, of small particles, one observes an exponential decay of the electro-optic effect with a time constant τ called relaxation time /46/:

$$\alpha = \alpha_o\, e^{-t/\tau} \qquad (2.24)$$

Where α_o is the value of the electro-optic effect at the time t = o at which the electric field is switched off.
The relaxation time, τ, is given by /47/:

$$\tau = \frac{1}{12D}$$

Where D is the rotational diffusion coefficient.
The common way /25,46,47,53/ to measure the relaxation times is to apply electric pulses across colloidal suspensions; the transient electro-optical

not well defined

signal is displaced on a very sensitive oscilloscope and simultaneously the oscilloscope traces are photographed and analysed later for quantitative determination of relaxation times. Using the relationship between the relaxation time and the rotational diffusion coefficient, the latter can be determined; such a measurement then provides important information on the shape and sizes of the particles of a colloidal suspension. see page 15.

The rotational diffusion coefficient is related to particles' geometrical parameters by the following relationships /46/:

1°) according to Perrin's equations for revolution ellipsoids,

$$D = \frac{3kT}{16\pi\eta a^3} \{2\ell n(\frac{2a}{b}) - 1\} \qquad (2.25)$$

Where η is the viscosity of the solvent, a and b are, respectively, the long and the short semi-axes;

2°) according to Burgers' equations, for particles of cylindrical shape,

$$D = \frac{3kT}{8\pi\eta a^3} \{\ell n(\frac{2a}{b}) - 0.8\} \qquad (2.26)$$

Where a is half-length and b the radius of the cylinder.

From equations (2.25) and (2.26), we can determine the "length" of the particle if its shape and axial ratio $(\frac{a}{b})$ are known (e.g., from electron microscopy).

For a polydisperse system, the analysis of relaxation curves is very complex: each electro-optic effect has its particularities /47/, and the average relaxation time depends, generally, on the field strength and on electrical and optical properties of the particles /25a/. However, for a polydisperse system of revolution ellipsoids with a discrete distribution of lengths, O'Konski and Haltner have proposed a general formula which may characterize the decay of all electro-optic effects /46,47/. According to that formula, the decay of the electric linear dichroism should be given by the following expression:

$$\Delta A_D(t) = \sum_i \Delta A_{o,i}\, e^{-t/\tau_i} = \sum_i \Delta A_{o,i}\, e^{-6D_i t} \qquad (2.27)$$

Where $\Delta A_{o,i}$ is the contribution to the steady-state electric dichroism originating from the ith species, τ_i and D_i are, respectively, the relaxation time and rotational diffusion coefficient of the ith species.

There are two methods of determining the average relaxation time of a polydisperse solution/25b,46,47/:

definition ?

1) One method uses the initial tangent to the decay curve of the electro-optic effect, $\alpha(t)$. By extrapolation, this method permits to determine the average relaxation time of a colloidal suspension if the latter doesn't contain more than three different species.

2) The other suggested by Yoshioka and Watanabe uses the area bounded by the decay curve of the electro-optic effect. The electro-optical average relaxation time is given by:

$$\bar{\tau} = \int_0^\infty \frac{\alpha_D(t)}{\alpha_o} dt \qquad (2.28)$$

2.3.3.2. Electro-optic determination of electric parameters

By applying electric pulses (square pulses, pused sine-wave fields, etc.) across a colloidal suspension, one may determine the electric parameters (electric polarizabilities, and permanent dipole moments) of the particles in suspension. One may distinguish the permanent dipole moment orientational mechanism from the induced dipole moment orientational mechanism. If both mechanisms are involved, it is possible to determine their relative contribution.
By using pulsed sine-wave electric pulses, the dependence of an electro-optic effect on the frequency of the applied electric field (dispersion curves) can be followed. The dispersion curves may provide information on the type of the most important electric polarizability.

see page 15

A. Analysis of the rive curves of the electric linear dichroims in square electric pulses

Equations for the time dependence of the electric birefringence in a suddenly applied square electric pulse have been established by Benoit for the case of cylindrically symmetric macromolecules with permanent dipole moment p_a along the symmetry axis /25a/. These equations may be applied to the electric linear dichroism; at low degrees of orientation, one can write /25a,25b,46/:

$$\frac{\Delta A_R(t)}{\Delta A_o} = 1 - \frac{3}{2}\frac{P/Q}{(P/Q)+1} e^{-2Dt} + \frac{(P/Q)-2}{2\,(P/Q)+1} e^{-6Dt} \qquad (2.29a)$$

Where $\Delta A_R(t)$ is the value of the electric linear dichroism after a time t following the application of the electric field, ΔA_o is the value of the electric linear dichroism at the moment at which the electric field is switched off. P and Q have the meaning stated above (See Eq.(2.22); page 22)

From equation (2.29a), it is possible to make a qualitative distinction of permanent dipole orientation mechanism from induced dipole orientation

mechanism and a qualitative determination of the direction of the electric polarizability with respect to the particle symmetry axis.

(1°) If P and Q have the same sign (i.e the permanent and induced dipole moments tend to orient the particle in the same direction), the larger is the ratio, (P/Q), the slower is the establishment of the steady-state: the rise time of the electro-optic effect is larger than the decay time.

(2°) In the case where permanent dipole moment orientation is negligible (i.e P/Q=o), equation (2.29a) gives,

$$\Delta A_R(t) = \Delta A_o (1 - e^{-6Dt}) \tag{2.29b}$$

The rise curve given by equation (2.29b) is symmetrical to the decay curve given by equation (2.24).

(3°) If the induced dipole moment orientation mechanism is negligeable (i.e $P/Q \to \infty$), equation (2.29a) gives:

$$\Delta A_R(t) = \Delta A_o\left(1 - \frac{3}{2} e^{-2Dt} + \frac{1}{2} e^{-6Dt}\right) \tag{2.29c}$$

The rise curve given by equation (2.29c) is tangent to the t axis for t = o.

(4°) If both orientation mechanisms are involved, we can estimate their relative contribution (ratio P/Q) from the initial slope to the curve given by equation (2.29a):

$$\frac{1}{D}\frac{d}{dt}\left(\frac{\Delta A_R(t)}{\Delta A_o}\right)_{t=o} = \frac{6}{(P/Q)+1} \tag{2.29d}$$

(5°) If P and Q are opposite in sign, the electric linear dichroism changes its sign during the rise phase (the electric linear dichroism may drop precipitously even if the square electric pulse is still on) /25a,46/.

Another possibility which may be used in order to estimate the ratio (P/Q) was suggested by Yoshioka and Watanabe /47/. According to them, the ratio of the areas bounded, respectively, by the rise curve given by equation (2.29a) and the ordinate, and by the decay curve given by equation (2.24) and the abcissa, after a steady-state has been reached, is given by (see figure below):

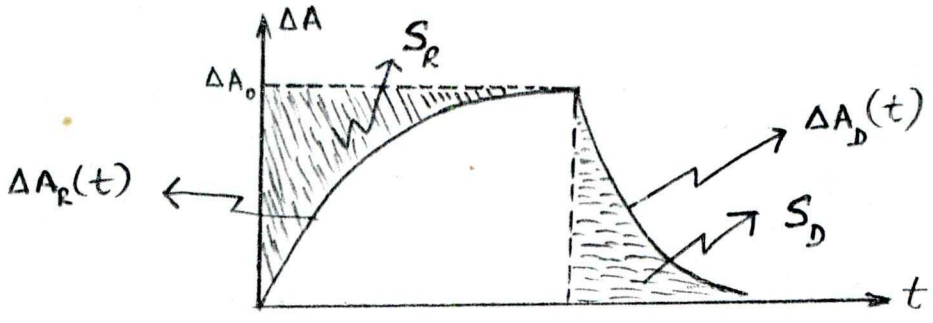

$$\frac{S_R}{S_D} = \frac{\int_o^\infty (\Delta A_o - \Delta A_R)dt}{\int_o^\infty \Delta A_D(t)\, dt} = \frac{4\,(P/Q) + 1}{(P/Q) + 1} \tag{2.30}$$

B. Transient electro-optic phenomena in pulsed sine-wave fields.

The use of sine wave electric pulses present the following advantages /25a,45-47/:

1) It limits the disturbing action of electrode polarization;
2) It limits the electrophoresis phenomena;
3) It permits to investigate the dispersion dependence of electro-optical phenomena;
4) The obtension of pulsed sine-wave fields doesn't require sophisticated electric pulse generators which are very expensive: by using an appropriate transformer, it is possible to obtain pulsed sine-wave electric fields which satisfy the requirements of some experiments.
5) By assuming the additivity of the permanent dipole orientation mechanism and the induced dipole orientation mechanism, it is possible to separate and to determine the effects due to permanent dipole moments and electric polarizabilities (see Section 2.4.4, page 40)

In alternating sinusoidal electric fields, the orientation distribution function, f, depends on the angle θ between the symmetry axis of the particle under consideration and the applied electric field, on the time, t, and on the angular frequency of the field. The explicit form of $f(\theta, \omega, t)$ may be obtained by solving the partial differential equation for the Brownian diffusion process (Eq.2.9). This equation has been solved for the case of low degrees of orientation /47/; the explicit form of the dependence of the electro-optic effects (electric birefringence and electric linear dichroism) on ω, E and t is given in this reference.
Let us assume that a sinusoidal electric field, $E = E_0 \sin \omega t$ (E_0 is the maximum amplitude) is applied across a colloidal suspension. We also assume that the period of the sinusoidal electric field, T, is much larger than the relaxation time of the particles, τ, so that the particle's permanent dipole moments can follow the oscillations of the electric field.

For low degrees of orientation (the Kerr law is valid), the electro-optic effect may be separated into two terms /25a,46,47/: a term $\alpha_i(t)$ which only depends on the induced dipole moments and a term $\alpha_p(t)$ which only depends on the permanent dipole moments. Peterlin and Stuart /25a/ have derived equations for the electric birefringence for rigid and axially symmetric macromolecules in alternating sinusoidal electric fields. These equations may be applied to the electric linear dichroism since the two electro-optic effects are proportional to a same orientation function.

The term of ΔA due to the induced dipole moments only is given by /25a,46,47/:

$$\Delta A_i(t) = \Delta A_{i,av} \left[1 \pm \frac{\cos(2\omega t - \phi_i)}{(1 + 4\omega^2\tau^2)^{1/2}}\right] \qquad (2.31)$$

Where $\Delta A_{i,av}$ is the average electric linear dichroism observed: it is the value which would be obtained if a steady electric field equal to $E_o/(2)^{1/2}$ was applied. ϕ_i is the phase angle between the electric linear dichroism and the applied electric field and is given by, $\tan\phi_i = 2\omega\tau$, where τ is the relaxation time of the macromolecules. Equation (2.31) shows that $\Delta A_i(t)$ is a sum of a constant term and a term which alternates with twice the frequency of the applied electric field.

At very high frequencies, only the term which is constant with time is observed. At extremly high frequencies ($\nu \geq 1$ MHz), the induced dipole moments cannot completly be formed; since this effect is not considered by the theory, the value observed doesn't agree with the expression (2.31).
In the case of a pure permanent dipole moment orientation, the electric linear dichroism takes the value /25a,47/:

$$\Delta A_p(t) = \Delta A_{p,o} \left[\frac{1}{1 + 9\omega^2\tau^2} + \frac{\cos(2\omega t - \phi_p)}{(1 + 9\omega^2\tau^2)^{1/2}\,(1 + 4\omega^2\tau^2)^{1/2}}\right] \qquad (2.32)$$

Where $\Delta A_{p,o}$ is the value of the electric linear dichroism which would be obtained if a steady electric value equal to $E_o/(2)^{1/2}$ was applied; ϕ_p is the phase angle between the electric linear dichroism and the applied electric field and is given by:

$$\tan\phi_p = \frac{5\omega\tau}{1-6\omega^2\tau^2}$$

Equation (2.32) shows that the electric linear dichroism consists of two components, one of which is constant with time, and the other of which alternates with twice the frequency of the applied electric field and differs in phase with the latter by the angle ϕ_p. However, in the pure permanent dipole orientation, case, both the time-independent and the time-dependent components decrease to zero at high frequency because the permanent dipole moments cannot follow the alternating electric field any longer.
In the general case where the permanent dipole moment orientation and induced dipole moment orientation mechanisms have to be taken into account, the electro-optic effect (electric birefringence and electric linear dichroism) is given by:

$$\alpha(t) = \alpha_i(t) + \alpha_p(t)$$

At low frequencies, $\alpha_p(t)$ predominates, while at very high frequencies, only $\alpha_i(t)$ remains, in the form of $\alpha_{i,av}$.
Thurston and Bowling have derived a general expression which shows that the variation of the electric birefringence with the frequency involves the ratio of the contributions of permanent dipole moments and induced dipole moments, (P/Q),/46/. This expression may be applied to the electric linear dichroism; then, for low degrees of orientation, the time-independent component of the electric linear dichroism is given by:

$$\frac{\Delta A_{av}}{\Delta A_o} = \frac{1}{(1 + P/Q)} \left[1 + \frac{P/Q}{1 + (\omega/2D)^2}\right] \qquad (2.33)$$

From equation (2.33), with appropriate extrapolations at $\omega \to \infty$, one may determine /46/ the ratio P/Q, the value of the permanent dipole moment, p, and the rotational diffusion coefficient, D.

2.3.4. Orientation of transition dipole moment

When one treats the interaction of light with matter, it may be helpful to consider the shape of two molecular orbitals describing the ground state and the excited state. In the absence of an electromagnetic radiation, it is assumed that all molecules in a solution are in the lowest electronic state, or ground state. When a molecule absorbs a photon of appropriate wavelength it can be excited to one of many rotation-vibration levels of the excited electronic state. Thus the charge distribution of the molecule is altered by the oscillating electric field of the electromagnetic wave. In order to describe the charge distribution of a molecule, one could consider each individual charge, but it is easier to expand the charge distribution in a multipole series. For electrically neutral molecules, the leading term in this expansion is the electric dipole term.
From the quantum mechanics point of view, it is appropriate to consider the dipole moment operator ($\vec{\underset{\sim}{\mu}}$) defined in the following way:

$$\vec{\underset{\sim}{\mu}} = \sum_i e_i \vec{\underset{\sim}{r}}_i$$

Where the sum is taken over each electronic charge (e_i) at position $\vec{\underset{\sim}{r}}_i$. ($\vec{\underset{\sim}{r}}_i$ is the position operator). Let us call ψ_e the wave-function of a particular excited electronic state of a molecule and ψ_g the wave-function of its ground state. The transition dipole moment of this particular electronic transition of the

molecule is defined by the following integral:

$$\vec{\mu}_{eg} = \langle \psi_e | \vec{\underset{\sim}{\mu}} | \psi_g \rangle = \int_V \psi_e^* \vec{\underset{\sim}{\mu}} \psi_g \, dV$$

Thus the transition dipole moment of a particular electronic transition is a matrix element of the dipole moment operator.

The value of the electric linear dichroism for infinitely high electric field strengths for which particles are fully oriented permits us to determine the direction of the transition dipole moment of the chromophore (which is responsible for light absorption) with respect to the molecular symmetry axis. In fact, let us assume that a particle is fully oriented; then its symmetry axis coincides with the direction of the applied electric field (e.g., direction of the OZ axis). Let us assume that the transition dipole moment lies at some fixed angle ψ to the OZ direction. Since the optical absorbance is proportional to the square of the transition moment, it follows that /46/:

$$A_Z = A_{\parallel} = k\mu_Z^2 = k\mu^2 \cos^2\psi = A_\mu \cos^2\psi .$$

Where k is a constant and A_μ is the optical absorbance for light polarized parallel to the direction of the transition moment. A_μ is connected to the absorbance (A_0) of the isotropic solution (i.e., molecular orientation are randomized) by /48/:

$$A_\mu = 3A_0$$

In consideration of the axial symmetry with respect to the direction of the applied electric field, μ_x and μ_y are randomly oriented, and it follows:

$$\bar{A}_x = \bar{A}_y = A_\perp = \frac{k\mu^2}{2}\sin^2\psi = \frac{A_\mu}{2}\sin^2\psi$$

$$\left(\frac{A_{\parallel} - A_\perp}{A_0}\right) = \frac{A_\mu}{A_0}\left(\cos^2\psi - \frac{1}{2}\sin^2\psi\right) = 3\left(\cos^2\psi - \frac{1}{2}\sin^2\psi\right) \qquad (2.34)$$

$$\frac{\Delta A_S}{A_0} = \frac{3}{2}\left(3\cos^2\psi - 1\right)$$

Thus, if there is only one chromophore in a macromolecule or any particle and if the structure of the latter is known precisely, electric linear dichroism measurements can be used to determine the direction of the transition dipole moment. Besides, if there is only one chromophore in a macromolecule and if the direction of its transition dipole moment is known, electric dichroism measurements can be used in order to get a better understanding of some aspects of macromolecular structure.

2.4. Electric field light scattering

2.4.1. Brief theoretical background on the conventional light scattering method

Under the effect of the electric field vector of an incident light beam, optical electrons of atoms or molecules of a medium may oscillate about their equilibrium position at the frequency of the incident light. Then, the electric field vector of the incident light beam may induce an oscillating electric dipole in any particle in its path. According to the classical theory of electromagnetism, an oscillating electric dipole is a source of an electromagnetic wave to which corresponds the scattered intensity.

In any optically homogeneous medium (the refractive index is constant) such as a transparent crystal where the molecular distribution is uniform, the wavelets scattered by the different scattering centers (volume elements much smaller than the wavelength of the incident light, so that the entire element can be considered as a single scattering source, which, however, are large enough to contain many molecules) are coherent and there is a complete destructive interference.

In fact, the particles of such a medium can always be paired off in such a way that the light paths from the two particles in each pair to an observer at any particular viewing angle θ' differ by essentially exactly one-half wavelength /56,57/. Consequently, no scattered intensity is observed in a pure optically homogeneous medium. However, in a pure liquid, a small amount of scattered intensity may be observed on account of the fluctuations in the density (fluctuations in local pressure and temperature) at any particular point /57/.

In optically heterogenous media (the refractive index varies on account of fluctuations in density or concentration), the more there is no correlation between the relative phase difference of the scattered wavelets from scattering elements, the more the scattered intensity is greater /56,57/. Consequently, light scattering is especially observed for colloidal suspensions, macromolecular solutions which contain small particles whose the refractive index differs from that of the solvent. The scattered intensity will depend on the concentration, the degree of correlation, electric properties (electric polarizabilities and permanent dipole moments) and geometrical properties of macromolecules in solution or dispersed particles.

The conventional light scattering method considers two cases according to the dimensions of dispersed particles.

(a) Light scattering by particles which are assumed to be uncharged, noninteracting, randomly positioned and oriented throughout the colloidal suspension, which don't absorb the incident light energy and whose linear dimensions are much smaller than the wavelength of the incident light, is described by the Rayleigh theory /58/. The main significant features of this theory are /56,57/:

(i) the scattered intensity is proportional to the inverse fourth-power of the wavelength of the incident light;

(ii) the polar scattering diagram (i.e the dependence of the scattered intensity on the viewing angle, θ') has a form of a revolution surface which is symmetric about the angle $\theta' = o$ (direction fo the incident light beam) and $\theta' = \frac{\pi}{2}$;

(iii) The scattered intensity is proportionnal to the square of the molecular weight of the scattering particles and it is also proportional to $(\frac{dn}{dc})$ (where n is the refractive index of the medium and c the concentration of particles in the suspension, in grams per cubic centimeter).

If one knows the weight-average concentration, by using expression derived by Rayleigh, he can determine the weight-average molecular weight, $\bar{M}_w$, of dispersed particles.

(b) Light scattering by particles whose linear dimensions are in the order of/or greater than the wavelength of the incident light is described by the Rayleigh-Gans theory /58/. An important approximation of Rayleigh-Gans is to assume that the local electric field is uniform in the whole volume elements of the scattering particle /57/. On account of the interference between wavelets scattered, the scattering particle's constituent volume elements, the polar scattering diagram is dissymmetric /56/: it has only one symmetry axis which coincides with the direction of the incident light ($\theta' = o$); it is dissymmetric about the angle θ' equal to $\frac{\pi}{2}$. This dissymmetry is characteristic of the size and shape of dispersed particles /57,58/; it is measured by a function $P(\theta')$ which takes into account the interference effects between wavelets scattered by a particle's constituent scattering elements.

The basic theoretical expression for the function P(θ') for any molecular shape is given by /57,58/:

$$P(\theta') = \frac{1}{N^2}\sum_{i=1}^{N}\sum_{j=1}^{N} < \cos(\vec{r}_{ij}\cdot\vec{h}) > = \frac{1}{N^2}\sum_{i=1}^{N}\sum_{j=1}^{N} <\cos(r_{ij}h\cos\xi) > \quad (2.35)$$

Where $\vec{h} = \vec{s} - \vec{s}_o$, $\vec{s}$ and $\vec{s}_o$ being the wave vectors in the direction of the incident and scattered light beams, respectively; $h = \frac{4\pi}{\lambda}\sin\frac{\theta'}{2}$ the vector $\vec{r}_{ij}$ joins the i and j scattering elements of which the particle has a total of N; ξ is the angle between the vectors $\vec{r}_{ij}$ and $\vec{h}$: ξ will be influenced by the orientation of the particle with respect to the direction of the incident light beam and hence it will be affected by the application of an external electric field.

The Rayleigh-Gans theory provides expressions which permit to determine the weight-average molecular weight, $\bar{M}_w$, and the z-average of the radius of gyration, $\bar{R}^2_z$, from the measurements of the intensity scattered by a colloidal suspension, as a function of the viewing angle θ' and the solute concentration /58/.

The Rayleigh-Gans theory is subjected to the two conditions /47/:

$$\frac{2\pi\ell}{\lambda}\left|\frac{n_p}{n_m} - 1\right| \ll 1 \text{ and } \left|\frac{n_p}{n_m} - 1\right| \ll 1 \quad (2.36)$$

Where ℓ is the average linear dimension of the particles; n_p and n_m are the refractive index of the particles and solvent, respectively; λ is the wavelength of the incident light.

2.4.2. Modification of the scattered intensity by an electric field

2.4.2.1. Introduction

Particle orientation in an electric field affects the scattering characteristics of a colloidal suspension in at least two ways /58/.

(i) First, by anology with other electro-optic effects, the preferential orientation of scattering elements in the direction of the applied electric field produces an optical anisotropy on a macroscopic scale and hence, affects the scattering properties of a colloidal suspension;

(ii) Second, for particles whose dimensions are in the order of and even greater than the wavelength of the incident light, the function of the geometrical parameters, $P(\theta')$, will vary upon particles preferential orientation in the direction of the applied electric field.

The theory of the electric field light scattering is subjected to the conditions of equation (2.36). A supplementary restriction is required in order to obtain scattered intensity changes noticeable enough to be measured /47/: for the case of optically but anisometric particles, their dimensions have to be in the order of (and even greater than) the wavelength of the incident light. However, this condition is not necessary for optically anisotropic particles. Then, the scattered intensity changes are especially related to the electric field-induced modification of the function $P(\theta')$, i.e. they are due to internal interference effects /58/.

Because of this, the theory for the electric field light scattering cannot simply be expressed in terms of the orientation function $F(p,\gamma,E,T)$ given by equation (2.8), page 19, for electric birefringence, electric linear dichroism,etc. it has been elaborated independently /47/.

The direction into which the particles tend to orientate when an external electric field is applied can be deduced from the changes in the polar scattering diagram /58/. Thus, like other electro-optic phenomena, the electric field light scattering permits to determine (in addition to $\bar{M}_w$ and $\overline{R_z^2}$) the electric parameters and the rotational diffusion coefficient, D, of dispersed particles. The simultaneous knowledge of the rotational diffusion coefficient, D, and the z-average radius of gyration ($\overline{R_z^2}$) provides information on the structure.

2.4.2.2. Electric field light scattering theory in continuous DC fields.

The electro-optic effect associated to light scattering is defined by Equation (2.6), page 17, $\alpha = \dfrac{I_E - I_o}{I_o} = \dfrac{\Delta I}{I_o}$

Where I_E is the intensity of the scattered light when an electric field of strength E is applied on the suspension and I_o is the intensity of the scattered light in the absence of the electric field.

I_o and I_E are given by /47/:

$$I_o = \frac{N}{4\pi} \int_\Omega i(\theta,\phi)d\Omega$$

$$I_E = N \frac{\int_\Omega i(\theta,\phi)e^{-U/kT}d\Omega}{\int_\Omega e^{-U/kT}d\Omega} \qquad (2.37)$$

Where $\int_\Omega \ldots d\Omega = \int_0^{2\pi} \int_0^{\pi} \ldots \sin\theta \, d\theta \, d\phi$ designates integration over a sphere of radius unity.

In the expressions given by Equation (2.37), N is the number of scattering particles per unit volume; U is the potential energy of the particle's permanent dipole moment and induced dipole moment and is given by Equation (2.11); $i(\theta,\phi)$ is the scattered intensity in the solid angle element, $d\Omega(\theta,\phi)$.
From Equation (2.37), we deduce :

$$\alpha = \frac{I_E}{I_o} - 1 = 4\pi \frac{\int_\Omega i(\theta,\phi) e^{-U/kT} \, d\Omega}{\int_\Omega e^{-U/kT} \, d\Omega \int_\Omega i(\theta,\phi) \, d\Omega} - 1 \qquad (2.38)$$

By using Equation (2.38), one may easily show that, for low degrees of orientation ($U \ll kT$), the electro-optic effect, α, is given by :

$$\alpha = \frac{\int_\Omega \frac{3\cos^2\theta - 1}{2} i(\theta,\phi) \, d\Omega}{\int_\Omega i(\theta,\phi) \, d\Omega} \cdot \left(\frac{p^2}{3k^2T^2} + \frac{\gamma}{3kT} \right) E^2 \qquad (2.39)$$

Suitable equations for the electric field-induced scattered intensity changes were first derived by Wippler (for rods or coils in relatively low-intensity fields), and then by Stoylov and others (for disks in low-intensity fields; for rods in high-intensity fields) /47,58/. In all these theories, it is assumed /58/ that the molecules are isolated as in an infinitely dilute solution, that they are optically isotropic, uncharged, and that the solution is monodisperse.

In 1954, Wippler has derived equations for the electric field light scattering by thin rods (strongly anisodiametric particles) in continous DC fields and for low degrees of orientation. He considered the distribution function for a thin rod in terms of a series of Legendre polynomials and produced, for the relative change in the scattered light, the following equation /47,58/:

$$\frac{\Delta I}{I_o} = \frac{3}{4P_o(\theta')} (1 - 3\cos^2\Omega) \, GE^2\phi(K)$$

$$\phi(K) = \frac{P_o(\theta')}{3} + \frac{\sin 2K}{4K^3} - \frac{1}{2K^2} \qquad (2.40)$$

$$G = \frac{p^2}{3k^2T^2} + \frac{\gamma}{3kT}$$

$$P_o(\theta') = \frac{1}{K} \int_o^{2K} \frac{\sin t}{t} \, dt - \left(\frac{\sin K}{K} \right)^2$$

$$K = \frac{2\pi\ell}{\lambda} \sin\left(\frac{\theta'}{2} \right)$$

In Equation (2.40), Ω is the angle between the direction of the electric field and the bisector of the viewing angle θ'; $\phi(K)$ is a function of optical parameters; $P_o(\theta')$ is defined as for Eq.(2.35); ℓ is the length of the rodlike particle.

According to Equation (2.40), for low degrees of orientation, $\frac{\Delta I}{I_o}$ is proportional to the square of the applied electric field (analogy with the Kerr law).

For frequencies higher than a "critical frequency" (frequency for which the permanent dipole moment contribution is half-completed or relaxed; above the critical frequency it is assumed that permanent dipole moments cannot follow the oscillations of the electric field), the initial slope to the curve $(\frac{\Delta I}{I_o}) = f(E^2)$ allows us to determine the electric polarizability, γ.

In fact, by setting $\Omega = \frac{\pi}{2}$, one has;

$$\left[\frac{\partial \alpha}{\partial E^2}\right]_{\substack{E\to O \\ \nu>\nu_c}} = \frac{3}{4P_o(\theta')} \times (G)_{\nu>\nu_c} \times \phi(K), \text{ where } \alpha = \frac{\Delta I}{I_o}$$

Since, above the critical frequency, the permanent dipole moments cannot follow the oscillations of the electric field, the contribution of the latter can be neglected:

$$\left[\frac{\partial \alpha}{\partial E^2}\right]_{\substack{E\to O \\ \nu>\nu_c}} = \frac{3}{4P_o(\theta')} \times \frac{\gamma}{3kT} \times \phi(K)$$

Since $\frac{3}{4}P_o(\theta') \cdot \phi(K) \xrightarrow[K\to\infty]{} \frac{1}{2}$, $\gamma = 6kT \left[\frac{\partial \alpha}{\partial E^2}\right]_{E\to o;\ \nu>\nu_c}$

$k = 1{,}38\ 10^{-16}$ erg/°K is the Boltzman constant; if we set T =293°K, we have

$$\gamma \simeq 2\,4 \times 10^{-13} \left[\frac{\partial \alpha}{\partial E^2}\right]_{E\to o;\ \nu>\nu_c} \qquad (2.41a)$$

$[\gamma] = cm^3$; [E] = Statvolt/cm

In MKSA units, we have:

$$\gamma \simeq 2.7 \times 10^{-29} \left[\frac{\partial \alpha}{\partial E^2}\right]_{E\to o;\ \nu>\nu_c} \qquad (2.41b)$$

$[\gamma] = F \times m^2$; [E] = V/m

Equation (2.40) may be used in order to interpret the measurements of the relative scattered intensity change as a function of the angle Ω between the direction of the applied electric field and the bisector of the viewing angle θ'

when the latter is maintained constant. In fact, for $K \ll 1$, equation (2.40) is transformed into /47/:

$$\frac{\Delta I}{I_o} = \frac{1}{45P_o(\theta')} (1 - 3\cos^2\Omega)GK^2E^2 \qquad (2.42)$$

Equation (2.42) may be written in the following manner:

$$(\frac{\Delta I}{I_o}) = (\frac{\Delta I}{I_{o\infty}})F(p,\gamma,E,T) \qquad (2.43a)$$

Where $F(p,\gamma,E,T)$ is the orientation function given by equation (2.13a)(page 21) and

$$(\frac{\Delta I}{I_o})_\infty = \frac{K^2}{9P_o(\theta')} (1 - 3\cos^3\Omega) \qquad (2.43b)$$

The term $(1 - 3\cos^2\Omega)$ is characteristic of rigid macromolecules /58/ for which:

$$\frac{(\Delta I/I_o)_{\Omega=0}}{(\Delta I/I_o)_{\Omega = \frac{\pi}{2}}} = -2. \qquad (2.44)$$

If the macromolecules are deformed by the electric field, the ratio of equation (2.44) is inferior to (-2); thus, equation (2.44) provides information on the mechanical properties of macromolecules in solution.

The case of arbitrary degrees of orientation has been studied by Stoylov/47/. He separately considered the permanent dipole moment orientation mechanism and the induced dipole moment orientation mechanism. The equations derived by Stoylov are restricted to the condition that $K<1$, which implies that observations should be made at small viewing angle θ' (since ℓ must be comparable to λ and even greater than λ otherwise the scattered intensity changes will be too small to measure). The equations derived by Stoylov permit to show that, for rod-like particles, the electro-optic effect for infinitely high electric fields for which it is assumed that molecular alignment is complete, is given by:

$$(\frac{\Delta I}{I_o})_\infty = \frac{1}{P_o(\theta')} \{\frac{\sin(K\cos\Omega)}{K\cos\Omega}\} - 1 \qquad (2.45a)$$

As expected, at saturation orientation, the relative scattered intensity change depends only upon the geometrical properties of the particles and the direction of alignment.

For $\Omega = \frac{\pi}{2}$, equation (2.45a) becomes:

$$(\Delta I/I_o)_\infty = \frac{1}{P_o(\theta')} - 1 \qquad (2.45b)$$

Thus, if complete orientation can be obtained or estimated, this method permits to evaluate the function $P_o(\theta')$, and consequently the square of the average radius of gyration, $\overline{R^2}$, since

$$P_o(\theta') = 1 - \frac{16\pi^2}{3\lambda^2} \overline{R^2} \sin \frac{\theta'}{2}$$

for the values of the viewing angle θ' which approache zero /56,57/.

2.4.3. Light scattering in continuous alternating electric fields

For low degrees of orientation ($U \ll kT$), all molecular models indicate a quadratic dependence of $(\Delta I/I_o)$ on the applied electric field strength /58/. Thus, the behavior of $(\Delta I/I_o)$ will be similar to that of the electric birefringence (or that of the electric linear dichroism): by analogy with electric birefringence equations derived by Peterlin and Stuart /25a/, $(\Delta I/I_o)$ consists of two components, one of which alternates with twice the angular frequency of the applied electric field and the other of which is time-independent (the latter is the value of the electro-optic effect which would be found if a dc field strength equal to $E_o/(2)^{1/2}$ was applied to the suspension, E_o being the maximum amplitude of the alternating field).
H. Plummer and B.R. Jennings have derived a rigorous equation for rodlike particles /58/:

$$\frac{\Delta I}{I_o} = \frac{1}{4} (1 - 3 \cos^2 \Omega) F(K) [S + A^{1/2} \sin (2 \omega t + \phi)] \qquad (2.46a)$$

Where S is the steady component coefficient,

$$S = \frac{(\beta')^2}{1 + (\omega^2/4D^2)} + 2\chi \qquad (2.46b)$$

A is the square of the alternating component coefficient,

$$A = \frac{(\beta')^4 + 4(\beta')^2\chi}{[1 + (\omega^2/4D^2)][1 + (\omega^2/9D^2)]} + \frac{4\chi^2}{1 + (\omega^2/9D^2)} \qquad (2.46c)$$

F(K) is a function of geometrical and optical parameters,

$$F(K) = \frac{1}{3} + \frac{1}{2P_o(\theta')} \left(\frac{\sin 2K}{2K^3} - \frac{1}{K^2}\right) \qquad (2.46d)$$

ϕ is the phase angle between the alternating component of $(\Delta I/I_o)$ and the applied electric field.
In the above expressions, $(\beta')^2 = \frac{p_a^2 - p_b^2}{k^2 T^2} E^2$, $\chi = \frac{\gamma_a - \gamma_b}{2kT} E^2$, where p_a, p_b, γ_a

and γ_b are defined as for Eq.(2.11)(see page 20); D is the rotational diffusion coefficient; $P_0(0')$ and K are defined as for Eq.(2.40) (see page 36).

2.4.4. Determination of electrical and geometrical parameters

The steady-state component, S, must be measured independently. From Eq.(2.46b), it is obvious that from the dispersion dependence of the steady-state electric field light scattering, the permanent dipole moment and induced dipole moment contributions can be isolated.
At low frequencies, both permanent dipole moments and induced dipole moments contribute to the steady-state component. If one plots the curve, $\alpha_{st} = (\Delta I/I_o)_{st}$ vs.E^2, from the initial slope $\{\frac{\partial}{\partial E^2}[\alpha_{st}(E^2)]\}_{E\to o;\nu\to o}$, he may determine the sum of permanent dipole and induced dipole moment contributions.
At high frequencies (above the critical frequency), only induced dipole moments contribute to the steady-state component, S, and then to $(\Delta I/I_o)$. The initial slope, $\{\frac{\partial}{\partial E^2}[\alpha_{st}(E^2)]\}_{E\to o;\nu>\nu_c}$, of the curve $\alpha_{st}(E^2)$ permits one to determine the electric polarizability, γ (see Eq.(2.41)).
As with other electro-optical properties, the rotational diffusion coefficient, D, can be determined from the dispersion curve of the steady-state electric field light scattering. One has to localize the critical frequency, ν_c, for which the permanent dipole moment contribution is half-completed or relaxed, i.e the frequency above which it is assumed that permanent dipole moments cannot follow the oscillations of the applied electric field. For $\omega = \omega_c$, the steady-state component of $(\Delta I/I_o)$ is given by (see Eq.(2.46b)):

$$S(\omega_c) = \frac{(\beta')^2}{1 + (\omega_c^2/4D^2)} + 2\chi$$

Since for $\omega = \omega_c$, the permanent dipole moment contribution is half-completed,

$$\frac{(\beta')^2}{1 + (\omega_c^2/4D^2)} = \frac{(\beta')^2}{2},$$

$$\frac{(\beta')^2}{1 + (\pi^2\nu_c^2/D^2)} = \frac{(\beta')^2}{2},$$

$$2 = 1 + (\pi^2\nu_c^2/D^2)$$

$$D^2 = \pi^2\nu_c^2$$

then, $\nu_c = \frac{D}{\Pi}$. (2.47)

From Eq.(2.47) the rotational diffusion coefficient is obtained.

For monodisperse colloidal suspensions, the rotational diffusion coefficient may be determined from the decay of the electro-optic effect in pulsed electric fields /47,58/:

$$\frac{\Delta I}{I_o} = \frac{\Delta I^\circ}{I_o} e^{-t/\tau} = \frac{\Delta I^\circ}{I_o} e^{-12Dt} \qquad (2.48)$$

Where $(\Delta I^\circ/I_o)$ is the relative scattered intensity change at the time t = o at which the electric field is switched off.

If one knows the rotational diffusion coefficient and the axial ratio of particles (by electron microscopy, for example) by using equations (2.25) or (2.26) (page 25) he can determine the average value of the linear dimensions of dispersed particles.

The case of polydisperse suspensions has been considered by Stoylov /47/. For the decay of the transient phenomena (electric field-induced scattered intensity change), one has a similar expression as Eq.(2.27) (see page 25). If the orientation of particles is complete and if $\Omega = \frac{\pi}{2}$, it is possible not only to determine the average lengths of the different classes of particles but also the relative proportion of each class.

2.4.5. Optically anisotropic particles

The polarizability, γ, is a tensor with principal values γ_1, γ_2, and γ_3 (where 1, 2 and 3 are the orthogonal principal axes of the particle). If the scattering particle is optically anisotropic, then the induced electric dipole in it is not (except at particle's orientations which coincide with the directions of the three principal polarizabilities) parallel to the electric vector of the incident light.

Whereas, for optically isotropic particles, the restriction $(\ell/\lambda) \geq 1$ is indispensable in order to obtain electric field-induced scattered intensity changes large enough to be measured, for optically anisotropic particles, this restriction is no more necessary in order to observe

appreciable electric field-induced scattered intensity changes /57/. The scattered intensity will depend on the state of polarization of the incident light.

The measurement of the relative scattered intensity changes due to infinitely high electric field (which achieve complete orientation) permits to determine the optical anisotropy, δ.
For very small values of K (i.e $K \ll 1$) and when $\Omega = \frac{\pi}{2}$, the dependence of $(\Delta I/I_0)_\infty$ on optical anisotropy is given by /47/:

$$\left(\frac{\Delta I}{I_0}\right)_\infty^{V_v} = \frac{20\,\delta + 16\,\delta^2}{5 + 4\,\delta} \qquad (2.49)$$

Eq.(2.49) is valid for positive optical and positive electrical anisotropies. The symbol V_v means that for an incident light vertically polarized (subscript v), the scattered light is, itself, vertically polarized (capital letter V).
For negative optical and electrical anisotropies, one has the following expression /47/:

$$\left(\frac{\Delta I}{I_0}\right)_\infty^{V_v} = \frac{-10\,\delta + \delta^2}{5 + 4\,\delta} \qquad (2.50)$$

In principle, the knowledge of the optical anisotropy, δ, of dispersed particles provide an important information on their atomic structure.

2.5. Materials and experimental methods

2.5.1. Preparation of chloroplasts

The chloroplasts were prepared following the methods described in references /44,59-63/, using 12 - 14 day old seedlings of green pea plants which had been grown in a greenhouse under sunlight.
A typical preparation consisted of grinding about 9.62g of green pea leaves in about 75ml of a buffer adjusted to pH 7.2 consisting of 2mM Tricine, 330mM Sorbitol and 5mM $MgCl_2$. The resulting homogenate was filtered through several layers of cheesecloth. The filtrate was then centrifuged at 2500 tours/minute for about 1 minute in a JANETZKI K24 ultracentrifuge equiped with a refrigeration system (0°C - 4°C). The sediment of this centrifugation was discarded while the supernatant was centrifuged at 6500 tours/minute for about 7 minutes. The supernatant of this centrifugation was discarded, leaving a pellet of chloroplasts. This pellet was resuspended in about 5ml of a medium containing 2mM Tricine buffer at pH 7.2 and 330mM Sorbitol.

Given that a suspension of chloroplasts is very polydisperse, electro-optic data obtained on such a suspension would be difficult to interpret. One way to obtain more or less homogeneous samples is to break up the chloroplasts, either by chemical methods (by treating chloroplast suspensions with detergents such as the digitonin, the triton X-100, etc...) or by physical methods (ultrasonic treatment of chloroplast suspensions) and then to proceed to the separation of the various sub-chloroplast fragments by differential centrifugation.
Another reason which incited us to break up the chloroplasts is that we tried to prepare open chloroplast fragments similar to purple membrane fragments. Open fragments manifest, in general /51/, much more pronounced electro-optic effects than those obtained using closed fragments.
In the particular case of chloroplasts, the achievement of open fragments would permit to determine the direction of transition dipole moments of the antenna complex pigments, and others with respect to the chloroplast membrane plane.

what was the real aim?

2.5.2. Preparation of sub-chloroplast fragments

a) Sub-chloroplast fragments obtained by digitonin treatment

Immediately after their isolation, chloroplasts were suspended in a medium containing 2mM Tricine pH 7.2 and 330mM Sorbitol. Such a suspension was incubated with 1 % digitonin for 30 minutes in the dark and at a temperature of 4°C. Then, the suspension was centrifuged at 10,000 x g for

20 minutes. The sediment thus obtained was resuspended in a medium containing 2mM Tricine buffer at pH 7.2 and 330mM Sorbitol. This sample has been divided into three categories of sub-chloroplast fragments by differential centrifugation. The first centrifugation, at 1000 x g, lasted 10 minutes; its sediment was resuspended in the suspending medium mentioned above.
We have called this sample, "large chloroplast fragments obtained by digitonin treatment". The supernatant of this first centrifugation was centrifuged at 5000 x g for 30 minutes; thus a second sediment was obtained and we resuspended it in our suspending medium (a medium containing 2mM Tricine buffer at pH 7.2 and 330mM Sorbitol). This fraction constitutes the sample that we call ,"intermediate chloroplast fragments obtained by digitonin treatment". Finally, the supernatant of the second centrifugation has been centrifuged at 5000 x g for 60 minutes. The sediment thus obtained was resuspended in the suspending medium mentioned above; this fraction constitutes the sample that we call, "Small chloroplast fragments obtained by digitonin treatment".

b) Sub-chloroplast fragments obtained by ultrasonic treatment

0.4ml of a concentrated chloroplast suspension were diluted in 9.5ml of a buffer adjusted to pH 7.2 consisting of 2mM Tricine, 330mM sorbitol and 5mM $MgCl_2$. The latter suspension was subjected to ultrasonic treatment for 5 minutes using "the ultrasonic disintegrator UD-11, 22 KHz, 250W". Three categories of sub-chloroplast fragments were separated by differential centrifugation, following the procedure described in the paragraph 2.5.2.a.

c) Sub-chloroplast fragments obtained by Na-deoxycholate treatment

A mixture of 5ml of a chloroplast suspension and 50µl of Na-deoxycholate has been subjected to ultrasonic treatment for 30 seconds. The suspension thus obtained was centrifuged at 5000 x g for 15 minutes and at a short distance fractions, one of small particles (supernatant), and the other of large particles (sediment).
We have prepared two other fractions of sub-chloroplast fragments in the following way: 5ml of a chloroplast suspension was subjected to ultrasonic treatment for 30 seconds , and then separated into two categories of sub-chloroplast fragments, following the procedure described at the paragraph 2.5.2.c.

2.6. Scheme of the apparatus used for electric linear dichroism and electric field light scattering, description of their components and the measurements.

2.6.1. Electric linear dichroism

For electric linear dichroism measurements, we have used either a conventional Perkin-Elmer UV-VIS Spectrophotometer Model 137 UV or a Specord UV-VIS Spectrophotometer, both adapted for electric linear dichroism measurements. The modifications brought about these conventional Spectrophotometers consist to synchronize the signal recording with the application of the electric field.

Below, we present the Scheme of the apparatus used for electric linear dichroism measurements and the description of its components.

Fig. 2.1. Scheme of the apparatus used for electric linear dichroism measurements.

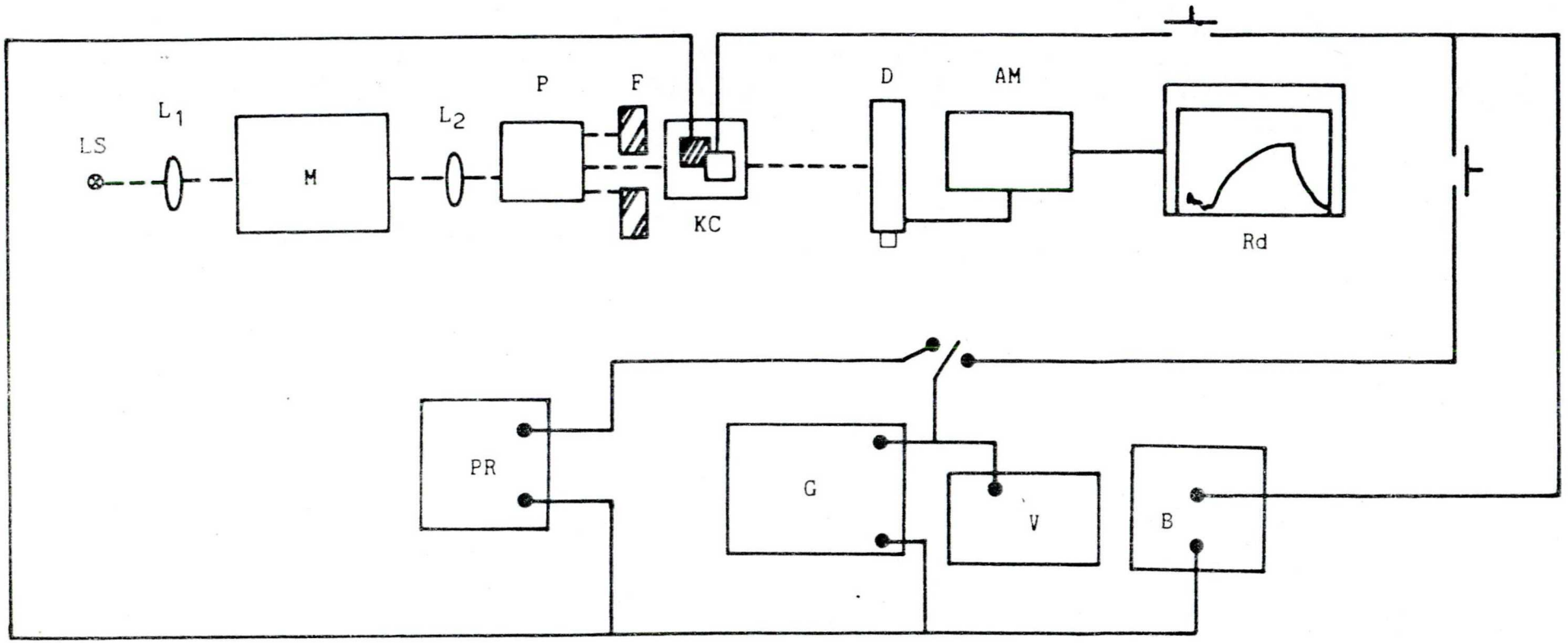

LS = light source; L_1 = focusing lens; M = monochromator; L_2 = collimating lens; P = polarizer; F = slit; KC = Kerr cell; D = detector; AM = amplifier; Rd = recorder; PR = resistance bridge; G = pulsed generator; V = voltmeter; B = bridge for measuring the conductivity of the solution.

Self-made or already done ?

2.6.1.1. Description of the components of the electric linear dichroism's apparatus

1°) Light source (LS) — specifications?

As in almost all conventional spectrophotometers, we used two light sources with their housing and supply: a tungsten lamp for the visible region and a deuterium lamp for the ultraviolet region. The light, focused by the lens, L_1, reached the inlet slit of a grating monochromator, M.

2°) Monochromator (M)

A high luminosity grating monochromator (Schoeffel Model GM 250) was used in order to select the electromagnetic radiation of an appropriate wavelength. We have adjusted the input and exit slits at 3mm and 1mm, respectively, which gives a spectral bandwidth of the order of 6-8nm. Indeed, the monochromator's position is such as its exit slit is located in the focus of a quartz lens, L_2; thus, the light from the exit slit of the monochromator is collimated by the lens, L_2.

3°) Polarizer (P)

Electric linear dichroism measurements require an incident light beam which is polarized, either parallel to the direction of the applied electric field, or perpendicular to it.

The polarizers used must satisfy the following requirements /55/:

(i) A high transmittivity in the wavelength range being investigated;

(ii) The ratio of the intensity transmitted by two crossed polarizing prisms (polarizer and analyser) to the intensity transmitted by the same prisms in the parallel position should be lower than 10^{-4} ($\frac{I_x}{I_{\parallel}} < 10^{-4}$).

In our experiments, the incident light beam was polarized by a Glan prism, and the focused in the Kerr cell (measurement cell).

4°) Kerr cell or measurement cell (KC)

The cell where we have put the colloidal suspension to be investigated consisted of a quartz cuvette in which two vertical platinum electrodes (horizontal electric field) are fitted; the electrodes were parallel to each other and set at a short distance (1.5 - 3 mm) from on onether By applying an appropriate voltage to the electrodes, one obtains a convenient electric field strength. As stressed by meany reaserchers

/46,47/, we have taken great care in the filling of the measurement cell with the sample, in order to avoid the presence of air bubbles which could favour sparking at high electric field strengths.

5°) Pulsed generators (G)

We used a Zopan pulse generator, type PGP-3, in order to generate rectangular electric pulses (10μs to 10ms duration).
For dispersion measurements, pulsed sine-wave electric fields were applied using a GF 11 sine generator (G.D.R.)
The use of electric pulses allows to minimize secondary effects such as the Joule heating, electrophoresis, etc... Besides, the electric pulse techniques permits to study transient phenomena from which relaxation times may be determined.

Indeed, any type of electric pulse generators may be used; however, the following requirements have to be fulfilled /46,47/:

(i) Stability and linearity;

(ii) The time response of the generator, i.e the time constant, RC, characterizing the rise and decay of the electric field must be almost 10 times shorter than the shortest disorientational relaxation time of the dispersed particles. The values of the capacitance of the last filter of the generator and its internal resistance have to be appropriately selected in order to fulfill the limitation concerning the time constants for the rise and decay of the electric field; residual capacitances of the cell circuit and its resistance must be minimized.

(iii) It is necessary to have an auxiliary device which permits to control the amplitude and form of the electric field in the macromolecular solution (or colloidal suspension) especially during the time when the electric field is switched on.

(iv) For a colloidal suspension of very small particles, it is necessary to use electric pulses of very high voltage in order to obtain an orientational electro-optic effect sufficient to be measured.

6°) A photomultiplier for the detection of the optical signal (D)

The specific parallel or perpendicular dichroism is measured as a change of weak light intensity (see next section). The optical signal from the Kerr cell is transformed into an electric signal by a relatively sensitive photomultiplier, the RCA 1P28 photomultiplier, and its load circuit.
This photomultiplier was powered by a d.c. high voltage source which was stabilized by high quality electronic voltage stabilizers (FEU-35, USSR).
After a suitable amplification, the transient electric signal was recorded by an X - Y recorder.

2.6.1.2. Electric linear dichroism measurements

(a) Experimental conditions

The concentration of the colloidal suspension (suspension of chloroplasts or that of sub-chloroplast fragments) to be investigated has been adjusted so that the absorbance in the absence of the electric field was about 0.3 to 1.2. In order to obtain a colloidal suspension of low conductivity, chloroplasts or sub-chloroplast fragments were suspended in a buffer of low ionic strength (2mM Tricine buffer at pH 7.2 and 330mM Sorbitol) and finally this suspension was very diluted using bidistilled water. not defined the final ionic strength

The main reasons to use a suspension of very low conductivity are /46,47,55/:

(i) Minimize the Joule heating effects;

(ii) Minimize the disturbing effects of electrode polarization;

(iii) Assure a greater electric polarizability in so far as the greater part of its value is of interfacial nature.

Our experiments of electric linear dichroism were carried out on chloroplast or sub-chloroplast suspensions with conductivity's values ranging from $10^{-4}\ \Omega^{-1}\ cm^{-1}$ to $10^{-3}\ \Omega^{-1}\ cm^{-1}$.

The pH of all suspensions was adjusted at about 7.2 after dilution? pH buffering at low ionic strength?

(b) Experimental procedure

The scheme of the apparatus used for electric linear dichroism measurements is presented on Fig.2.1 (page 46). The incident light beam was polarized, either parallel to the direction of the applied electric field, or perpendicular to it.

For each state of the incident light beam polarization, we have directly measured the optical density, O.D., of chloroplast suspensions or sub-chloroplast fragment suspensions, in the absence and presence of the electric field, respectively. We assume that the optical density, O.D., is equal to the optical absorbance, A. The ratio of the transmittances permits to determine the electric linear dichroism. In fact:

$$(O.D.)_{\parallel} = A_{\parallel} = -\log \frac{I_E^{\parallel}}{I_o} = -\log T_E^{\parallel}$$

$$(O.D.)_{\perp} = A_{\perp} = -\log \frac{I_E^{\perp}}{I_o} = -\log T_E^{\perp} \qquad (2.48)$$

$$(O.D.) = A_o = -\log \frac{I}{I_o} = -\log T$$

Where I_o is the light intensity impinging on the Kerr cell; I is the light intensity transmitted by the solution in the absence of the electric field;

$I_E^{\parallel}$ and $I_E^{\perp}$ are the light intensities transmitted by the solution in the presence of the electric field when the incident light beam is polarized parallel to the direction of the applied electric field and perpendicular to it, respectively; $T_E^{\parallel}$ and $T_E^{\perp}$ are transmittances of the solution in the presence of the electric field, for parallel and perpendicular polarized light, respectively; and T is the transmittance of the solution in the absence of the electric field (transmittance of the isotropic solution).

$$\Delta A_{\parallel} = A_{\parallel} - A_0 = \log \frac{T}{T_E^{\parallel}}$$

$$\Delta A_{\perp} = A_{\perp} - A_0 = \log \frac{T}{T_E^{\perp}} \qquad (2.49)$$

Since, according to Eq.(2.18)(page 22), $\Delta A = 1.5 \Delta A_{\parallel} = -3 \Delta A_{\perp}$, one has:

$$\Delta A = 1.5 \log \frac{T}{T_E^{\parallel}} = -3 \log \frac{T}{T_E^{\perp}} \qquad (2.50)$$

In our measurements, both the two spectrophotometers used were adjusted so that the transmittances of the sample were included between 80 % and 100 %. The measurement of T and T_E for one state of the incident light polarization, with respect to the applied electric field, suffices in order to determine the electric linear dichroism, ΔA.
However, for sensitivity reasons, it is preferable to measure the electric field induced change of absorbance for polarization direction parallel to the applied electric field /46/.

2.6.2. Electric field light scattering

In order to measure the relative scattered intensity changes resulting from the application of an electric field across a suspension of chloroplasts or a suspension of sub-chloroplast fragments, we have used either an apparatus with a fixed angle of observation of 90° described by Stoylov /47/, or a Russian-made light-scattering apparatus, FPS-3 (angle of observation varying between 30° and 150°), which was adapted to electric field light scattering measurements.
The scheme below (Fig.2.2) indicates the principal components of the electric field light scattering experimental apparatus.

Fig.2.2. Scheme of the apparatus used for electric field light scattering.

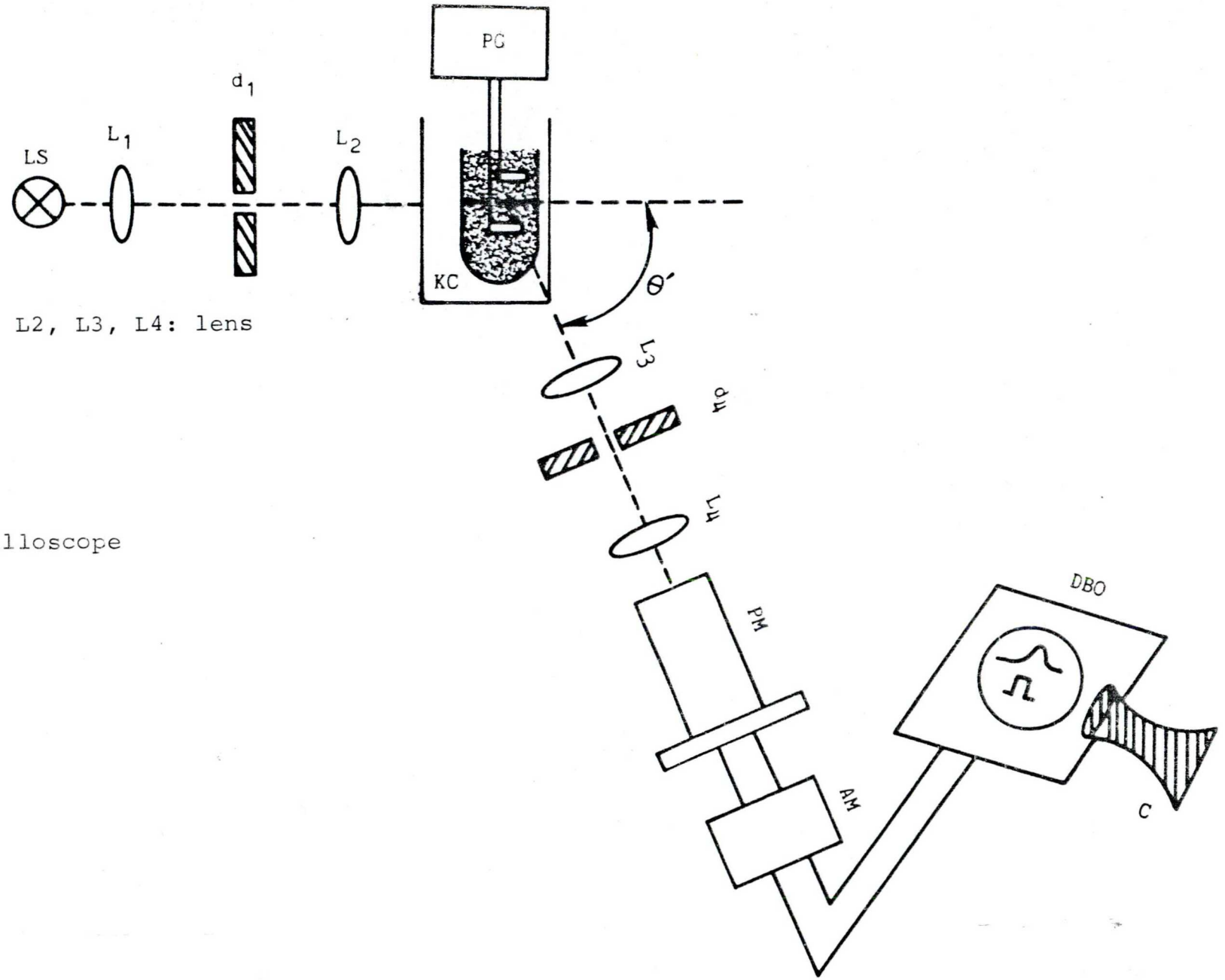

LS = Light source; L1, L2, L3, L4: lens
d1, d2 = Diaphragms
KC = Kerr cell
PG = Pulse generator
PM = Photomultiplier
AM = Amplifier
DBO = Double beam oscilloscope
C = Camera

2.6.2.1. Description of the main components of the electric field light scattering experimental apparatus.

1°) Light Source (LS)

We have used a helium-neon laser (Spectra-Physics, Model 125; λ = 632.8nm) Neutral density filters were used in conjunction to attenuate the incident intensity to an appropriate level.

2°) Kerr cell or measurement cell (KC)

All were used?

We have used four types of cells schematized in Fig.2.3.

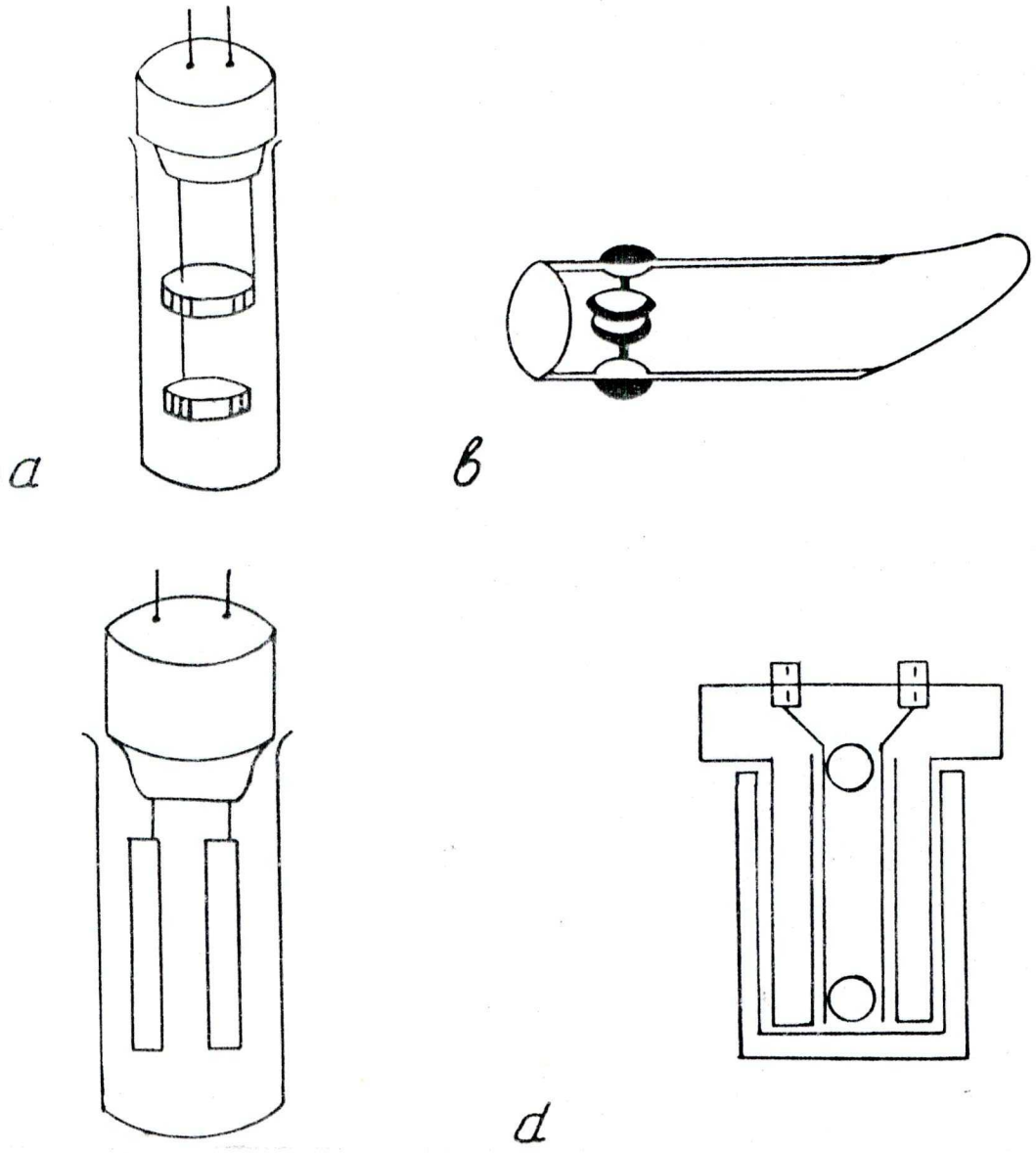

Fig.2.3. Cells used in our electro-optic measurements

a) Light scattering cylindrical cell; the electrodes are two horizontal discs- vertical electric field. The viewing angle θ' may be varied but Ω has a fixed value of 90°.
b) Light scattering cell with an optical horn and horizontal disc electrodes - vertical electric field. The viewing angle θ' is fixed at 90°.
c) Light scattering cylindrical cell with vertical electrodes - horizontal electric field. The angles θ' and Ω are variable.
d) Rectangular cell with vertical electrodes. This electro-optic cell has been used in the two spectrophotometers used for electric linear dichroism measurements.

3°) Pulse generator (PG) Is it necessary even to mention?

Electric generators used for the electric field light scattering investigations present similar requirements as those used for electric linear dichroism studies (see paragraph 2.6.1, page 48). In our electric field light scattering measurements, we have used a commercially available electric pulse generator, "Cober Electronics, Model 605 P".

4°) Signal detection and recording

The transient "light signal" scattered at an angle θ' is collected by an appropriate optical system and it is brought to the photocathode of a very sensitive photomultiplier (e.g., EMI 9558Q). The role of this photomultiplier is to convert the transient optical signal into a transient electric signal. The photomultiplier was supplied by a d.c. high voltage source which was stabilized by high quality electronic voltage stabilizers (FEU-35,USSR). After a suitable amplification, the transient electric signal was displayed on a double-beam storage oscilloscope (TR 4653, Hungary) together with the attenuated electric pulses. This oscilloscope has a good amplification and a good sensitivity (1mV/div $\leq$ S $\leq$ 25mV/div). The attenuation of the electric pulse signals was achieved by means of a calibrated resistor bridge. Photographs of the oscilloscope transient signals were taken with a suitable camera. We have analysed the cliché of the photos thus obtained in order to determine the electric and hydrodynamic parameters of chloroplasts or those of sub-chloroplast fragments.

2.6.2.2. Measurements

We have measured the intensity I_o scattered in the absence of the electric field for various values of the viewing angle θ'. For the same values of θ' and different values of Ω, we have applied across a suspension of chloroplasts or a suspension of sub-chloroplast fragments an electric pulse consisting of several oscillations of a sine wave and we have measured the intensity, I_E, scattered in the presence of the electric field. The scattered intensity change is $\Delta I = I_E - I_o$. We have recorded I_o and ΔI for a required set of conditions of θ', Ω and E, following the procedure described by Fredericq and Houssier /46/. For the measurement of the intensity I_o scattered in the absence of the electric field, we use the oscilloscope in the conventional mode. Its time base is set in "free run" (no triggering and the highest frequency scale, e.g., 50µs/div). The intensity I_o is proportional to the distance between two continuous horizontal traces observed on the oscilloscope screen, one of the traces presenting

the position of the oscilloscope trace when the shutter of the photomultiplier is closed and the other, the oscilloscope trace when the shutter of the photomultiplier is opened. For the measurement of the scattered intensity changes, the oscilloscope functions in the "memory mode" and a lowest frequency scale (e.g., 0.5s/div) is chosen. The oscilloscope is set in the external triggering position. The shutter of the photomultiplier is opened. With the polarity-reversing switch in the ON - position, an electric pulse is manually initiated with the Model 605P Cober Electronics pulse generator and applied to a suspension. The resulting photocurrent signal appears on the oscilloscope screen. Generally, in order to be better compared to I_0, the photocurrent signal has been amplified (by adjusting the amplification factor or sensibility of the oscilloscope).

For a given value of θ', we have measured the scattered intensity changes as a function of the applied electric field strength. This measurement permitted us to obtain the graphs $(\frac{\Delta I}{I_0})$ vs.E^2 from which we have determined the electric parameters of chloroplasts or those of sub-chloroplast fragments.

We have estimated the disorientational relaxation times of chloroplasts or those of sub-chloroplast fragments from the decay curve of the photocurrent signal after switching off the electric field. In fact, assuming that each suspension investigated is monodisperse, we have:

$$\Delta I_d(t) = \Delta I^\circ \, e^{-t/\tau}$$

$$\Delta I_d(\tau) = \frac{\Delta I^\circ}{e} = \frac{\Delta I^\circ}{2.718} \simeq \frac{\Delta I^\circ}{3} \qquad (2.51)$$

Where ΔI° is the value of ΔI at the time t = o as the electric field is switched off.

2.7. Results and discussions

2.7.1. Electric linear dichroism

The orientation of whole green pea chloroplasts or that of green pea chloroplast large fragments is observed in a series of rectangular pulses for field strengths as low as $20V.cm^{-1}$ and complete orientation is achieved at about $60V.cm^{-1}$ (see fig.2.4.). Our absorption spectrum (fig.2.5., page 56) of whole chloroplasts suspended in a medium containing 2mM Tricine buffer at pH 7.2 and 330mM sorbitol is similar to that obtained by Gagliano et al./45/. The characteristic absorption spectrum of whole chloroplasts and those fragmented by the Na-deoxycholate are compared in Fig.2.6. There is a slight shift in the absorption peak from 14600 cm^{-1} for whole chloroplasts to 14720 cm^{-1} for the chloroplast fragments. Otherwise the qualitative aspects of the absorption spectrum are independent of the particle size and the conclusion of Gagliano et al./45/ is confirmed: form dichroism plays no substantial role in our measurements.

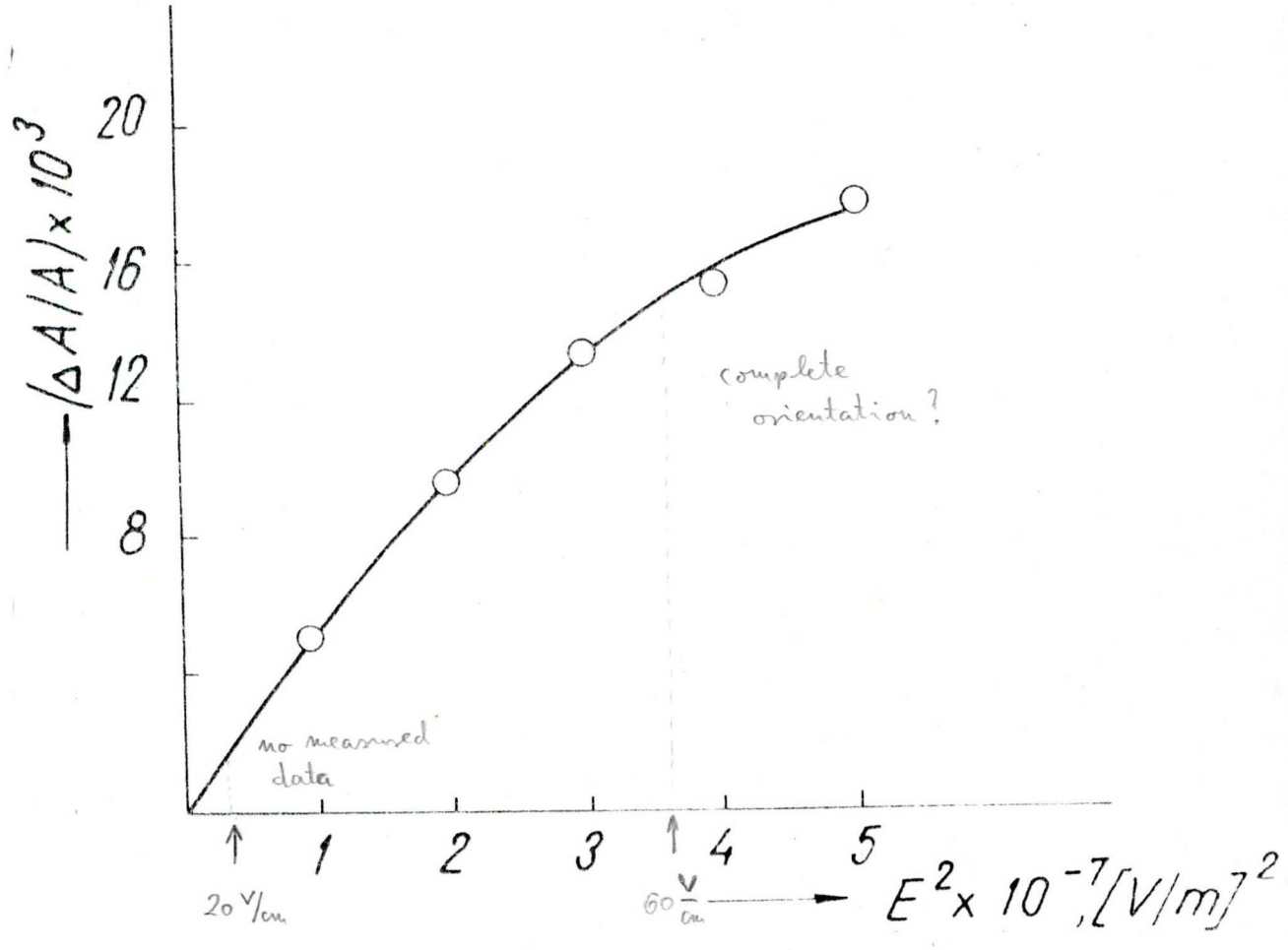

Fig.2.4. Dependence of the specific parallel dichroism on the square of the electric field-strength ($\frac{\Delta A_{\parallel}}{A} = f(E^2)$) for chloroplasts suspended in a medium containing 2mM Tricine buffer at pH 7.2 and 330mM sorbitol. ν = 1 KHz; λ = 680nm.

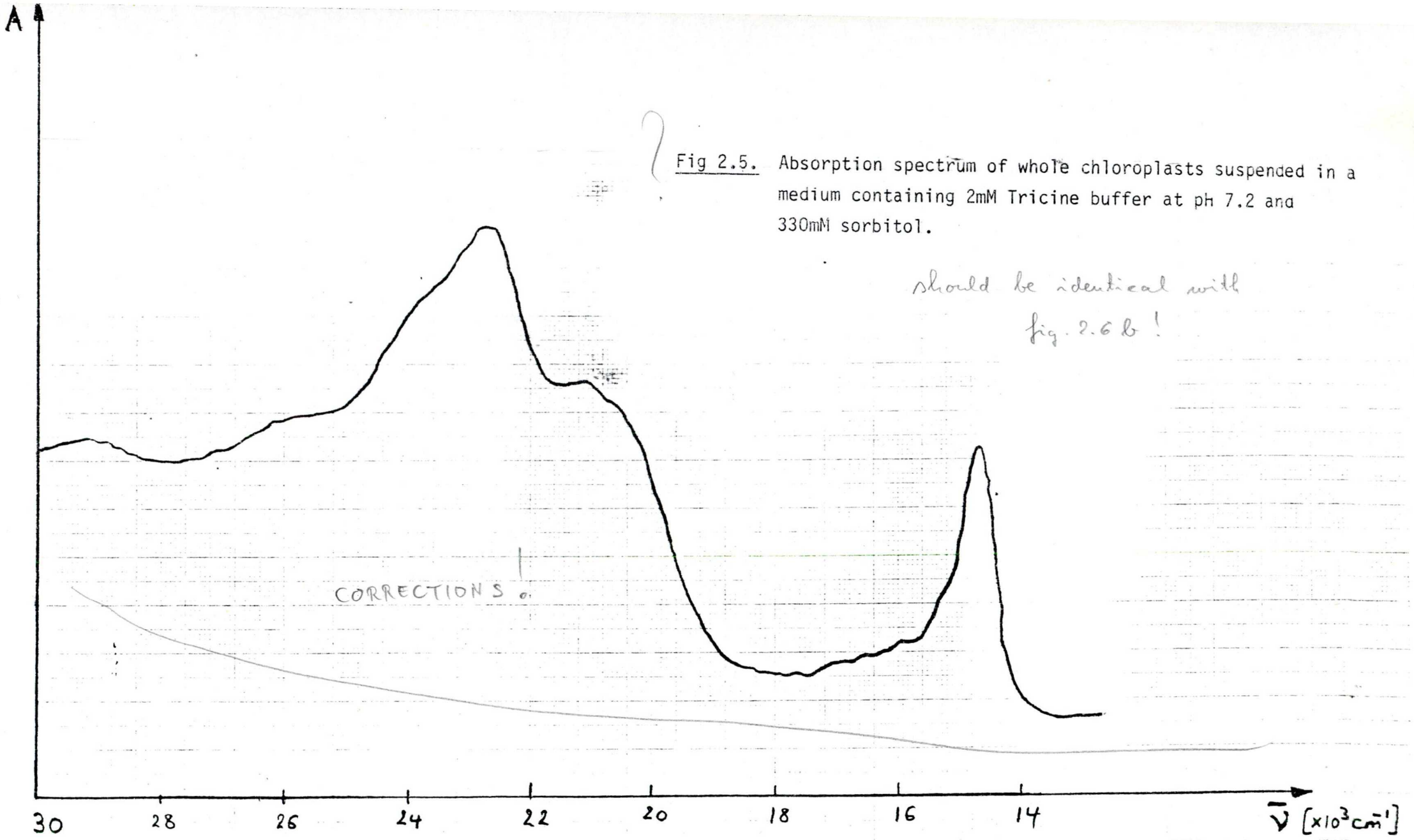

Fig 2.5. Absorption spectrum of whole chloroplasts suspended in a medium containing 2mM Tricine buffer at pH 7.2 and 330mM sorbitol.

should be identical with fig. 2.6b!

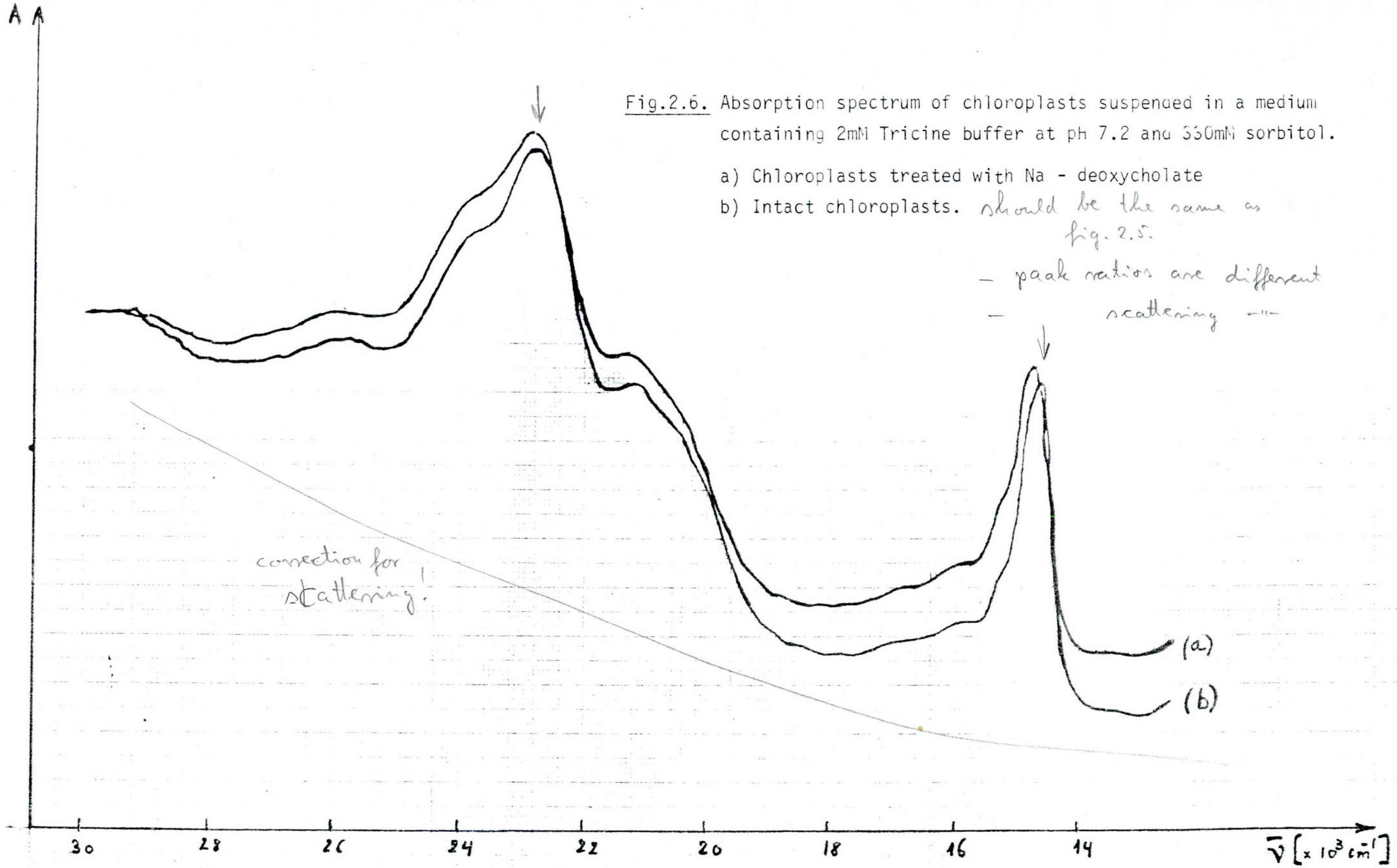

Fig.2.6. Absorption spectrum of chloroplasts suspended in a medium containing 2mM Tricine buffer at pH 7.2 and 330mM sorbitol.

a) Chloroplasts treated with Na - deoxycholate

b) Intact chloroplasts. should be the same as fig. 2.5.

– paak ratios are different

– scattering –"–

The dependence of the specific electric dichroism at 680nm on the square of the electric field-strength is presented in Fig.2.4. (for whole chloroplasts) and in Fig.2.7 to Fig.2.10 (for chloroplast fragments). Assuming that at the frequency of 2KHz, the permanent dipole moments cannot follow the oscillations of the electric field, from Figs.2.7. and 2.8., we determine the approximative value of the electric polarisability for chloroplasts suspensions ultrasonicated for 30s. We assume that at the beginning of the non-linear dependence of $(\Delta A_{\parallel}/A_0)$ or $(\Delta A_{\perp}/A_0)$ on the square of the electric field-strength, the potential energy of induced electric dipole moments is in the order of kT (where k is the Boltzmann constant and T the absolute temperature):

$$\frac{U_{or}}{kT} \simeq 1, \text{ i.e } \frac{\gamma E_{int}^2}{2kT} = 1, \text{ or } \gamma = \frac{2kT}{E_{int}^2}$$

The approximate value of the square of the intermediate electric field extrapolated in Figs.2.7 and 2.8 is $3.6 \times 10^3 (V/cm)^2$, or $4 \times 10^{-2} (Statvolt)^2 \times cm^{-2}$. Consequently, the polarizability γ is approximately equal to 2×10^{-12} cm^3 (at usual temperatures, e.g., T = 293°K).

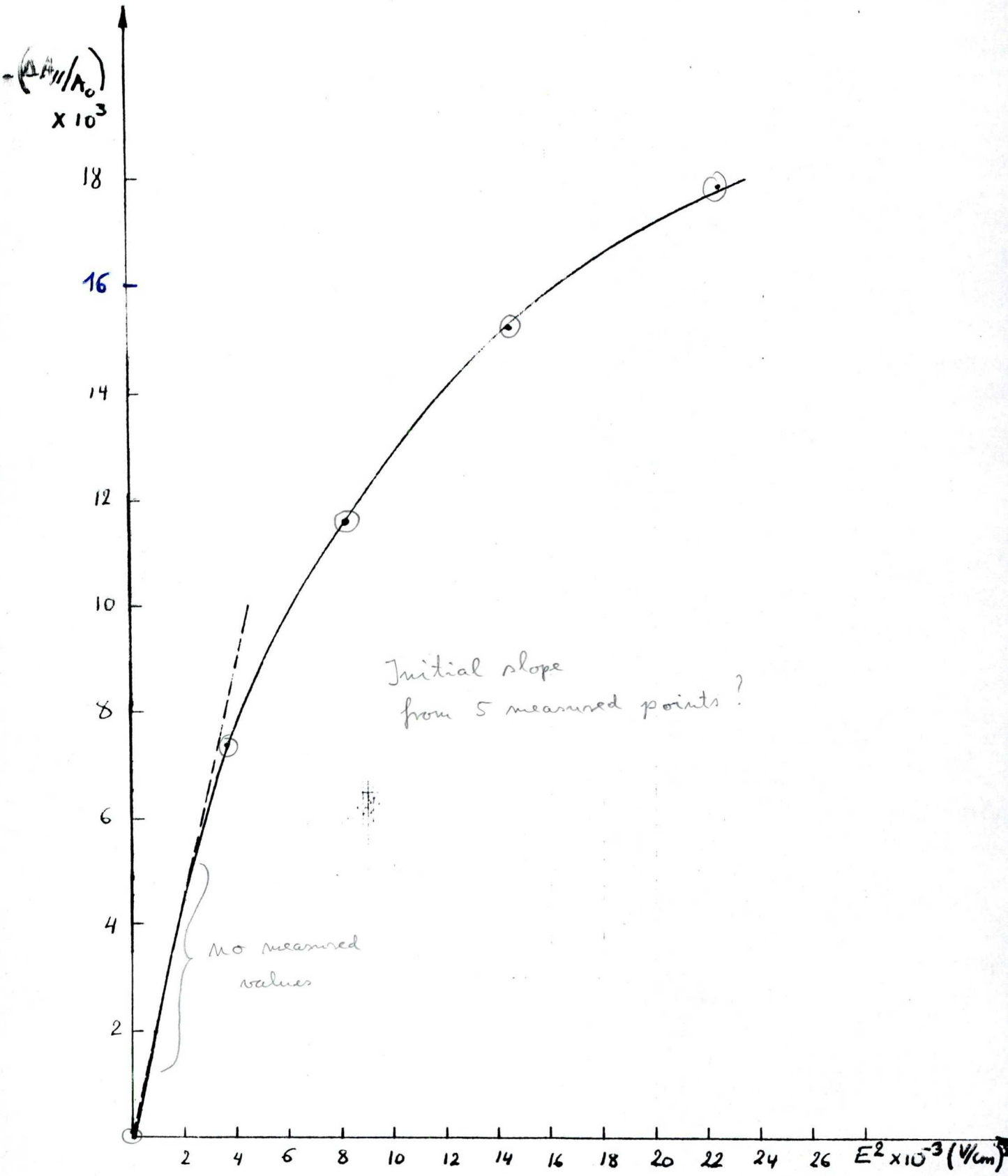

Fig.2.7 Dependence of the specific parallel dichroism on the square of the electric field-strength ($\frac{\Delta A_{//}}{A_o} = f(E^2)$) for chloroplasts ultrasonicated during 30s. ν = 2 KHz. $\lambda = {}^{o}680$nm. Suspension of chloroplast fragments in a medium containing 2mM Tricine buffer at pH 7.2 and 330mM sorbitol. The broken line indicates the initial slope.

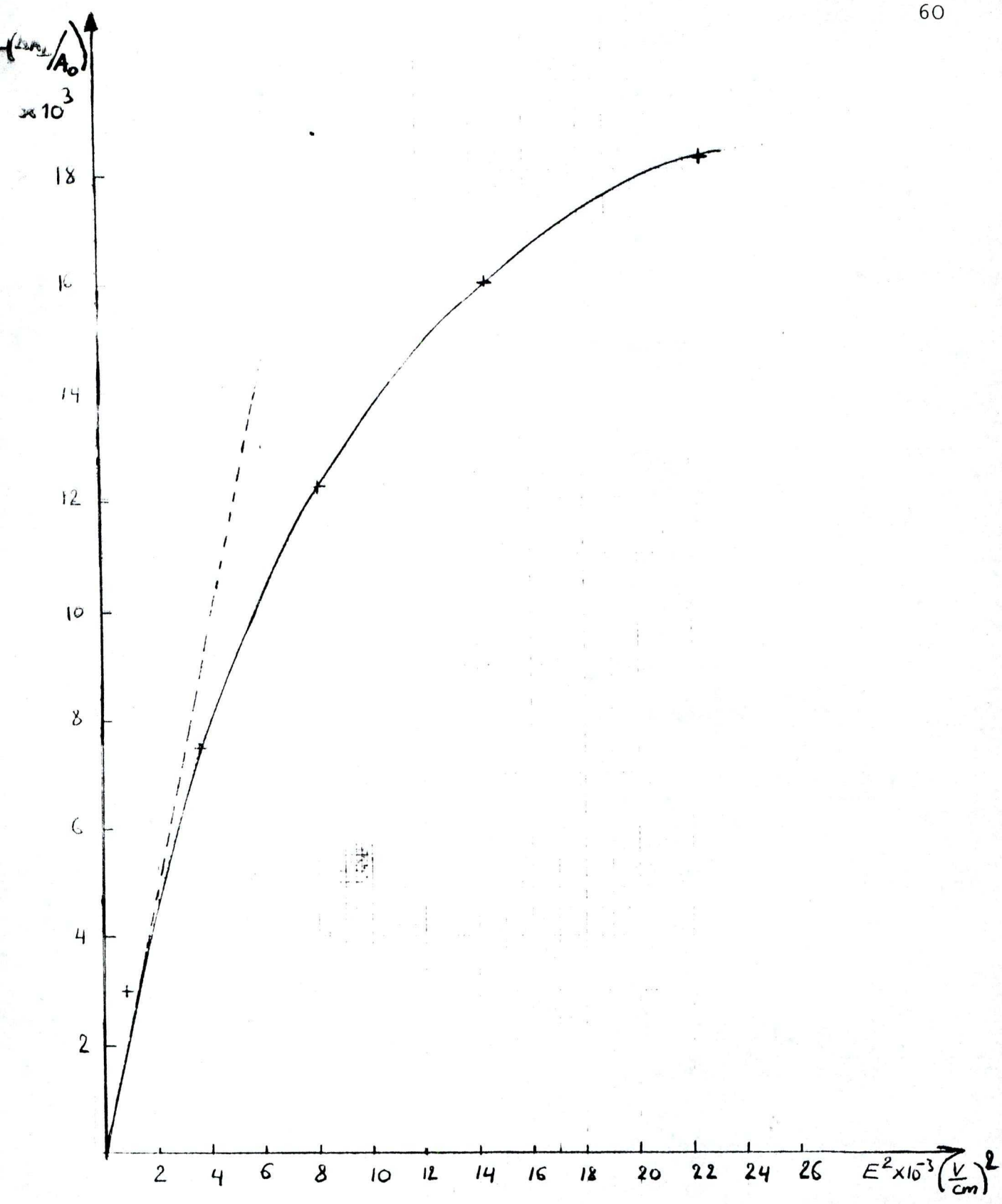

Fig.2.8 Dependence of the specific perpendicular dichroism on the square of the electric field-strength ($\frac{\Delta A_\perp}{A_o} = f(E^2)$) for chloroplasts ultrasonicated during 30s. ν = 2 KHz. $\lambda = {}^{o}$680 nm. Suspension of chloroplast fragments in a medium containing 2mM Tricine buffer at pH 7.2 and 330mM sorbitol. The broken line indicates the initial slope.

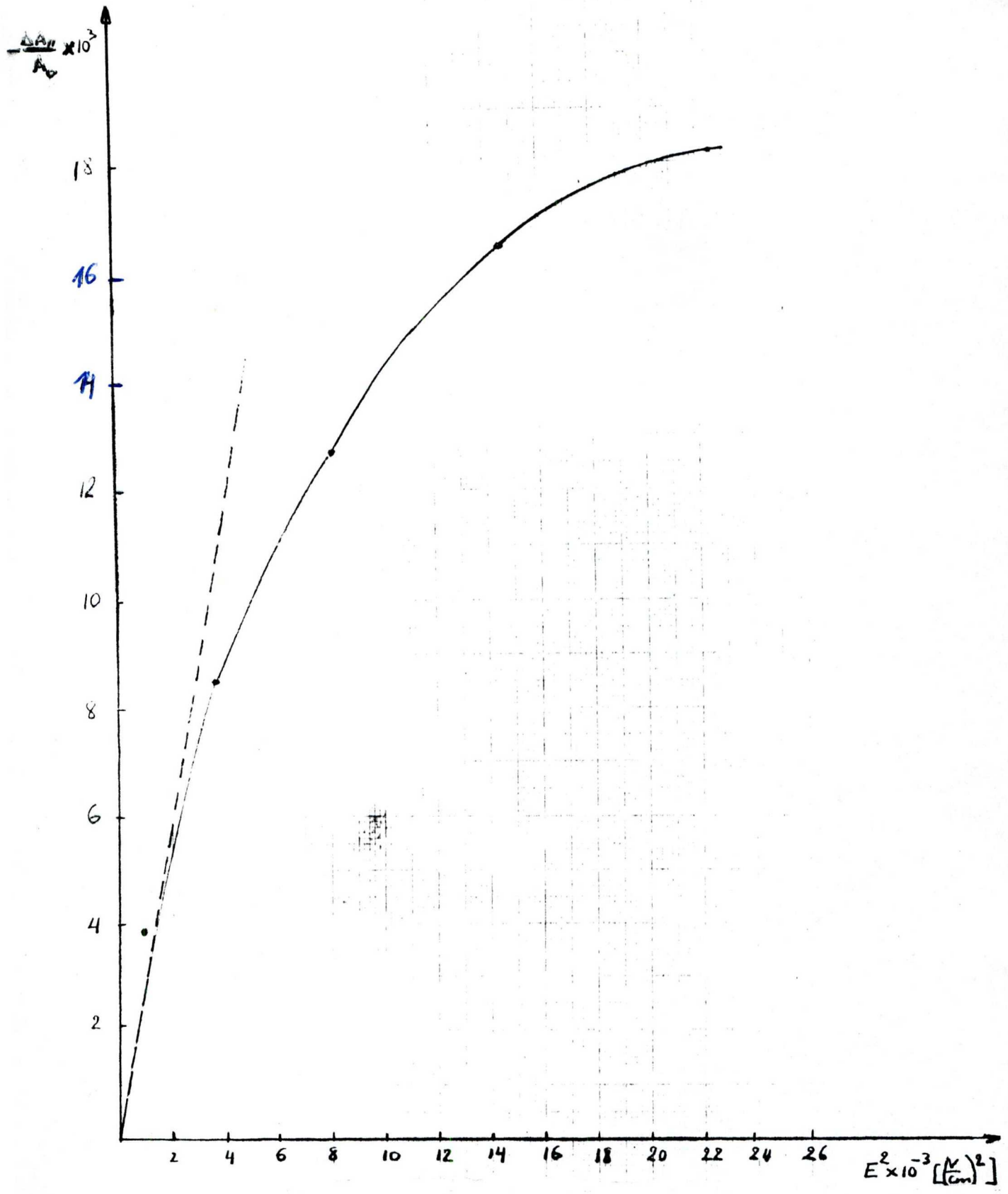

Fig.2.9 Dependence of the specific parallel dichroism on the square of the electric field-strength ($\frac{\Delta A_{//}}{A_0} = f(E^2)$) for chloroplasts ultrasonicated during 30s. ν = 200Hz. λ = 680nm. Suspension of chloroplast fragments in a medium containing 2mM Tricine buffer at pH 7.2 and 330mM sorbitol. The broken line indicates the initial slope.

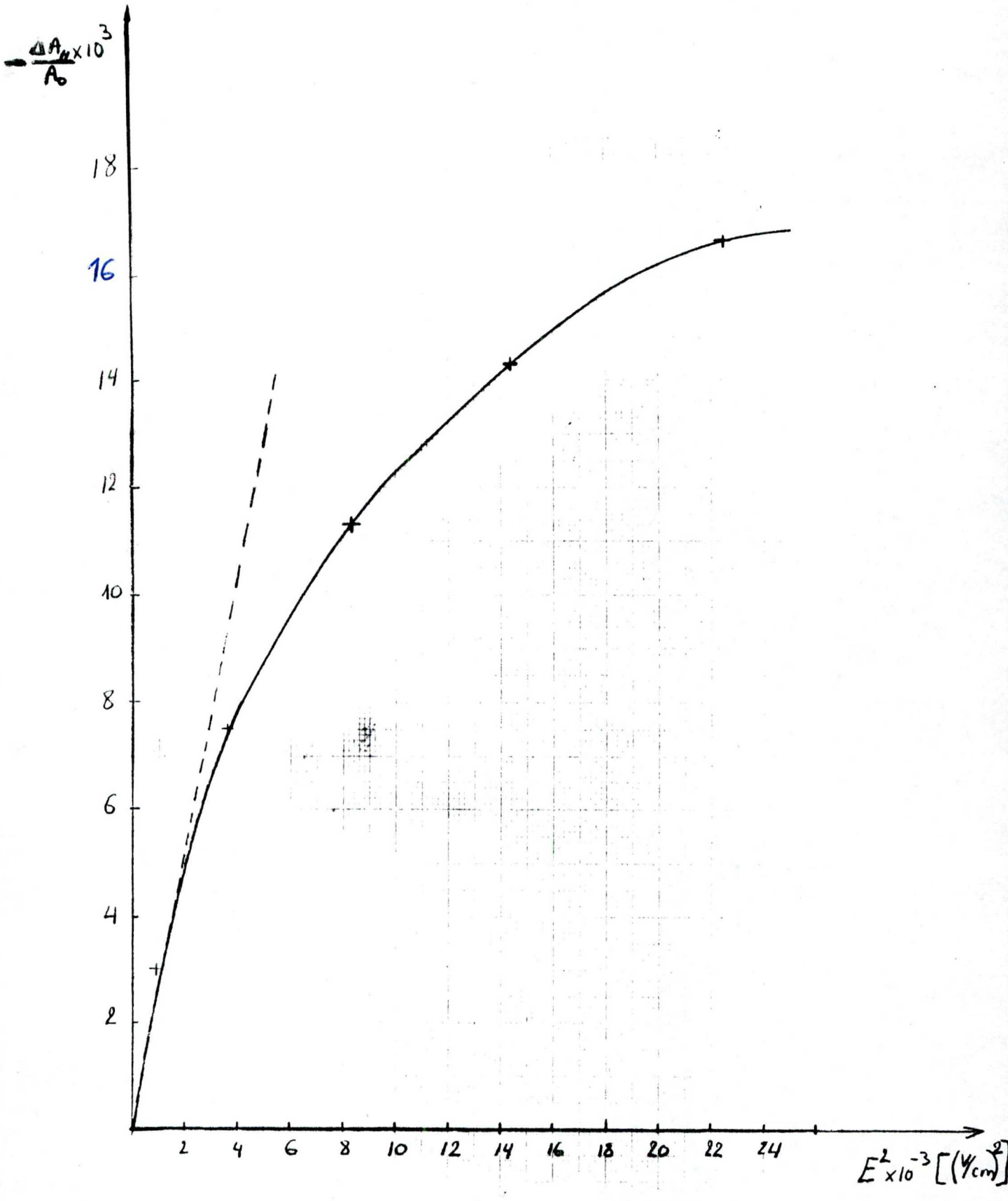

Fig.2.10 Dependence of specific parallel dichroism on the square of the electric field-strength ($\frac{\Delta A_{//}}{A_0} = f(E^2)$) for chloroplasts ultrasonicated during 30s. λ = 680nm. ν^0 = 20Hz. Suspension of chloroplast fragments in a medium containing 2mM Tricine buffer at pH 7.2 and 330mM sorbitol. The broken line indicates the initial slope.

Electric linear dichroism measurements are perturbed by secondary effects such as form dichroism and light scattering effects which deform the photocurrent signal. Our electric linear dichroism measurements showed that the effects of light scattering prevailed whenever whole chloroplasts and large chloroplast fragments were studied, which did not permit us to determine the direction of the transition dipole moment with respect to the chloroplast membrane plane. Another obstacle to the determination of the direction of the transition dipole moment was due to the fact that the chloroplast fragments remain closed (whatever be the fragmentation method used) such as it is shown by an electron micrograph of the morphological structure of chloroplast fragments (Fig.2.14., page 67). However, for all other purposes, these studies could be equally exploited. The general impression is that the electric linear dichroism's values obtained for chloroplast large fragments are considerably lower than those obtained for purple membrane fragments /50/. The results obtained for the whole chloroplasts and the chloroplast large fragments are in agreement with those obtained by other workers /45,65-67/: magnitude of the electro-optic effects, absorption spectrums, relaxation times, frequency dependence of the electro-optic effect,etc.

Fig.2.11 shows a typical curve for the frequency dependence of the specific parallel dichroism in the frequency range 20Hz - 100kHz. The measurements were made at a value of the electric field-strength equal to 4.5×10^3 V/m. At this value of the electric field strength, $(\Delta A_{\parallel}/A)$ is on the linear part of the curve $(\Delta A_{\parallel}/A) = f(E^2)$, so that the condition of low degrees of orientation is fulfilled ($U \ll kT$).

On the dispersion curve, it is seen that several dispersions can be followed, which corresponds to what has already been observed /65-67/. The interpretation of these dispersions is premature since a more detailed experimental study is necessary for this. At present, only an average value for the electric polarizability's relaxation time was estimated from the relationship $\tau = \frac{1}{2\pi\nu_c}$, where ν_c is the frequency at which the electro-optic effect is half-completed or relaxed and τ is the relaxation time of the electric membrane charge or the time required by the latter to reach an equilibrium distribution after the disappearing of an external perturbation. The mean value obtained is: $\tau = 6 \times 10^{-5}$s. An electric polarizability's relaxation time of this order of magnitude (frequency $\nu_c = 2.6 \times 10^3$ Hz) is characteristic of the interfacial charge dynamics. We conclude in qualitative manner that the structure of chloroplast membranes (or that of chloroplast large fragments) is similar to the structure of polyelectrolytes or macroions around which are located small ions or counterions. In this case, there would be a strong electrostatic interaction between the polar head groups of the chloroplast membrane constituent molecules

and the counterions and the latter would form a diffuse electric double layer/25b/. We think that this diffuse electric double layer may play a fundamental role in the spatial separation, by the thylakoid membrane, of the photoproducts of the photochemical step of natural photosynthesis. The orientation of chloroplasts or that of chloroplast large fragments in an electric field is due to the induced interfacial polarization (polarization due to the deformation of the diffuse electric double layer by the electric field). In the case of purple membrane fragments, Dunne et al./97/ suggest that the observed electric polarizability would be due to the coherent oscillations of electrons of bacteriorhodopsine molecules within these fragments. We have made complementary experiments in which we have varied the pH or the ionic strength of chloroplast fragment suspensions. We have ascertained that the electric polarizability increased when the ionic strength of chloroplast fragment suspensions decreased: this has indicated to us that the measured electric polarizability was of interfacial nature.

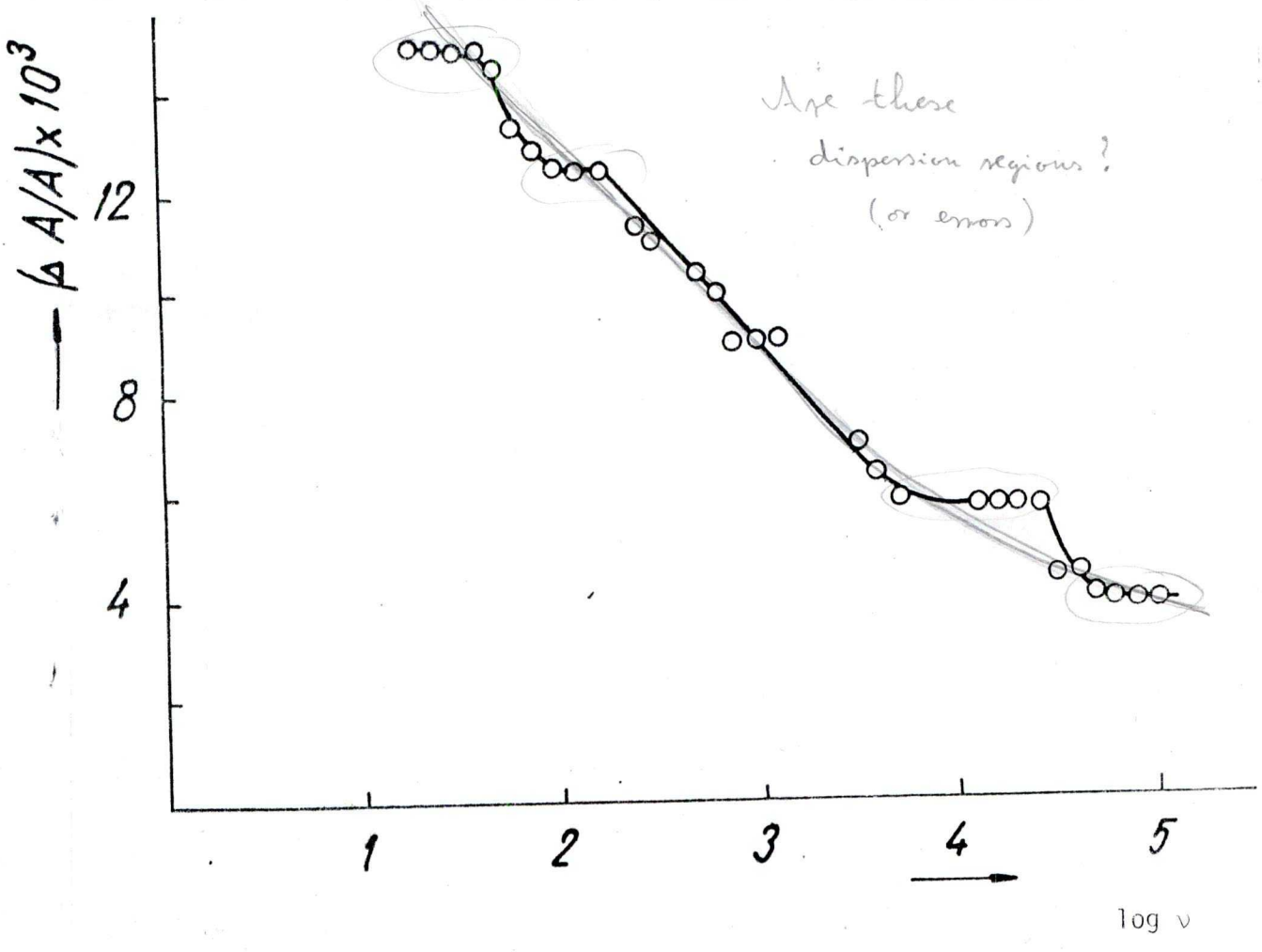

Fig.2.11 Dependence of the specific parallel dichroism on the frequency of the electric field ($\frac{\Delta A}{A} = f(\log \nu)$) for chloroplast large fragments suspended in a medium containing 2mM Tricine buffer at pH 7.2 and 330mM sorbitol. $E = 4.5 \times 10^3$ V/m. $\lambda = 680$nm.

The time dependence of the electric linear dichroism induced by a rectangular voltage pulse in a suspension of whole chloroplasts is shown in Fig.2.12. Since the rise of this electro-optic effect is slower than its decay, referring to the techniques discussed by O'Konski et al./25/, Fredericq and Houssier /46/ (see page 27), we conclude in qualitative manner that permanent dipole moments contribute to the mechanism of orientation. In a quite good agreement with the observations of Gagliano et al./45/, there is also a residual signal which persists for times longer than 5-10ms after the field has been switched off. This component may be due to the polydispersity of the chloroplast suspension. The relaxation time estimated in Fig.2.12 is: τ = 25s.

compare page 69

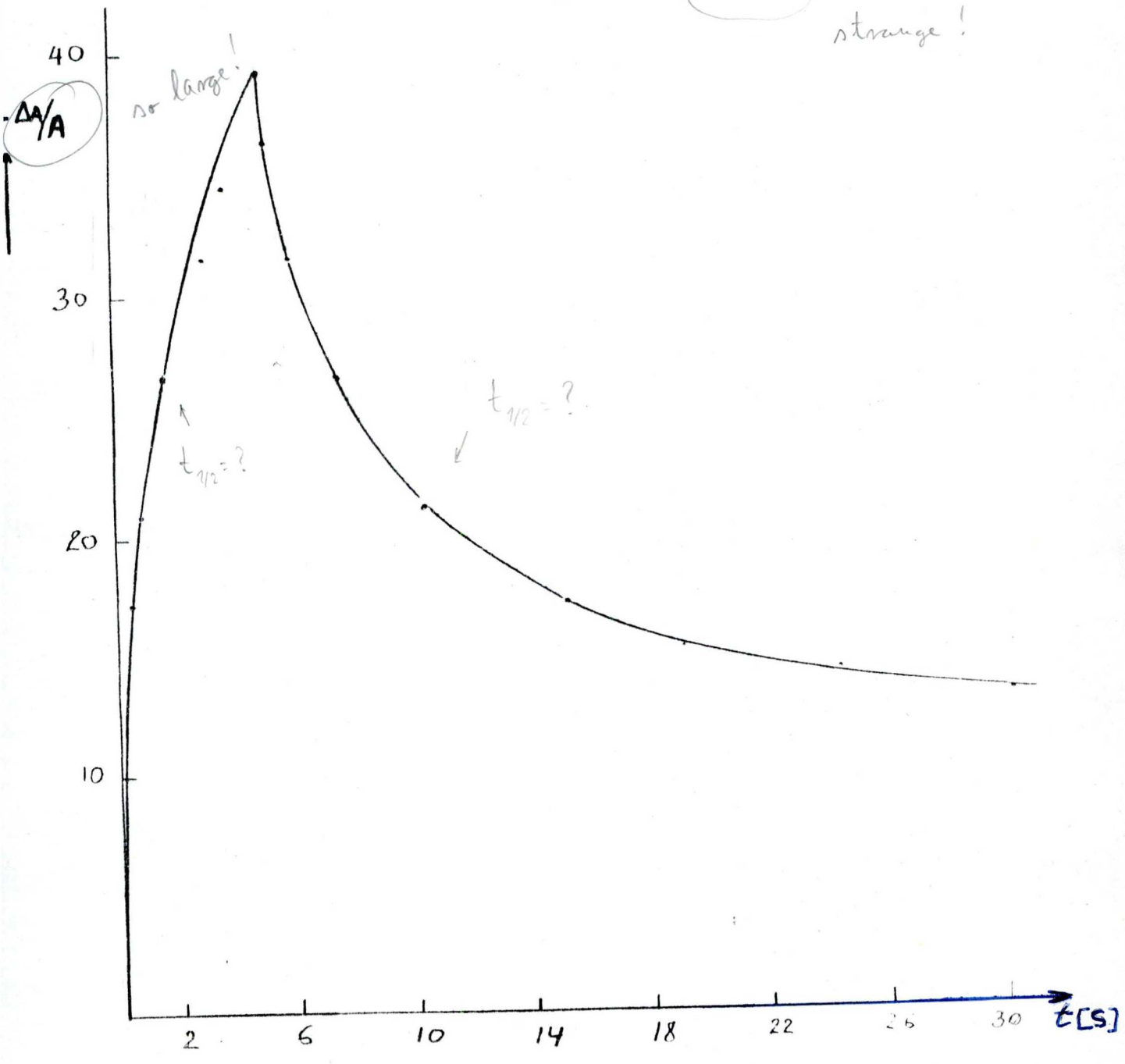

Fig.2.12 Transient electric linear dichroism signal induced by a rectangular voltage pulse in a suspension of whole chloroplasts suspended in a medium containing 2mM Tricine buffer at pH 7.2 and 330mM sorbitol. E = 120V/cm, ν = 2KHz; λ = 680nm.

2.7.2. Electric field light scattering

A typical oscillogram of a transient electric field-induced scattered intensity change from a suspension of chloroplasts or that of sub-chloroplast fragments is shown in Fig.2.13. The measurements were made using suspensions of very low ionic strength (final solvent = 2mM Tricine buffer + 330mM Sorbitol + bidistilled water, pH 7.2) and in the frequency range 20Hz - 200 kHz.

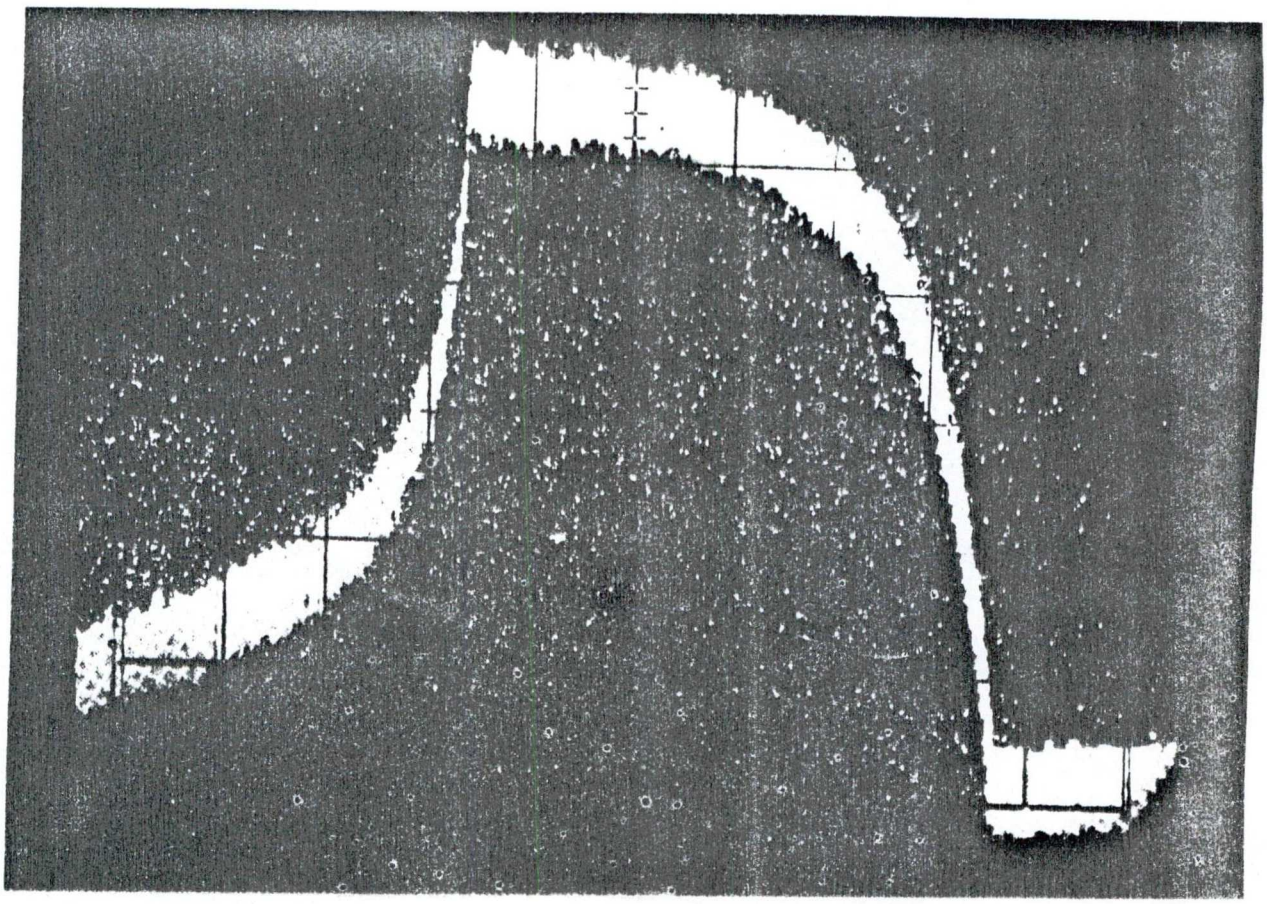

Fig.2.13 Oscillogram of a transient electric field-induced scattered intensity change from a very diluted suspension of chloroplast fragments. Chloroplast fragments were prepared by subjecting whole chloroplasts to ultrasonic treatment. The suspension was submitted to an electric pulse consisting of several oscillations of a sine wave. E = 200V/cm, ν = 1KHz; time base = 50ms/div; sensibility = 5mV/div; λ = 632.8nm.

intrinsic time constant of the set-up (cell)?

From the decay curves of transient electric field-induced scattered intensity changes in pulsed sine-wave electric fields, we have determined the approximate values of the disorientational relaxation times (τ) of chloroplast fragments. The principle of measurement is indicated in Eq.(2.51): after a time equal to τ following the removal of the electric field, the electro-optic effect is reduced to about the third of its initial value. The values of τ measured for the whole chloroplasts down to the smallest chloroplast fragments studied range between 20s and 2×10^{-2}s. Then we have determined the rotational diffusion coefficients from the relationship, $D = \frac{1}{12\tau}$.

Electron micrographs of chloroplast fragments show that we can approximate their form to elongated ellipsoids of axial ratio from 2 to 4 (see Fig.2.14).

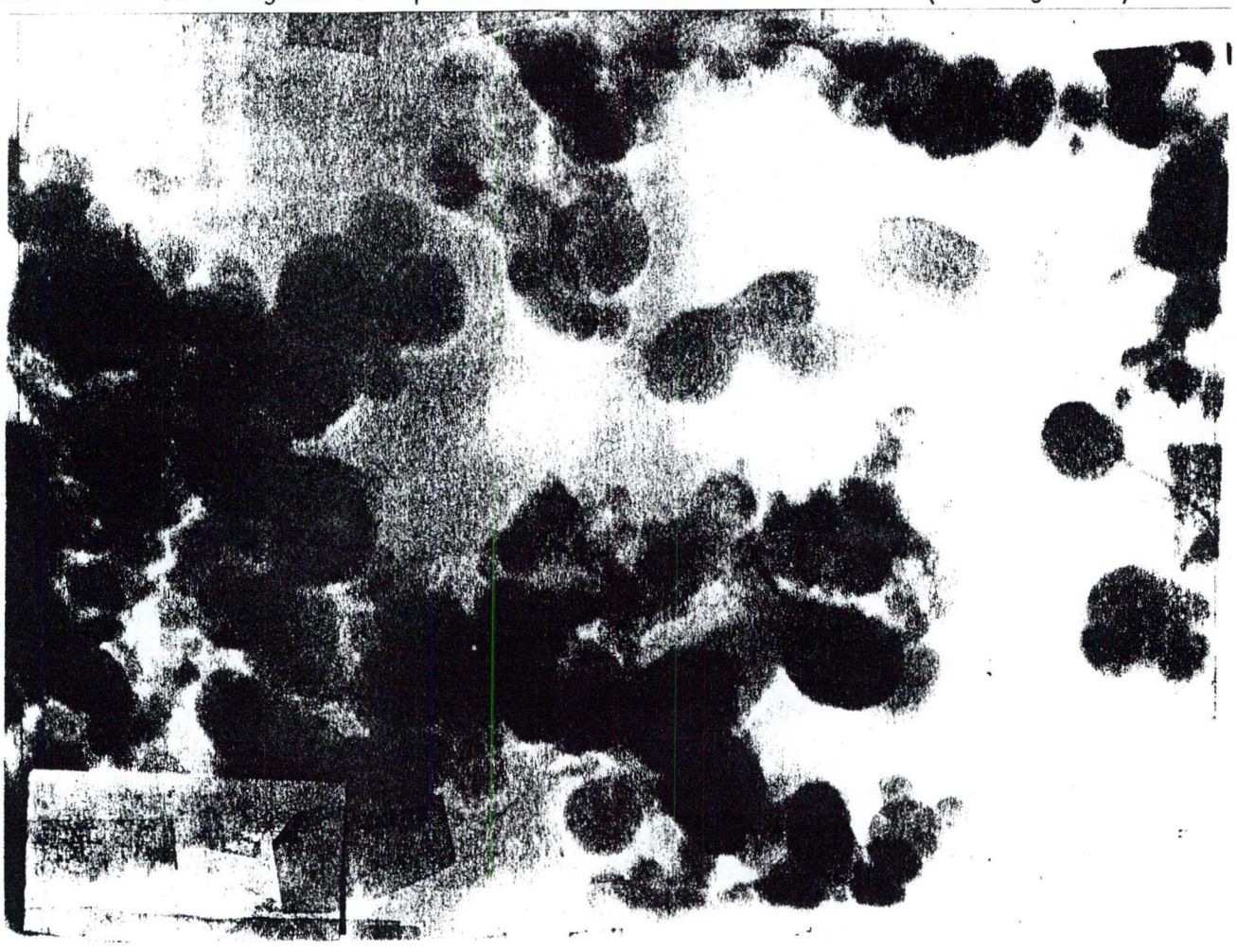

Fig.2.14 Electron micrograph of the morphological structure of chloroplast fragments obtained by subjecting whole chloroplasts to digitonin treatment. Magnification : 200,000.

What's that?

Since for revolution ellipsoids, $D = \frac{3kT}{16\pi\eta a^3} [2\ \ell n\ (\frac{2a}{b}) - 1]$, we deduce the long semi-axis a of each ellipsoid. In our calculations, we have used the following approximate values: T = 293°K, $\eta = 1g \times cm^{-1} \times s^{-1}$, and $\frac{a}{b} = 3$. Under these conditions, $a = (\frac{6.202}{10D})^{1/3} \times 10^{-4}$ [cm]. The results obtained for D and a at different values of the electric field-strength and for different frequencies are indicated in tables 2.1a and 2.1b. The dimensions that we have obtained for chloroplast large fragments are in agreement with those obtained by Geancitov et al./98/ from magnetic field-induced transient fluorescence intensity change and they correspond to what is observed by electron microscopy.

Table 2.1a

Rotational diffusion coefficients and dimensions of chloroplast fragments obtained by subjecting whole chloroplasts to digitonin treatment.

	E[V.cm^{-1}]	ν[Hz]	D[S^{-1}]	a [μm]
Large fragments	157,5	10^3	0,104	1.81
	235,5	10^3	0,170	1.54
	141	10^3	0,104	1.81
	157,5	2×10^5	0,07	2.06
	235,5	10^3	0,07	2.06
	235,5	20	0,083	1.95
	141	10^3	0,083	1.95
	141	10^3	0,12	1.73
	78,75	10^3	0,083	1.95
Small fragments	78,5	10^3	0,12	1.73
	157,5	10^3	0,166	1.55
	235,5	10^3	0,278	1.31
	157,5	2×10^5	0,208	1.44
	235,5	10^3	0,278	1.31
	235,5	20	0,208	1.44

Table 2.1b

Rotational diffusion coefficients and dimensions of chloroplast fragments obtained by subjecting whole chloroplasts to ultrasonic treatment

	$E[V.cm^{-1}]$	ν[Hz]	$D[s^{-1}]$	a[μm]
Large fragments	78,75	10^3	0,064	2.13
	141	10^3	1,665	1.55
	157,5	10^3	0,083	1.95
	157,5	2×10^5	0,083	1.95
	235,5	20	0,083	1.95
	235,5	10^3	0,139	1.64
	235,5	10^3	0,083	1.95
Intermediate fragments	78,75	10^3	0,104	1.81
	157,5	10^3	0,166	1.55
	157,5	2×10^5	0,166	1.55
	235,5	20	0,139	1.64
	235,5	10^3	0,139	1.64
	235,5	10^3	0,208	1.44
Small fragments	78,75	10^3	0,278	1.31
	141	10^3	2,085	0,667
	157,5	10^3	0,333	1,23
	235,5	10^3	0,416	1.15

The figures 2.15, 2.16, 2.17, and the table 2.2 present the relative scattered intensity change as a function of the square of the electric field-strength at a frequency of 1kHz. The curves $(\frac{\Delta I}{I}) = f(E^2)$ manifest saturation effects at high electric field strengths, whereas for very weak electric field-strengths a linear dependence is observed as expected from equation (2.46). Assuming that, at a frequency of 1kHz, the contribution of permanent dipole moments to the mechanism of orientation is negligible, the initial slope to each curve permits us to estimate the value of the electric polarizability. In fact, assuming the Rayleigh-Debye-Gans approximation and a maximum value (for the large dimensions and large axial ratios) of 0.5 for the function of the optical parameter, $\phi(K)$, the electric polarizability may be determined from Eq.(2.14). The values obtained are indicated in table 2.3 (page 74)

Table 2.2

Dependence of the electric field-induced relative scattered intensity change in suspensions of various chloroplast fragments on the electric field-strength

	Fragments obtained by digitonin treat.		Fragments obtained by ultrasonic treatment			Remarks
E_{eff} [V.cm^{-1}]	$(\Delta I/I_o)$ [%]		$(\Delta I/I_o)$ [%]			
	Large fragments	Small fragments	Large fragments	Intermediate fragments	Small fragments	
39.2	8.9	4.7	2.5	1.5	1.25	$\Theta = 30°$
78.75	25.6	20.0	15.0	5.0	3.75	$\nu = 1$ KHz
157.5	50.0	42.7	27.5	12.0	10.0	
235.5	60.0	55.05	18.0	18.0	15.0	

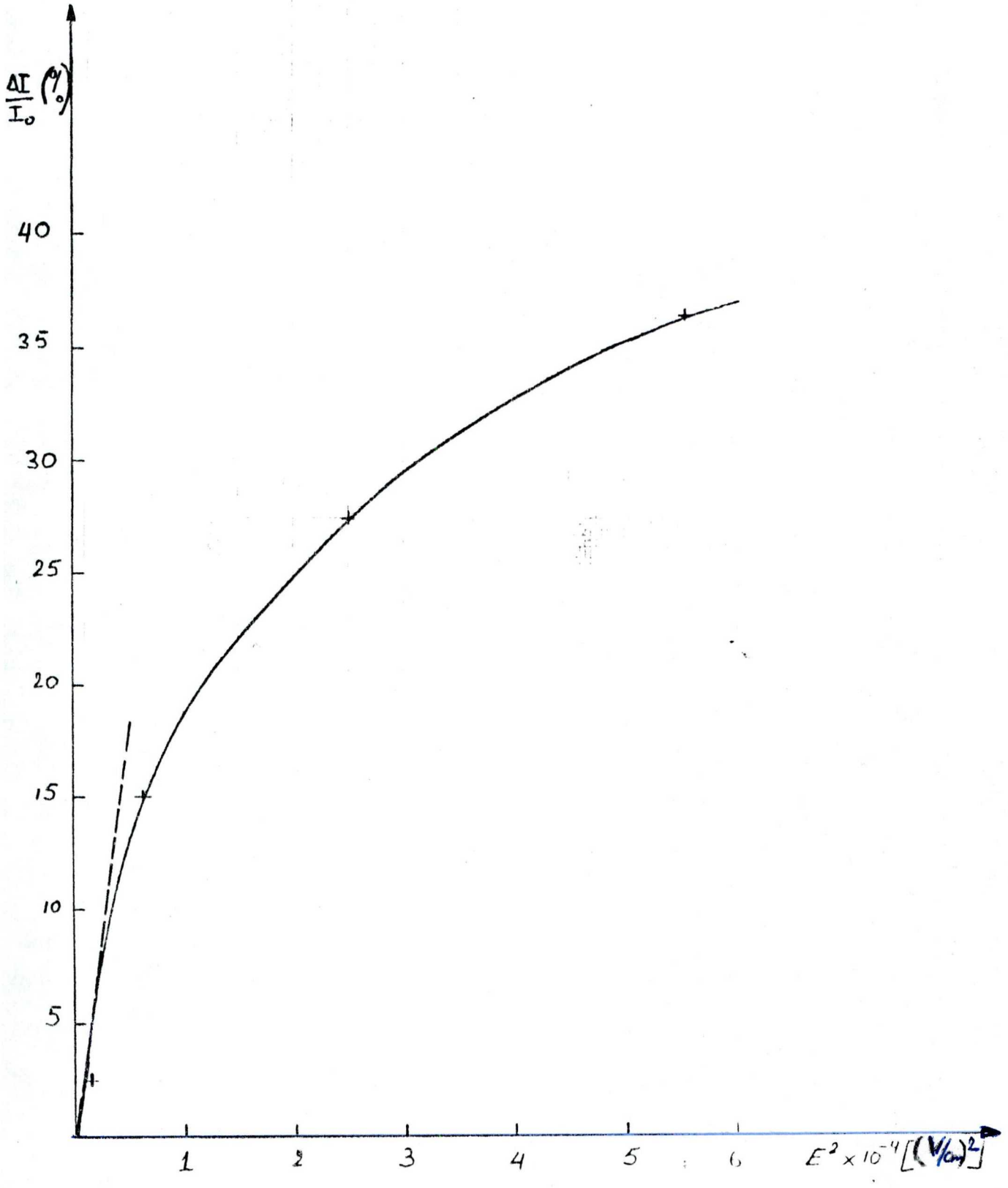

Fig. 2.15.

Dependence of the relative electric field-induced scattered intensity change on the square of the electric field-strength $(\frac{\Delta I}{I_0} = f(E^2))$ for chloroplast large fragments obtained by subjecting a suspension of whole chloroplasts to ultrasonic treatment. λ = 680 nm. ν = 1KHz. The broken line indicates the initial slope.

why have measured the scattering?

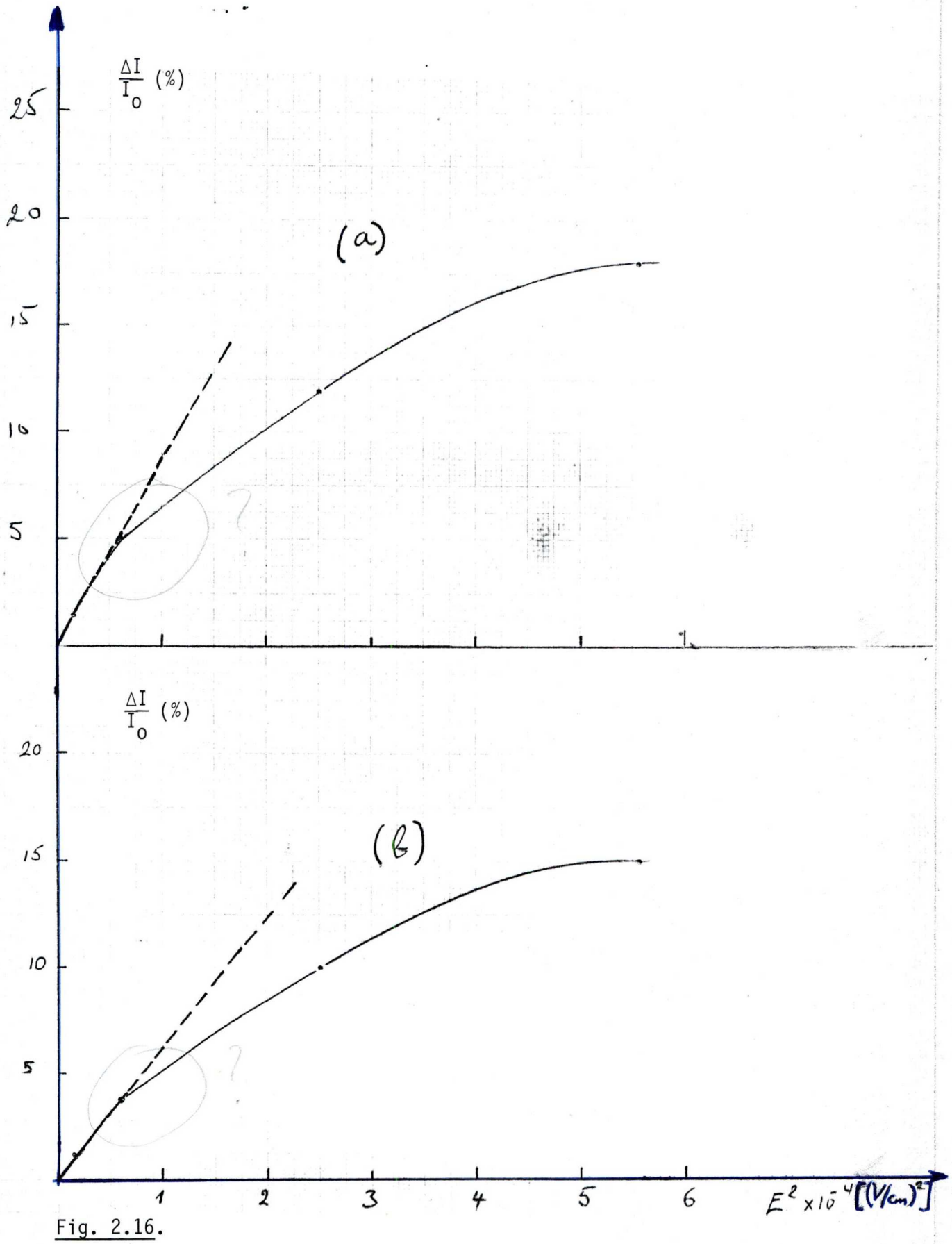

Fig. 2.16.

Dependence of the relative electric field-induced scattered intensity change on $E^2(\frac{\Delta I}{I_o} = f(E^2))$ for intermediate and small chloroplast fragments obtained by ultrasonic treatment. (a) Intermediate fragments; (b) small fragments. ν = 1 KHz ; λ = 680 nm. The broken lines indicate the initial slopes.

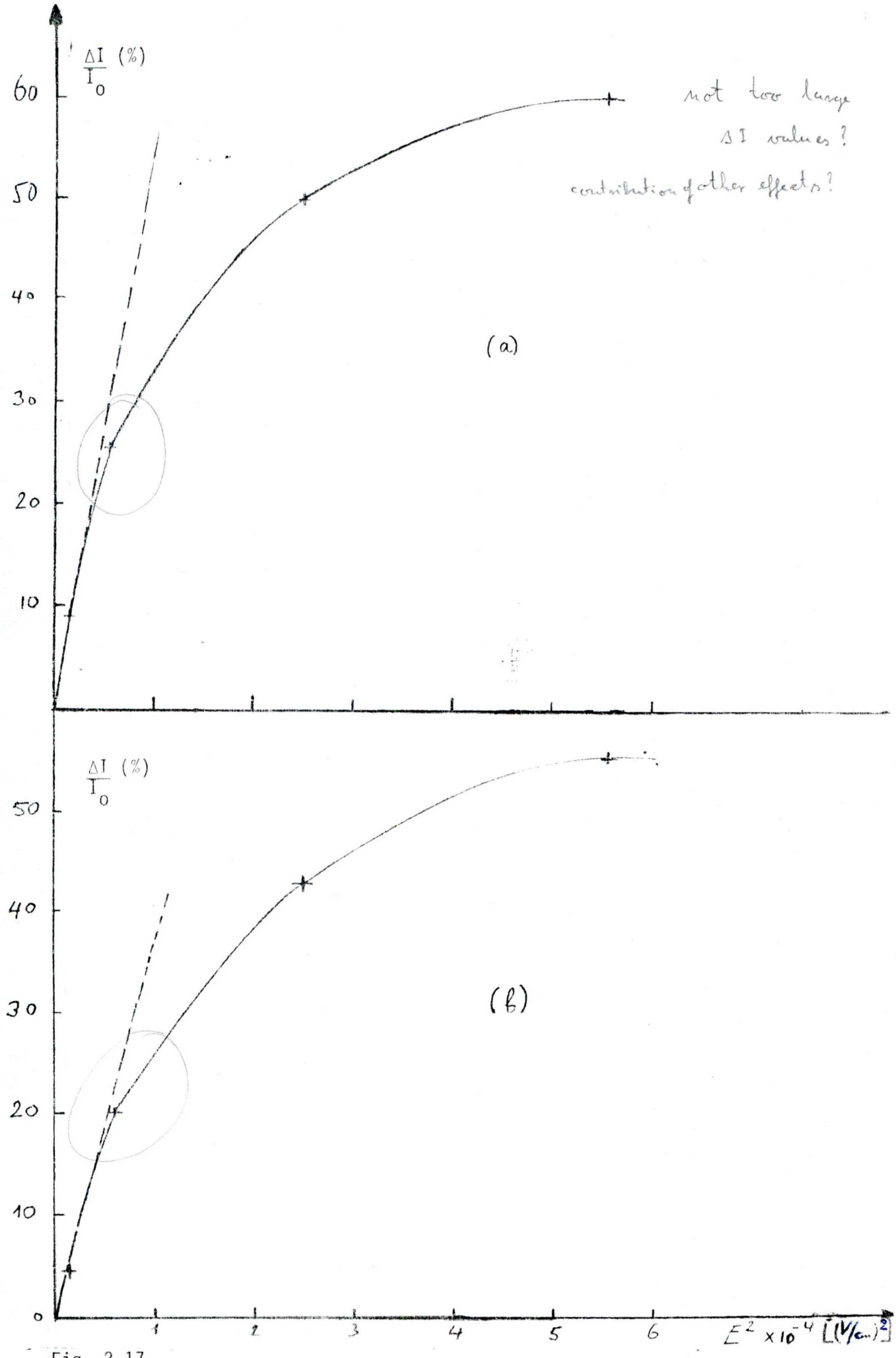

Fig. 2.17.

Dependence of the relative electric field-induced scattered intensity change on $E^2(\frac{\Delta I}{I_0} = f(E^2))$ for chloroplast fragments obtained by digitonin treatment. (a) Large fragments; (b) small fragments. ν = 1 KHz ; λ = 680 nm. The broken lines indicate the initial slopes.

Table 2.3.

Electric polarizabilities of chloroplast fragments obtained by the electric field light scattering method.

Sample	$\left(\frac{\partial \alpha}{\partial E^2}\right)_{E=0}^{(u.e.s.c.g.s)}$ ν = 1 KHz	$\gamma = 2{,}4 \times 10^{-13} \left(\frac{\partial \alpha}{\partial E^2}\right)_{E=0}$ ν = 1 KHz
Large fragments obtained by the digitonin treatment	4.95	12×10^{-13} cm^3
Small fragments obtained by the digitonin treatment	3.285	7.9×10^{-13} cm^3
Large fragments obtained by ultrasonic treatment	3.15	7.55×10^{-13} cm^3
Intermediate fragments obtained by ultrasonic treatment	0.7875	1.89×10^{-13} cm^3
Small fragments obtained by ultrasonic treatment	0.5625	1.35×10^{-13} cm^3

Can they be compared?

MKSA units!

The electric polarizability of chloroplast large fragments prepared by digitonin treatment is approximately 1.2×10^{-12} cm^3. This value is close to those obtained for other large particles (bacteria, purple membrane, fixed erythrocytes, etc.) /68/ and it is in agreement with the values of the electric polarizabilities that we have obtained by the electric linear dichroism method (see page 58). As we have already mentioned (see page 28), we have used pulsed sine-wave electric fields in order to limit secondary effects such as the Joule heating, electrophoresis, etc. Since we have not used continuous d.c. electric fields, we could not determine the mean value of the permanent dipole moment associated to each species of chloroplast fragments.

really close? see (68)

Discussion?

completely lacking!

Conclusions?

CHAPTER III

ARTIFICIAL PHOTOSYNTHETIC SYSTEMS

3.1. Introduction

Artificial photosynthetic systems are constituted by natural or synthetic chemical compounds and they seek to mimic some aspects of the photophysico-chemical reactions of natural photosynthesis. When these compounds exist in a perfectly homogeneous liquid solution, one has an homogeneous photochemical system. If the system is not homogeneous but contains appropriate interfacial systems or supramolecular assemblies, one has an heterogeneous photochemical system.

Artificial photosynthetic systems are investigated for their potential utilization in the conversion and storage of solar energy. If, by means of artificial photosynthetic systems, sunlight energy could be used to generate an easily storable chemical, the problem of sunlight energy storage would be solved.

Given that artificial photosynthetic systems have to simulate some aspects of the primary photophysico-chemical reactions of natural photosynthesis, they have to perform at least the following functions of the photosynthetic thylakoid membrane of the chloroplast/1/:

(i) the quantum capturing function

(ii) the photoinduced electron transfer from a lower to a higher energy state.

In this chapter, we describe briefly artificial photosynthetic systems (wireless homogeneous and heterogeneous photochemical systems), and we present the mechanisms of photochemical conversion and storage of solar energy in the systems used in this work. Special emphasis is given to the utilization of artificial photosynthetic systems in order to achieve the dye-sensitized photodecomposition of water to H_2 and O_2. This interest is understandable since such a process constitutes an important approach to the production of renewable hydrogen fuel using visible light. Finally, we investigate the possibility of photochemically oxidizing a Mn(III)-tetrapyridyl porphyrin derivative by a Zn- tetrapyridyl porphyrin derivative (sensitizer) in aqueous micellar solutions of sodium dodecyl sulfate. This interest is understandable since in artificial photosynthetic systems, it is believed that polynuclear manganese complexes are most probable candidates which may mediate the multi-electron-transfer process of the photochemical oxidation of water. In fact, since manganese has many states of oxidation, in principle manganese complexes are able to remove four electrons from two molecules of water and make molecular oxygen without the production of free oxygen atoms, or hydroxyl radicals, or other intermediates which would

destroy the system /8a, 17, 22/. It is also known that a manganese-containing complex is involved in the light-driven reactions of PSII, in which water is oxidized to O_2/23/.

3.2. Description of artificial photosynthetic systems (wireless homogeneous and heterogeneous photochemical systems)

Artificial photosynthetic systems attempt to mimic our current knowledge on the natural photosynthesis process in order to convert sunlight energy into chemical energy and/or electricity. According to its role, an artificial photosynthetic system will involve the following elements/1, 2, 10b/ :

(i) Species which absorb in the visible range of the solar spectrum. These species perform a role similar to the quantum capturing function of the chloroplast.

(ii) Electron acceptors and electron donors, which perform the photo-induced electron transferring function of the photosynthetic electron transport chain of the thylakoid membrane.

(iii) A physical way to organize reactants and to keep separated spatially the photoproducts of the photoinduced electron transfer reactions. In natural photosynthesis this role is accomplished by the thylakoid membrane of the chloroplast.

These were already mentioned on the previous page

The choice of the components of an artificial photosynthetic system stems from our current knowledge on the natural process and on the role that must be assumed by each system.

MAIN COMPONENTS OF AN ARTIFICIAL PHOTOSYNTHETIC SYSTEM

(a) A dye or sensitizer (S). It is a substance which has a strong absorptivity in the visible range of the solar spectrum. As soon as it has absorbed a photon of suitable wavelength, the sensitizer is electronically excited; this excited state is a better electron donor or electron acceptor than the ground state and, it can initiate photoinduced electron transfer reactions (or photoinduced redox reactions). The sensitizer assumes the role of a photocatalyst and it is the reaction-centre trap analogous to that in natural photosynthesis (e.g., PSI and PSII are these reaction-centre traps). A very important requirement in the choice of a sensitizer is that its excited state should have a long lifetime and it should be energetic enough to carry out the desired photochemical reactions. Sensitizers excited to the singlet state (Fig. 3.1.) very quickly lose their energy (lifetime in the range 10^{-5}-10^{-9}s) and for this reason their excited singlet states cannot be used to store the light energy. But for some sensitizers excited to the singlet state, there may be a spin inversion (Fig. 3.1.) and the molecule goes to the excited triplet state in a mechanism

called inter-system crossing. The excited triplet state is more stable (lifetime of the order of 10^{-3}s) than the corresponding excited singlet state, because the electrostatic repulsion is reduced there. Sensitizer molecules which are excited to the triplet state are long lived and they may diffuse towards other molecules in a liquid solution and the interaction with the latter permits us to store part of the light energy in the form of chemical energy. In order to obtain an appreciable quantum efficiency for the photochemical conversion and storage of light energy, the quantum yield for the excited triplet state should be high and this, excited triplet state should have good redox properties.

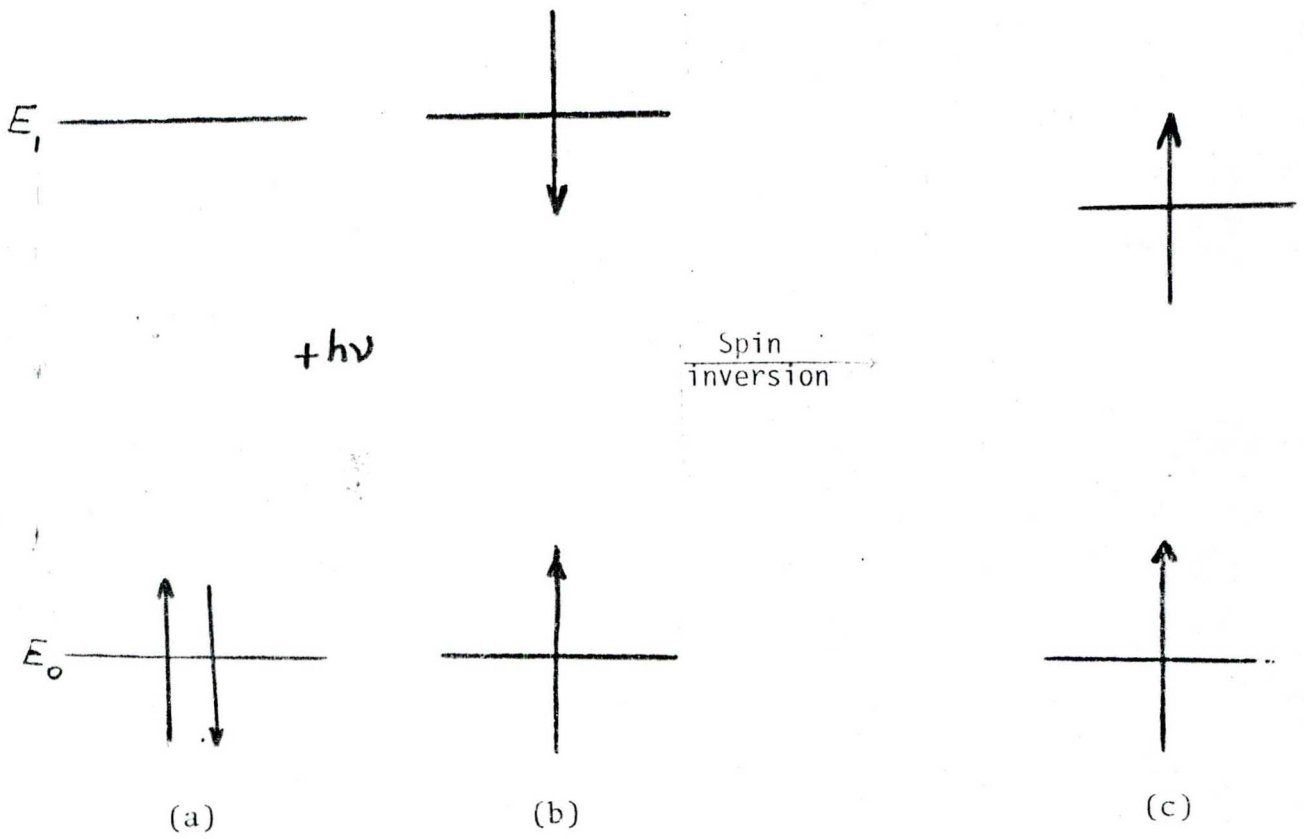

Fig. 3.1.

Energy level diagram indicating some electronic states of a sensitizer The effect of light absorption on a pair of electrons in a molecular orbital of the sensitizer is also shown. The arrows indicate the directions of the electron spins with respect to a local magnetic field. (a) Ground singlet state. (b) Excited singlet state. (c) Excited triplet state. According to the theory of quantum mechanics, this excited triplet state is lower in energy than the corresponding excited singlet state.

It is known /29/ that natural photosynthesis makes extensive use of organometallo-porphyrins (e.g.) chlorophyll molecule) as chromophores in the primary phorochemical reactions. Synthetic sensitizers of similar structure have been used in artificial photosynthetic systems /30/. One of the sensitizers that we have used, a Zn-tetrapyridyl porphyrin derivative ($ZnTP_yP - C_{16}$, Fig. 3.2b.) resembles the chlorophyll molecules which are the major light-absorbing pigments of green cells. The actual structures of various chlorophyll molecules were established from degration studies by FISCHER in 1940 and unequivocally proved by WOODWARD who first synthesized chlorophyll in vitro, in 1960 /14/. From these studies, we know that chlorophyll molecules are surfactants: they have a hydrophylic "head" attached to a hydrophobic core. The hydrophilic head or porphyrin head is formed by a tetrapyrrole ring, in the center of which a magnesium atom is co-ordinately bound. The hydrophobic core is a hydrophobic terpenoid side chain, consisting of the alcohol phytol. The Zn-tetrapyridyl porphyrin derivative ($ZnTP_yP - C_{16}$) is a surfactant: its hydrophilic head or porphyrin head is formed by a tetrapyridyl ring, in the center of which a zinc atom is co-ordinately bound; the C_{16} tail represents its hydrophobic core. Like chlorophyll molecules, the $ZnTP_yP - C_{16}$ sensitizer has a large number of double bounds in conjugation and this property is relevant for the effectiveness in absorbing electromagnetic radiation in the visible region of the solar spectrum. The $ZnTP_yP - C_{16}$ absorbs in the blue region of the solar spectrum (λ = 430 nm). Not only the $ZnTP_yP - C_{16}$ complex has almost the same chemical structure and the same organization for quantum capture as chlorophyll molecules, but especially it presents the following advantage over chlorophyll molecules: it is more stable than chlorophyll molecules extracted from plants for their use in artificial photosynthetic systems.

Another sensitizer that we have used in an experiment of dye-sensitized photoreduction of water to hydrogen, is the tris (2, 2'-bipyridinium) ruthenium (II) ($Ru(bpy)_3^{2+}$; Fig. 3.2a). The oxidized $Ru(bpy)_3^{3+}$ complex (redox potential: $E°(Ru(bpy)_3^{3+}/Ru(bpy)_3^{2+})$ = 1.26V/30/) is thermodynamically capable of oxidizing water to oxygen at pH7 (redox potential: $E°(O_2/H_2O)$ = 0.82V/1/). Besides, the tris - (2,2'-bipyridine) - ruthenium (II) complex has a strong absorptivity in the visible range of the solar spectrum: in fact, the peak of its absorption is located at a wavelength λ = 452 nm, a value which is close to position of the maximum of the solar spectral irradiance distribution /69/.

(b) Electron donors(D) and electron acceptors (A)

Generally, after a sensitizer molecule has absorbed a photon of suitable wavelength and it has been excited to the singlet state, either it very quickly comes back to its ground state by emitting a photon of

longer wavelength (fluorescence phenomena) or it very quickly undergoes a radiationless deactivation (e.g., the absorbed light energy is transformed into thermal energy due to collisions with other molecules). Even for a sensitizer molecule which is in the excited triplet state, if it does not undergo any photochemical process and does not chemically react with a neighboring molecule, it finally deactivates either by a radiative process (e.g., phosphorescence phenomena) or by a radiationless process.

The role of electron acceptors and electron donors is to intercept, by electron transfer from or to the excited sensitizer, the decays pathways mentioned above. The photoproducts of the photoinduced electron transfer reactions should retain most of the light energy initially stored in the excited sensitizer. One of the requirements for the choice of electron donors and electron acceptors is that they may not interact with the sensitizer in its ground state. In addition, the redox potential of the D^+/D or A/A^- couples should be appropriate. The electron donors and electron acceptors are the analogues of the photosynthetic electron transport chain.

Following are the electron donors that we have used :

(i) Ethylene diamine tetraacetic acid disodium salt (EDTA; Fig. 3.2.f), tris (2-hydroxyethyl) amine or triethanolamine (TEA). These two compounds contains a tertiary nitrogen atom with many carboxymethyl groups and, consequently, thay are good electron donors/70/. However, the pH of the solution must be equal to the pK_a value of the group state protonation equilibria of the electron donor/36,70/. In acid pH, the protonation of the amino functional group reduces the electron donation properties of the electron donor. If the pH is appropriate, these two electron donors present the following advantage : as soon as they are oxidized, they are unstable and they irreversibly decompose into other products (they are called sacrificial electron donors). Thus, a kinetic control of the rates of the photoinduced electron transfer reactions as well as a kinetic control of the rates of the thermal back reactions are feasible (e.g., the thermal back electron transfer between the photoproducts is prevented).

(ii) A manganese-tetrapyridyl porphyrin derivative complex ($Mn^{III}TP_yP\text{-}C_{16}$, Fig. 3.2d) and an olefin (5-hexenoic acid).

Following are the electron acceptors that we have used :

(i) N,N' - bis (sulfonato-n-propyl)-4,4' bipyridyl or propyl viologen sulfonate (PVS°, Fig. 3.2.c).

(ii) 1, 1' - dimethyl - 4,4' bipyridinium dichloride or methyl viologen (MV^{2+}, Fig. 3.2e).

The main reasons which motivated us to choose these two electron acceptors are the following :

(1°) Each of the compounds may accept a single electron into its conjugate system and then it forms a stable radical which does not dimerize/31/.

(2°) The essential feature of the structure of these compounds is the dipyridyl or dipyridium. The dipyridyl, or dipyridinium, viologen is colorless, and when each compound has accepted an electron it turns to the blue color, allowing the reaction to be followed.

(3°) The most used electron acceptor (PVS°) is a special one because it is a dipolar ion with no net charge and when it accepts an electron it becomes negatively charged. Being negatively charged, the PVS^- radical may be expelled from the negatively charged interface between the water bulk phase and the organic phase of a micelle in an aqueous micellar solution of sodium dodecyl sulfate. Since all the sensitizers that we have used become positively charged after the photoinduced electron transfer from the excited sensitizer to an electron acceptor, thay are attracted by the negatively charged interface of an SDS micelle. Thus, the thermal back reaction between the negative ion radical (PVS^-) and the oxidized sensitizer is retarded or inhibited.

(c) Catalysts

The role of these components is to mediate multi-electron transfer processes such as the dye-sensitized photooxidation of water to oxygen or the dye-sensitized photoreduction of water to hydrogen. In photoinduced electron transfer reactions, the role of the catalysts is to lower the activation energy by interacting with energetic but unstable photoproducts to facilitate stable compounds formation. Catalysts are enzymes analogous to natural photosynthesis.

We have achieved a dye-sensitized reduction of water to hydrogen using an homogeneous photochemical sacrificial system in which colloidal platinum mediated the two-electron transfer process for the reduction of water to hydrogen.

(d) Supramolecular Assemblies or Interfacial Systems

By means of hydrophobic-hydrophilic interactions between the reactants and/or the photoproducts an interfacial system can assume the

following functions/1/ :

(i) to provide a selective solubilization of the reactants and allow a close proximity between them;

(ii) to organize reactants;

(iii) to stabilize or keep spatially separated the oxidized and reduced species of the photoinduced redox reactions.

Interfacial systems are the analogues of the photosynthetic thylakoid membrane. Several interfacial systems such as micelles/36,71/, vesicles/28,74,75/,colloidal SiO_2 particles/72/; polyelectrolytes - polyacrylates particles/77/, etc., have been used, in artificial photosynthetic systems, as a model for the thylakoid membrane of the chloroplast. In our work, we have used micelles of sodium dodecyl sulfate as a model for the thylakoid membrane (see section 3.4. for details).

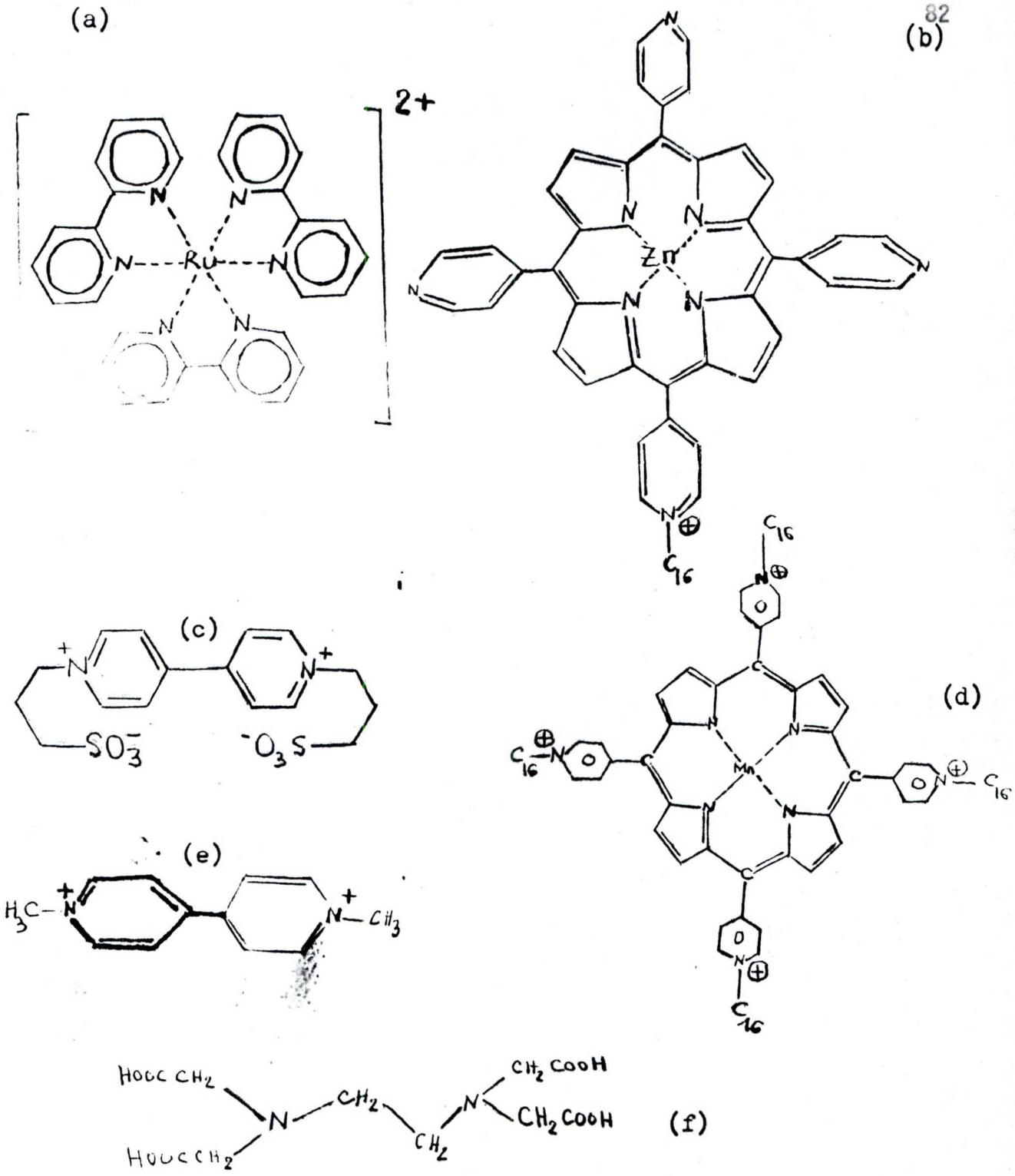

Fig. 3.2. Chemical Structure of the Sensitizers, Electron Acceptors and Electron Donors Which Have Been Used.

(a) Tris (2,2' - bipyridinium) ruthenium (II) chloryde hexahydrate $Ru(bpy)_3^{2+}$;

(b) Zn - tetrapyridyl porphyrin derivate complex with a hydrophobic core ($Zn\ TP_yP\text{-}C_{16}$);

(c) Propyl viologen sulfonate (PVS°);

(d) Mn(III) - tetrapyridyl porphyrin derivative complex with a hydrophobic core ($MnTP_yP\text{-}C_{16}$);

(e) Methyl viologen (MV^{2+});

(f) Ethylene diamine tetraacetic acid disodium salt (EDTA)

3.3. Photochemical conversion and storage of light energy

3.3.1. Mechanisms of light energy conversion into chemical energy in artificial photosynthetic systems

The kinetics and mechanisms of dye-sensitized photoinduced electron transfer reactions, which follow immediately upon light absorption by the sensitizer, have been extensively investigated by "flash photolysis techniques" /8a, 29, 36, 37, 77, 78/. Flash photolysis technique involves the excitation of a sensitizer by an intense, short light flash (provided either by a flashlamp-pumped laser or a mode-locked laser) and then the decays processes are followed either by transient absorption change studies at a given wavelength (kinetic spectroscopy) or by measuring a complete spectrum at a pre-set time after the flash (flash spectroscopy).

Let us consider the simplest photochemical system existing in a solution containing a certain amount of the sensitizer (S), of the electron acceptor (A) and of the electron donor (D). When the sensitizer absorbs a photon of appropriate wavelength it is excited to some vibrational level, s_{1v}, of the excited singlet state (Eq.3.1a). By internal conversion, this excited state very quickly transforms to the lowest excited singlet state, s_{10}, (Eq.3.1.b).

$$S \xrightarrow{h\nu} S^{*\,s_{1v}} \qquad (3.1a)$$

$$S^{*\,s_{1v}} \longrightarrow S^{*\,s_{10}} \qquad (3.1b)$$

Of all the deactivation processes of the excited singlet state (fluorescence, and others) we are interested in its transformation into an excited triplet state (mechanism called inter-system crossing) since only excited triplet states are long lived so that electron transfer may take place between the excited sensitizer and the electron acceptor. The lowest excited singlet state has a very short lifetime ($\tau = 10^{-5}$-10^{-9}s), and it very quickly crosses to a vibrational level of the excited triplet state, T_{1v}, isoenergetic to the lowest excited singlet state; by internal conversion, this excited state decays to the lowest excited triplet state, T_{10} (Eq.3.1c). The lowest excited triplet state is a metastable state and it is long lived (its lifetime is in the order of several milliseconds) and can perfom some chemistry.

$$S^* \, {}^{S}1_0 \longrightarrow S^* \, {}^{T}1_v \longrightarrow S^* \, {}^{T}1_0 \text{ (milliseconds)} \qquad (3.1c)$$

For simplification let us consider the case where the excited sinsitizer is a good electron donor (oxidative quenching). The lowest excited triplet state of the sensitizer (S) transfers an electron to the electron acceptor (A) and goes to S^+ while the electron acceptor is reduced to A^- (Eq. 3.2) :

$$S^* \, {}^{T}1_0 + A \longrightarrow S^+ + A^- \qquad (3.2.)$$

$$S^+ + A^- \longrightarrow S + A \qquad (3.2')$$

Generally, the sensitizer (S) is chosen so that its oxidized species (S^+) is an oxidant strong enough to take an electron from the donor (D); in such a case, the electron donor (D) reduces S^+ to S, while D is oxidized to D^+ (Eq. 3.3) :

$$A^- + S^+ + D \longrightarrow S + A^- + D^+ \qquad (3.3)$$

$$A^- + D^+ \longrightarrow A + D \qquad (3.3')$$

If, the thermal back electron transfer (equations (3.2') and (3.3')) could be prevented, the redox gradient of A^- and D^+ represent a chemical stored energy, ΔG, which is the difference between the energy of the materials in the final state and that in the initial state (Figure 4). The photochemical reaction described above can be followed spectrophotometrically by measuring the optical density of D^+, or that of A^-, as a function of the illumination time (see paragraph 3.5.2a).

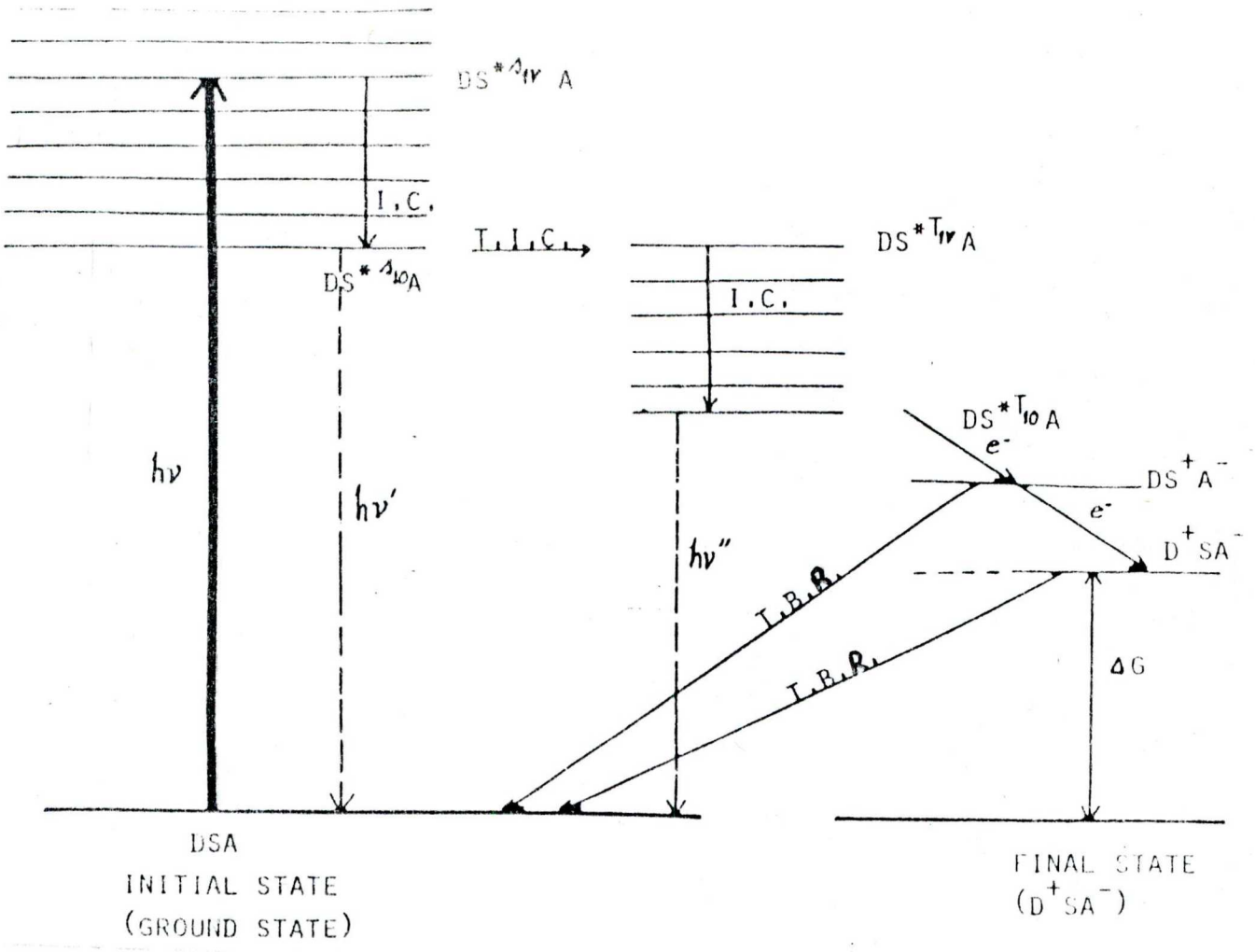

Fig.3.3. Schematic diagram for the photochemical conversion and storage of light energy via photoinduced redox reactions (see text for details).

Abbreviations and symbole: S_{iv} and T_{iv} represent, respectively, a vibrational level of the excited singlet state and excited triplet state of the sensitizer (S). I.C. means internal conversion; T.I.C. means transition inter-system crossing; T.B.R. means thermal back reaction. ν is the frequency of the photon absorbed by the sensitizer; ν' and ν" represent the frequencies of photons which could be emitted in fluorescence and phosphorescence phenomena, respectively. ΔG is the net chemical energy stored in the photochemical reaction.

(Reprinted from reference /1/ , p.12)

3.3.2. Chemical utilization of the photoproducts in the dye-sensitized photodecomposition of water to O_2 and H_2.

If the redox potential of the A/A^- couple is below the redox potential of H^+/H_2 couple, then A^- can reduce water to hydrogen in the presence of a charge storage catalyst (Cat.1) (Eq. 3.4) :

$$2A^- + 2H_2O \xrightarrow{\text{Cat.1}} 2A + 2OH^- + H_2 \qquad (3.4)$$

Reduced bipyridinium salts (viologen radicals) are capable of reducing water to hydrogen in the presence of colloidal platinum particles stabilized by a negatively charged polymer/27, 30/.

In the same manner, if the redox potential of the D^+/D couple is above the redox potential of the O_2/H_2O couple, D^+ can oxidize water to oxygen in the presence of a suitable charge-storage catalyst (Cat. 2) (Eq. 3.5) :

$$4D^+ + 2H_2O \xrightarrow{\text{Cat.2}} 4D + 4H^+ + O_2 \qquad (3.5)$$

For a practical utilization of the photochemical conversion and storage of light energy, water itself should be the ultimate electron donor/29, 36, 37/. In such a case, one should choose the sensitizer (S) so that S^+ be thermodynamically capable of oxidizing water to oxygen; the redox potential of the S^+/S couple should be above that of the O_2/H_2O couple (i.e., $E°(S^+/S) > E°(O_2/H_2O) = 0.82$ V). In these conditions, the regeneration of the sensitizer would be coupled to water oxidation (Eq. 3.5') :

$$4S^+ + 2H_2O \xrightarrow{\text{Cat.2}} 4S + 4H^+ + O_2 \qquad (3.5')$$

The oxidized $Ru(bpy)_3^{3+}$ complex is thermodynamically capable of oxidizing water to oxygen ($E°(Ru(bpy)_3^{3+}/E°(Ru(bpy)_3^{2+}) = 1.26V$) in the presence of transition metal oxides such as RuO_2/27, 41/, IrO_2/42/, PtO_2/27/ and CoO/9/, etc.

However, in general, in homogeneous solutions, the rapid thermal back reaction between S^+ and A^- to give S + A or between D^+ and A^- to give D + A does not allow this type of photochemical solar energy conversion and storage.

In homogeneous photochemical systems, two cases are an exception:

(i) When a sacrificial electron donor which undergoes an irreversible oxidation is present in the system, a dye-sensitized reduction of water to hydrogen (Eq. 3.4) is observed/27, 29, 36, 37, 70/;

(ii) When a sacrificial electron acceptor which undergoes an irreversible reduction is present in the system, a dye-sensitized oxidation of water to oxygen is observed/36, 41, 42/.

These homogeneous photochemical sacrificial systems produce H_2 and O_2 at the expense of consuming the sacrificial electron donor and the sacrificial electron acceptor, respectively.

A simultaneous photodecomposition of water to H_2 and O_2 upon illumination with visible light requires the use of heterogeneous photochemical systems (i.e., systems comprising appropriate interfacial systems or ultrathin membranes). Bolton/11, 80/ has proposed a cycle for the dye-sensitized photodecomposition of water into H_2 and O_2. The proposed cycle involves two photochemical reactions coupled in series by an ultrathin membrane which is permeable to electrons and protons. This membrane is the analogous of the pool of plastiquinone molecules which lies in the photosynthetic electron-transfert chain and constitutes the essential link for electron flow from PSII to PSI (i.e., the photoinduced transfer of electrons and protons across the thylakoid membrane). This system of two photochemical reactions operating in series (so that two photons are absorbed for every electron transferred in the ultimate reaction) would better simulate the photochemical step of natural photosynthesis; it would permit us to utilize an appreciable fraction of photons in the visible region of the solar spectrum and to convert light energy into chemical energy with an optimal quantum efficiency. The complete dye-sensitized photodecomposition of water into H_2 and O_2 following the scheme proposed by Bolton, has not yet been achieved. The homogeneous photochemical sacrificial systems mentioned above constitute an approach where separate reduction half-reaction to produce H_2 or oxidation half-reaction to produce O_2 , are realized.

Some groups of investigators have achieved the dye-sensitized photodecomposition of water to H_2 and O_2 using a single photosystem (i.e., one-photon process). For example, Brugger et al./27/ have achieved a dye-sensitized decomposition of water into H_2 and O_2 using a microheterogeneous aqueous solution containing platinum particles protected by the cationic polysoap PVP-C_{16}, $Ru(bpy)_3^{2+}$ or $ZnTMP_yP^{4+}$ as sensitizers, $C_{14}MV^{2+}$ as an electron acceptor relay and RuO_2 as the

oxygen-generating catalyst. Gratzel et al./83/ have achieved the photodecomposition of water to O_2 and H_2 using colloidal TiO_2 doped with chromium ions and CdS colloidal dispersions both coated with ultrathin platinum particles and RuO_2. Calvin and Coworkers/31/ have achieved the dye-sensitized decomposition of water to O_2 and H_2 using negatively charged colloidal SiO_2 particles as interfacial systems. Other researchers/69, 81, 82/ have achieved this goal using photoelectrolytic cells. However, the quantum efficiencies obtained by all those investigators were very low because they used a single photosystem.

Generally, in artificial photosynthetic systems, interfacial systems which keep spatially separated the intermediate photoproducts are necessary in order to store the light energy. In some of our experiments, heterogeneous photochemical systems were constituted in aqueous micellar solutions of sodium dodecyl sulfate ($C_{12}H_{25}\ SO_4^-\ Na^+$: SDS). In such micellar aqueous solution of SDS, one has two sub-phases with a negatively charged interface in between. These sub-phases are: a bulk or aqueous phase and an organic phase (the hydrophobic core in the micelle).

3.4. Formation and properties of micelles

3.4.1. Micelle formation

A surfactant or surface active agent is a molecule possessing two portions: a long saturated hydrocarbon chain or hydrophobic tail (water-repelling) and a hydrophilic polar head group (water-attracting) /84, 85/. Micelles or surfactant aggregates are spontaneously formed when surfactant molecules are dissolved in water at any molar concentration above a critical value called "Critical micelle concentration (CMC)"/37,85/. Above this value, each additional surfactant molecule is found in the form of additional micelles. Thus, the molar concentration of micelles (C_M) is given by :

$$C_M = \frac{C - CMC}{N_{ag}}$$

Where C is the overall concentration of surfactants; N_{ag} is the aggregation number (i.e., the number of monomers in a micelle). N_{ag} determines the size and geometry of the micelle.

All the physico-chemical methods for the determination of the CMC's are based on the same principle /84, 85/: one measures the change in a physical property (see examples below) of a solution of surfactants as a function of surfactant concentration (C), and then he may observe

a narrow concentration range where there is a sudden, not abrupt, but rather gradual change in the physical property. Such a narrow concentration range is attributable to the association of surfactants forming aggregates or micelles. In order to determine the CMC of a surfactant, one plots the curve corresponding to the change in a given physical property as a function of the surfactant concentration. The curve thus obtained presents two distinct portions, one of which represents the behavior of the physical property below the CMC, and the other of which represents the behavior above the CMC. Since the two portions of the curve have different slopes at any points, the intersection of two appropriate slopes permits us to determine the approximate value of the CMC.

Following are some physical properties which have been used for the determination of the CMC's of the most used surfactants/84, 85/:

(i) the interfacial tension;

(ii) the electric conductivity;

(iii) the freezing point lowering and vapor pressure lowering;

(iv) calorimetric properties (the specific heat and the heat of dilution);

(v) the transport properties such as the viscosity of the solution and the sedimentation coefficient of the surfactants;

(vi) the optical and spectroscopic properties of a solution (e.g., measurements of scattered light intensity at a viewing angle equal to 90°, measurements of the turbidity of the solution, of the refractive index, of the absorbance at a given wavelength, of fluorescence spectra, etc.).

In this work, we have determined the CMC of the sodium dodecyl sulfate surfactant (SDS) by measuring the change in the A.C. conductivity of aqueous solutions of SDS as a function of the SDS concentration (see paragraph 3.5.2c).

3.4.2. Properties of micelles

(i) At low concentrations ($C<0.1M$) the micelles have almost a spherical shape (radius in the range 15A° - 30A°)/37,71/.

(ii) The hydrophobic chains form the interior of a micelle while the hydrophilic polar head groups are located at the interface between the interior organic phase and the water bulk phase.

(iii) If the hydrophilic polar head groups are charged, the surface of the micelle is surrounded by a counter ions atmosphere. The latter are, to a certain degree, attracted to form a diffuse electric double layer /71, 84, 85/. In such a case, the surface of the micelle is characterized by some electric field so that it can kinetically control the rates of the dye-sensitized electron transfer reactions as well as the rates of the thermal back reactions between the photoproducts. Thus, the diffuse electric double layer of an ionic micelle may play a crucial role in the photochemical conversion and storage of light energy.

(iv) Depending on their chemical structure, molecules may be solubilized in the hydrophobic core in a micelle or at its hydrophilic interface. Surfactant molecules are solubilized in a micelle in such a way that their hydrophobic chains are located in the hydrophobic core of the micelle while their polar head groups are located at the inner or outer periphery of the micelle. Thus, one may solubilize sensitizer molecules, electron donor and electron acceptor molecules either in the hydrophobic environment or the hydrophilic one, depending on the structural properties of these molecules. Then micelles permit us to organize reactants at the molecular level and allow a close proximity between them, which contribute to kinetically control the rates of the dye-sensitized electron transfer reactions.

Micelles are not static species but rather exist in a dynamic equilibrium/85/. The monomer-micelle equilibria equation which also describes the formation and dissociation must obey to the chemical equilibria laws/71, 85/ (Eq. 3.6) :

$$M_n \underset{k_f}{\overset{k_d}{\rightleftharpoons}} M_{n-1} + M \qquad (3.6)$$

where M_n is a micelle constituted by n surfactant molecules and M is a single surfactant molecule; k_f and k_d are the rate constants for micelle formation and micelle dissociation, respectively. These rate constants may be determined by relaxation techniques. In fact, the relaxation time (τ) for micelle dissociation is given by /85/ :

$$\frac{1}{\tau} = k_f C - k_d \qquad (3.7)$$

Where C is the overall concentration of surfactants.

Similary, an adsorption-desorption equilibrium exists; it obeys to the following equation /71/ (Eq. 3.8) :

$$B(mic) \underset{k_+}{\overset{k_-}{\rightleftharpoons}} B + mic \qquad (3.8)$$

k_- and k_+ are the rate constants for adsorption and desorption of the molecule B, respectively. B(mic) represents an adsorbed molecule. From Eq. (3.8) it is obvious that an adsorbed molecule may be transported to another micelle via desorption-adsorption at the new micelle after a short stay as free entity B in the bulk solution. Molecule exchange between the bulk solution and micelles is also predicted by Eq. (3.8). This equation determines the rate at which the photoproducts of the photoinduced electron transfer reactions may be formed as well as the rate at which they may recombine. Since a micelle can solubilize several molecules of different species (e.g., a sensitizer and an electron acceptor), there may be a photoinduced transfer of electrons between these molecules.

The fact that micelles are in constant dynamic change constitutes one of the difficulties of using them as interfacial systems in artificial photosynthetic systems/10a/. It is hard to change micellar size, to insert more or less sensitizer molecules into micelles in order to improve the quantum efficiency for the conversion of light energy into chemical energy.

In artificial photosynthetic systems, surfactant vesicles present several advantages with respect to micelles/28/: surfactant vesicles can solubilize and organize large number of sensitizers, electron donors and electron acceptors per aggregate and they are amenable to electrostatic modification and chemical functionalization. Given that the vesicles are more efficacious in keeping spatially separated the oxidized and reduced species of the photoinduced redox reactions, one expects that, for the same experimental conditions, the quantum efficiency of the photochemical conversion of light energy obtained by using vesicles as interfacial systems will be greater than that he would obtain by using micelles as interfacial systems.

3.5. Materials and experimental procedure

3.5.1. Materials

One of the sensitizers used, (5 - [(1'-hexadecylpyridinium-4'-yl] -10, 15, 20 -tris- [4'-pyridyl] -21H, 23H - porphine) - zinc perchlorate and one of the electron donors used, bromo-aquo-(5-[1'-hexadecylpyridinium 4' yl] - 10, 15 , 20 - tris [4' pyridyl] - 21H, 23H - porphine) - manganese perchlorate, were prepared by Roland Wohlgenouth and Ester Nemethy (C/O Solar Energy Group of the Lawrence Berkeley Laboratory, University of California, Berkeley) according to the procedure described by OKUNO et al./86/. They have dissolved an appropriate amount of the compounds meso-tetra (4 - pyridyl) - pophyrin (TP_yP) and 1 - bromohexadecane ($1\text{-}C_{16}H_{33}Br$) in dimethylformamide. By refluxing that solution under nitrogen, a quaternization of TP_yP leads to the formation of the mono-, di-, tri-, and tetraquaternized porphyrins. These different species of surfactant porphyrins were separated by gel-permeation chromatography with Sephadex LH-20. By reacting a mono-quaternized porphyrin and a manganese salt (manganese acetate tetrahydrate) or a zinc salt (zinc acetate dihydrate) in dimethyl-formamide, they have obtained the two compounds mentioned above. Equation (3.9) summarizes the different steps of these reactions:

$$(TP_yP) + (1 - C_{16}H_{33}Br) \xrightarrow[N_2]{\text{dimethylformamide}} (TP_yP\text{-}C_{16}) \xrightarrow{Mn^{III}} MnTP_yP\text{-}C_{16}$$

$$(TP_yP) + (1 - C_{16}H_{33}Br) \xrightarrow[N_2]{\text{dimethylformamide}} (TP_yP\text{-}C_{16}) \xrightarrow{Zn^{II}} ZnTP_yP\text{-}C_{16} \qquad (3.9)$$

The purity was checked by high purity liquid chromatograph (HPLC) on a rheodyne NH_2 column in a mixture of $CHCl_3/CH_3OH$ (95/5) /87/.

The most used electron acceptor, N, N'- bis (sulfonato-n-propyl) - 4,4' - bipyridyl or propyl viologen sulfonate (PVS°) was prepared by reacting 4, 4' - bipyridine dihydrate with 1, 3 - propanesultone, following the procedure described by Wohlgemuth et al./87/.

The colloidal suspension of ultrafine platinum catalysts was prepared by the reduction of hydrogen hexachloroplatinate hydrate (H_2PtCl_6, Aldrich Chemical Co., Inc.) with a 1 percent sodium citrate solution, following the method of Turkevich et al./88/. These ultrafine platinum catalysts were stabilized by a negatively charged polymer,

carbowax - 20M. The concentration of colloidal platinum was estimated by use of a spectrophotometer, the extinction coefficient at 450 nm being taken as 2.3 x $10^3 M^{-1}$ x cm^{-1}/27/. The concentration thus obtained was about 40 µg Pt/ml.

The other chemical compounds used: 5 - hexenoic acid, hexanoic acid, sodium dodecyl sulfate, methyl viologen (MV^{2+}), ethylenediamine tetraacetic acid disodium salt (EDTA), tris (2 - hydrixymethyl) amine (TEA), tris (2, 2' - bipyridinium) ruthenium (II) chloride hexahydrate ($Ru(bpy)_3^{2+}$), methanol and chloroform, were obtained from commercial supplies (Fluka Chemical Corporation, Hauppauge, NY 11787 and Strem Chemicals, Newsburyport, Mass 01950) and were used without further purification. Water was deionized first, then was twice deionized by a Millipore, Milli. Q Water Purification System.

Sample solutions

For the experience of the dye-sensitized reduction of water to hydrogen, the sample consisted of 3.5 ml of an aqueous solution containing the tris (2, 2' - bipyridine) - ruthenium (II) complex, $Ru(bpy)_3^{2+}$ ($4x10^{-5}M$), as a sensitizer; methyl viologen, MV^{2+} ($4x10^{-3}M$), as an electron acceptor relay; ethylenediamine tetraacetic acid disodium salt dihydrate, EDTA (1.5 x $10^{-2}M$), as a sacrificial electron donor; and colloidal platinum ($10^{-5}M$: Carbowax - 20 M protected Pt particles of 32 - A° diameter), as a charge storage catalyst. A Corning pH meter was used to measure the pH of the solution; in this experiment, the pH was adjusted to 6.0 by adding concentrated NaOH or HCl.

For other experiments in which the Mn- tetrapyridyl porphyrin derivative ($MnTP_yP\text{-}C_{16}$) was used as the first electron donor or in which we wanted to check the photocatalyst importance of the latter, the sample consisted of a 3 ml of an aqueous micellar solution containing the following chemicals: sodium dodecyl sulfate (1.1 x $10^{-2}M$ SDS), Zn-tetrapyridyl porphyrin derivative(5 x $10^{-6}M$ Zn $TP_yP\text{-}C_{16}$), Mn(III) - tetrapyridyl porphyrin derivative (6.3 x $10^{-6}M$ $MnTP_yP\text{-}C_{16}$) and propyl viologen sulfonate (4.6 x 10^{-4} M PVS°). For some experiments these 3 ml also contained either an appropriate amount of 5 - hexenoic acid or that of hexanoic acid.

3.5.2. Experimental procedure

(a) Experimental precautions

Prior to sample illumination, each sample solution was deaerated by repeated evacuation and flushing with highly purified argon gas. Ar gas was purified by active copper at 150°C.

The use of deaerated sample solutions is indispensable because the presence of oxygen would inhibit the dye-sensitized photochemical reactions in at least two ways.

(i) First, oxygen reactswith the excited states of the sensitizers that we have used; for example, since oxygen is a very strong electron acceptor, it would compete with the electron acceptors chosen for the photochemical conversion and storage of light energy.

(ii) Second, the reduced ion radicals of the electron acceptors (viologens) that we have used, in this work, are unstable in the presence of oxygen. In the case of methyl viologen (MV^{2+}), the reduced positive ion radical ($MV^{+\cdot}$) very quickly reacts with oxygen in the following manner /36,37/(Eq.3.10):

$$MV^{+\cdot} + O_2 \rightarrow MV^{2+} + O_2^{-} \qquad (3.10)$$

(b) Sample irradiation

Sample solutions irradiation was carried out with a highly collimated (parallel) beam from an oriel 1000 watt xenon arc lamp (the operating voltage and current are 25V and 40A, respectively). The xenon arc lamp power supply (the oriel 8540 regulated D.C. power supply) contains an ignition system which provides high voltage (20-30KV) RF energy for a fraction of second to start the lamp. In fact, this high voltage ionizes the xenon gas and creates a conduction nate.
An arc is then established and maintained by a low voltage D.C. current flow. When cold xenon gas fills the xenon arc lamp to a few atmospheres pressure. During the operating conditions, the pressure appreciably increases (50-70 atmospheres). The high pressures and corresponding high molecular densities allow the dissipation of a large amount of power in a small space. The light source thus created is extremely small and intense and is perfectly convenient (suitable) for any application requiring a high intensity on a small target or a highly collimated beam.

Infrared radiation was removed by passing the incident light beam through a 10-cm aqueous cupric sulfate solution (100 g/ℓ). Visible light impinging on the sample solutions was restricted to some specific narrow bands using either a UV filter with a cutoff at 400nm or two narrow band interference filters with maximum transmittance at 430nm and 460nm, respectively, and a transmittance bandwith equal to 10nm.

(c) Measurement of the rates of formation of oxidized or reduced species

Absorption spectra of oxidized or reduced species resulting from the photoinduced redox reactions were recorded with a Hewlett-Packard 8450A UV/VIS Spectrophotometer with a HP 7225A Graphics Plotter. All sample solutions were placed into a 1.0 cm optical pathlength quartz cuvette or a glass cuvette. Each sample solution was continuously stirred by means of a teflon stirring bar throughout the irradiation period in order to avoid the accumulation of photoproducts in the irradiated area.

The number of moles of reduced species (PVS^- and MV^+) or that of oxidized species (Mn^{IV} TP_yP - C_{16}) produced by illumination of sample solutions were determined by measuring the optical densities of these species at some specific wavelengths: λ = 602nm (for PVS^- and MV^+) and λ = 424nm (for Mn^{IV} TP_yP - C_{16}).
The molar extinction coefficients of these compounds are /77,87/:

$$\varepsilon_{602}(PVS^-) = 1.41 \times 10^4\ M^{-1} \times cm^{-1}$$

$$\varepsilon_{602}(MV^+) = 1.13 \times 10^4\ M^{-1} \times cm^{-1}$$

$$\varepsilon_{424}(Mn^{IV}) = 7.4 \times 10^4\ M^{-1} \times cm^{-1}$$

(d) Measurement of the critical micelle concentration (CMC) of sodium dodecyl sulfate (SDS)

We have determined the CMC of SDS dissolved either in bidistilled water or in a mixture of bidistilled water and methanol, by measuring the A.C electric conductivity of SDS solutions as a function of SDS concentration, using the YSI Model 31 conductivity bridge.

The measurement of the electric conductivity of SDS solutions requires an alternating voltage source in order to minimize the effects of polarization at the surface of the electrodes. If a D.C voltage source was used, there would be a permanent accumulation of charges at the surface of the electrodes; the accumulated charges would create an antagonist electric field with respect to the applied electric field. In addition, charge accumulation at the electrode surface would involve inhomogeneous concentration in the measurement cell.

The electrodes of the cell (YSI Model 3401 conductivity pyrex cell) used for electric conductivity measurements are coated with platinum black. The aim of this coating is to minimize the effect of electrode polarization

which might happen during a half-period: in fact, platinum black is a porous substance which increases the surface of electrode contact with the solution and diminishes the charge of polarization per unit surface.

With the YSI model 31 conductivity bridge, the conductance of solution is directly measured. The conductivity of the solution is the conductance value in micromhos/cm times the "cell constant" (K). This constant depends on the geometrical configuration of electrodes. Cells with constants K equal to 1.0 or greater normally have widely spaced electrodes while cells with constants of 0.1 or less have large electrodes which are closely spaced. The former should be used for solutions with resistivities less than about 50,000 Ω x cm and conductivities of more than 20 μmhos/cm. In our measurements, we have used a conductivity pyrex cell (YSI 3401 conductivity cell) with constant K = 1.0.

The principle of electric conductivity measurement is the following. The YSI Model 31 conductivity bridge utilizes a manually balanced AC bridge which can operate either at 60 Hz or 1 KHz. The bridge output is amplified and applied to the grid of an indicator tube. As the bridge output approaches zero, a rectangular "shadow" appears on the screen of the indicator tube. When a maximum "shadow" is obtained, the corresponding conductance is then read from a readout dial.

(e) Measurement of the number of moles of hydrogen produced in the dye-sensitized reduction of water

Hydrogen in the gas phase was detected by gas chromatography using the Varian Model 3700 Gas Chromatograph. After illumination time intervals equal to one minute, by means of a Hamilton 700-series microliter syringe, we have withheld beforehand 250 μℓ of gas on the top of the appropriate sample solution and we have injected them in the Varian 3700 G.C. Hydrogen was detected by the Gow-Mac thermal conductivity detector of the Varian 3700 G.C. with a detection limit of 10^{-9} moles. The Varian 3700 G.C. is provided with a molecular sieve 5A° column which is designated to protect the thermal conductivity detector from moisture and the eventual impurities of the carrier gas (argon).

The results of the measurement were quantitated by relating the peak areas to a calibration curve. This curve was established from measurements of area peaks corresponding to well-known H_2 concentrations in a H_2/Ar mixture.

(f) Determination of the quantum efficiency for the dye-sensitized reduction of water to hydrogen

The efficacy of a photochemical process is expressed in terms of the quantum efficiency, which is the ratio of the number of moles of a compound produced in that process, for a given period of time, to the number of moles of monochromatic photons absorbed, during the same time, by the sensitizer:

$$\phi = \frac{N_C}{N_{ph}}$$

Where N_C and N_{ph} are the number of moles of compound and of that of photons, respectively.

f.1 Measurement of the light intensity

1°) Chemical actinometry method

Referring to the procedure described by Wegner and Admson /32/, chemical actinometry with Reinecke salt ($K[Cr(NH_3)_2(NCS)_4]$) was chosen for the measurement of the incident light intensity (incident photon flux). We have dissolved 0.15 g of Reinecke salt in 10 ml of deionized water, and the solution was filtered just before use. The pH of the solution thus obtained was adjusted to about 3.5 by adding concentrated H_2SO_4. A portion of the solution of Reinecke salt was kept in the dark to be used as a reference. Another portion was illuminated and, after a certain period of illumination, an aliquot of 0.1 ml was withdrawn from both the illuminated solution and that kept in dark and each added into a 2.9 ml solution of 0.1M $Fe(NO_3)_3$ in 0.5M H_2SO_4. In the illuminated solution, a ferrothiocyanate complex is formed /32/ (Eq.3.11):

$$K[Cr(NH_3)_2(SCN)_4] \xrightarrow{h\nu} [K\ Cr(NH_3)_2]^{4+} + 4(SCN^-) \quad (3.11)$$

$$4(SCN^-) \downarrow (Fe^{3+}) \rightarrow 4[Fe(SCN)]^{2+}$$

We have taken the absorption spectrum of the $[Fe(SCN)]^{2+}$ complex using the solution kept in dark as the reference. The peak of the absorption spectrum of the $[Fe(SCN)]^{2+}$ complex is located at a wavelength λ = 450nm and the molar extinction coefficient at this wavelength is, $\varepsilon_{450} = 4.30 \times 10^3\ M^{-1} \times cm^{-1}$. Since the complex does not react, the optical density at this wavelength allows us to determine the concentration of the $[Fe(SCN)]^{2+}$ complex, which is equal to the concentration of SCN^- ions or that of photons absorbed by the Reinecke salt. With the 1000 W xenon arc lamp, the light intensity impinging on each sample solution was measured to be approximately 7.61×10^{-6} einsteins/-$cm^2 \times min$.

2°) Direct measurement using a photometer

The incident light intensity was directly measured with the EG & G Model 450 Photometer (EG & G Inc., 35 Congress. St., Salem, Massachussetts 01970) in conjunction with a B 1669 flat filter and OD-4 neutral density filter. The latter filter which uniformely attenuated the incident light intensity in the spectral region being investigated, also aimed to protect the photometer which does not support an irradiance greater than 2×10^{-3} W/cm^2. The B 1669 flat filter corrected the reponse of the detector and maintained it at a sensibility of the order of 7 %.

The value of the incident photon flux obtained by direct measurement with EG & G photometer is almost equal to that obtained by the chemical actinometry method.

f.2 Determination of the number of moles of photons absorbed by the sensitizer

The number of moles of photons impinging on the cell containing a sample solution and whose wavelengths are included in the interval between λ and $\lambda + \lambda d$ is given by:

$$dN_1 = N_o \, T_f(\lambda) d\lambda \qquad (3.12)$$

Where N_o is the number of moles of photons impinging on the filter being used, and $T_f(\lambda)$ is the transmittance of this filter at the wavelength λ. The fraction which is absorbed by the sensitizer is given by:

$$1 - T_S(\lambda) = 1 - 10^{-A_S(\lambda)} \qquad (3.13)$$

Where $T_S(\lambda)$ and $A_S(\lambda)$ are respectively, the transmittance and absorbance of the sensitizer at the wavelength λ. The number of moles of photons absorbed in the interval of wavelengths between λ and $\lambda + d\lambda$ is given by:

$$dN_2 = N_o[1 - T_S(\lambda)]T_f(\lambda)d\lambda = N_o[1 - 10^{-A_S(\lambda)}]T_f(\lambda)d\lambda$$

Thus, the number of moles of photons absorbed by the sensitizer is given by the following integral:

$$N_2 = \int_{\lambda min}^{\lambda max} N_o[1 - 10^{-A_S(\lambda)}]T_f(\lambda)d\lambda \qquad (3.14)$$

In the case of the filters that we have used in our experiments, the interval of their transmittance is such that we may restrain λ_{min} at 400nm and λ_{max} at 480nm.

Normally, the convolution between the filter function and the absorption curve of the sensitizer should enable one to determine the number of moles of photons absorbed by the sensitizer. In order to avoid the difficulties related to numeric integration, we have determined the relative number of moles of photons absorbed from the ratio between the area under the transmittance curve of the filter being used and the area under the absorption spectrum of the sensitizer.

In fact, the number of moles of photons impinging on the cell containing the sample solution is proportional to the area under the transmittance curve, which is:

$$a_1 = \int_{\lambda min}^{\lambda max} T(\lambda)d\lambda. \qquad (3.15)$$

The number of moles of photons absorbed by the sensitizer is proportional to the area under the curve $[1 - 10^{-A_S(\lambda)}]T_f(\lambda)$, which is:

$$a_2 = \int_{\lambda min}^{\lambda max} [1 - 10^{-A_S(\lambda)}]T_f(\lambda)d\lambda \qquad (3.16)$$

The ratio between the areas mentioned above is equal to the ratio between the weights of the pieces of papers under the transmittance curve and the absorption spectrum curve. Thus, the ratio between the two weights permits us to determine N_2:

$$N_2 = N_1 \times \frac{m_2}{m_1}$$

far away from the convolution method!

Where m_1 and m_2 are the weights of the pieces of papers corresponding to a_1 and a_2, respectively; N_1 has the same meaning as in equation (3.12).

This method of determining the number of moles of photons absorbed by the sensitizer, from the convolution between the filter function and the absorption curve of the sensitizer, is a crude way. For the method to work even approximately, the following conditions must be fulfilled:

(i) First, the filter function and the absorption spectrum of the sensitizer should be centered at the same wavelength.
Obviously if they are very far apart the absorption would be near zero, yet the product of the areas would still be the same. The filter that we

have used in the experiment dealing with the dye-sensitized reduction of water to hydrogen, has a maximum transmittance at 460nm. Besides, the peak of the absorption spectrum of the tris (2, 2' - bipyridine)-rutherium (II) sensitizer is located at (460 ± 10)nm. Then the condition mentioned above is almost satisfied.

(ii) Second, the simple product of convolution is only applicable if the absorbance of the solution is low. If most of the light is being absorbed already, then increasing the concentration, and thus the area under the absorption curve, will not produce much of a further increase.

3.6. Results and discussions

3.6.1. Dye-sensitized reduction of water to hydrogen

In the topic of the dye-sensitized reduction of water to hydrogen, one of the well-investigated /27,70,78/ systems is the following four-component system: (EDTA/$Ru(bpy)_3^{2+}$/MV^{2+}/Pt). We have used this system in order to determine the quantum yield for production of hydrogen under optimized experimental conditions (e.g., the pH of the solution, the concentrations of the various reactants, the size of the platinum catalyst and the polymer used to protect the platinum particles). Although this system has been widely investigated various experimental condition have been used, different methods have been used to detect hydrogen, different methods have been used to determine the quantum yield for its production and in many publications, the quantum yield (an important experimental feature of a photochemical reaction) is not reported.

The concentrations of the various reactants of the system (EDTA/$Ru(bpy)_3^{2+}$/MV^{2+}/Pt) as well as the pH of the sample solution are indicated at page 92. The kinetics and mechanisms of the primary photoinduced electron transfer reactions which follow immediately after light absorption by the sensitizer have been extensively investigated by means of flash photolysis techniques /29,77,78/. When the system is irradiated at 460nm wavelength (value which is close to the absorption maximum of the sensitizer) the $Ru(bpy)_3^{2+}$ sensitizer is excited to some vibrational level of the excited singlet state. This excited singlet state very quickly transforms to an excited triplet state. The lowest excited triplet state is a metastable state and it has a long life time ($\tau \cong 10^{-3}$ s) so that it can be detected chemically. In a diffusion controlled mechanism, the lowest excited triplet state of $Ru(bpy)_3^{2+}$ transfers an electron to methyl viologen (MV^{2+}) and goes to $Ru(bpy)_3^{3+}$ while methyl viologen is reduced to the monocation radical ($MV^{+\cdot}$)(Eq.3.18):

$$Ru(bpy)_3^{2+} \xrightarrow{h\nu} [Ru(bpy)_3^{2+}]^{*S} \xrightarrow{h\nu} [Ru(bpy)_3^{2+}]^{*T}$$

$$[Ru(bpy)_3^{2+}]^{*T} + MV^{2+} \longrightarrow MV^{+\cdot} + Ru(bpy)_3^{3+} \qquad (3.18)$$

$Ru(bpy)_3^{3+}$ is a very strong oxidant; it takes an electron from EDTA. Then, the initial state of the sensitizer is regenerated. EDTA is a sacrificial electron donor and it undergoes an irreversible oxidation: the oxidized EDTA, $(EDTA)_{OX}$, is unstable and decomposes rapidly into CO_2, formaldehyde, and ethylenediamine triacetic acid /70a/. The thermal back electron transfer reaction between $Ru(bpy)_3^{3+}$ and $MV^{+\cdot}$ is prevented by this irreversible process. The electrostatic repulsion between the two positively charged photoproducts is another factor which may help to retard the thermal back electron transfer.

When the three-component system ($EDTA/Ru(bpy)_3^{2+}/MV^{2+}$) has been perfectly degassed, stable $MV^{+\cdot}$ is photogenerated and it can be detected easily: while the non illuminated three-component system is colorless, the system turns to blue color as soon as the solution is illuminated; this indicates that $MV^{+\cdot}$ is formed and this fact allows the reaction to be followed quantitatively. For quantitative measurements, it is known that methyl viologen reduced to one electron stage has characteristic absorption maxima at 395nm and 602nm. We have followed spectrophotometrically the rate of reduction of methyl viologen by measuring the optical density of the monocation radical ($MV^{+\cdot}$) at 602nm; the molar extinction coefficient of $MV^{+\cdot}$ at 602nm is /77/: $1.13 \times 10^4\ M^{-1} \times cm^{-1}$. On figure 3.4, we present the number of moles of $MV^{+\cdot}$ photogenerated as a function of the number of moles of photons absorbed by the $Ru(bpy)_3^{2+}$ sensitizer. From figure 3.4, the quantum yield for production of $MV^{+\cdot}$, determined using an interferentiel filter with a transmittance maximum at (460 ± 10)nm is (0.75 ± 0.05).

In the four-component system ($EDTA/Ru(bpy)_3^{2+}/MV^{2+}/Pt$), the photogenerated $MV^{+\cdot}$ is thermodynamically capable of reducing water to hydrogen (Eq.3.19): first, the redox potential of the $MV^{2+}/MV^{+\cdot}$ couple is equal to - 0.44V, while that of the H^+/H_2 couple is equal to - 0.41V, at pH = 7; second, the partial pressure of hydrogen that is produced is very low. Since the standard redox potentials are almost equal, actually, what makes the reaction go in this case is the very low partial pressure of H_2 that is produced.

$$2MV^{+\cdot} + 2\ H_2O \xrightarrow{Pt/carbowax} 2\ MV^{2+} + 2\ OH^- + H_2 \qquad (3.19)$$

In fact, the build up of the blue color characteristic of $MV^{+\cdot}$ was no more observed in the presence of colloidal platinum; instead hydrogen was produced and its evolution could be detected by the Gow-Mac thermal conductivity

detector of the Varian Model 3700 Gas Chromatograph (see details at page 96).

Figure 3.5 summarizes the main features of the four-component system used for the dye-sensitized reduction of water to hydrogen. As it is shown, the system photoproduces hydrogen at the expense of consuming the sacrificial electron donor, EDTA. One molecule of EDTA is consumed whenever a molecule of H_2 is produced. The rate of H_2 formation should remain constant yielding one H_2 molecule per one EDTA molecule consumed until the quantity of EDTA remaining in the solution is insufficient for regenerating all the sensitizer molecules. If we take into account our experimental conditions (see page 93) we may predict that the rate of H_2 formation should remain constant until more than 97 % of the EDTA is consumed.

Figure 3.6 presents the rate of H_2 evolution as a function of the number of moles of photons absorbed by the $Ru(bpy)_3^{2+}$ sensitizer. The number of moles of H_2 evolved varies linearly with time and this should be expected as long as the quantity of EDTA remaining in the solution is sufficient to recycle all the sensitizer molecules. From Figure 3.6, we have determined the quantum yield for production of hydrogen: if we take into account that it takes two quanta to produce one H_2 molecule, the value obtained is (0.32 ± 0.02).

The values obtained for the quantum yield for photoproduction of MV^+ and H_2 are in agreement with those obtained by Harriman et al./29/, using as a sensitizer, the zinc-meso-tetramethyl(4-pyridyl) porphine ($ZnTMP_yP^{4+}$).

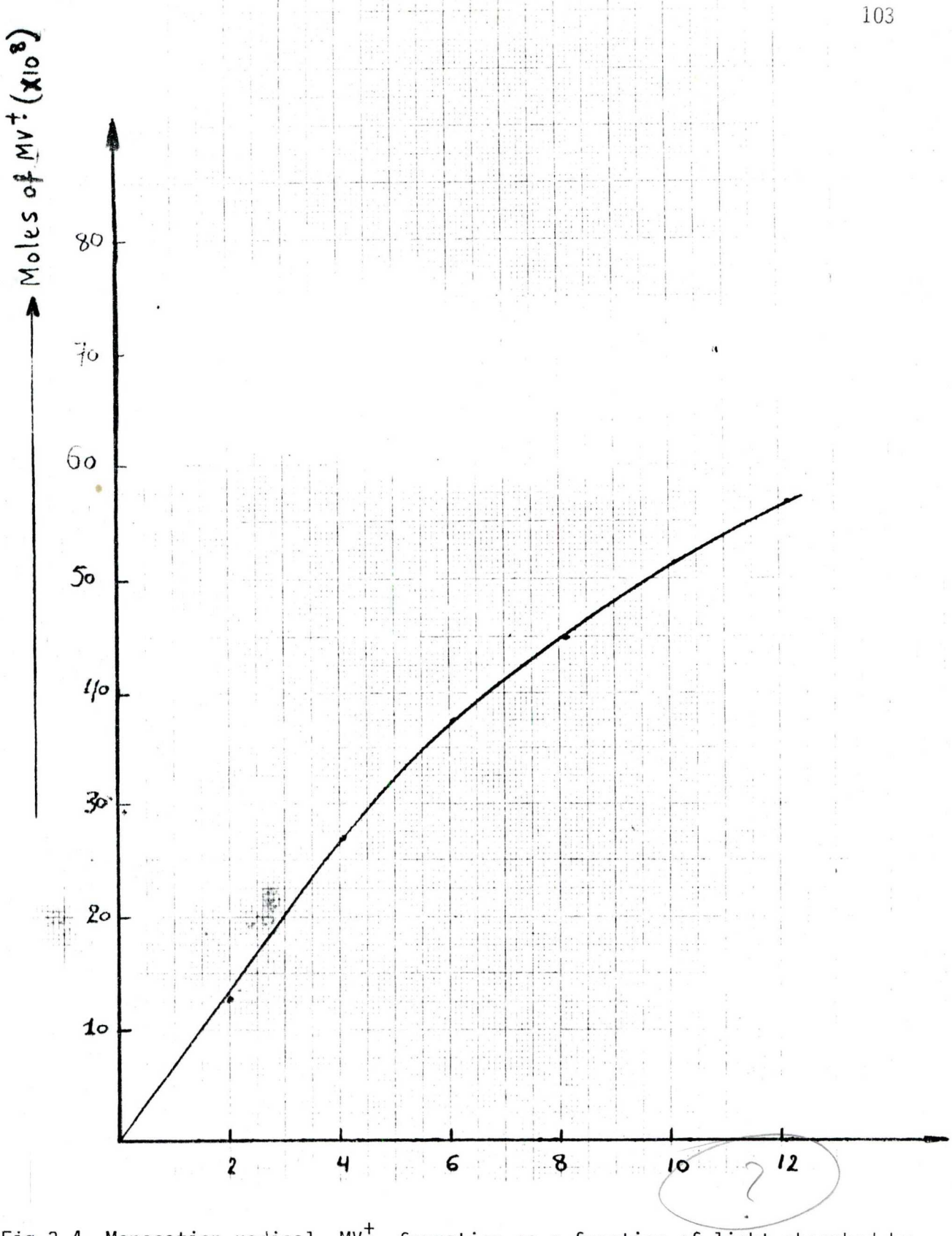

Fig.3.4. Monocation radical, MV^{+}, formation as a function of light absorbed by $Ru(bpy)_3^{2+}$ (4×10^{-5}M) in the presence of the sacrificial electron donor, EDTA (1.5×10^{-2}M). The concentration of MV^{+} has been determined by measuring its optical density at 602nm (see details in the text).

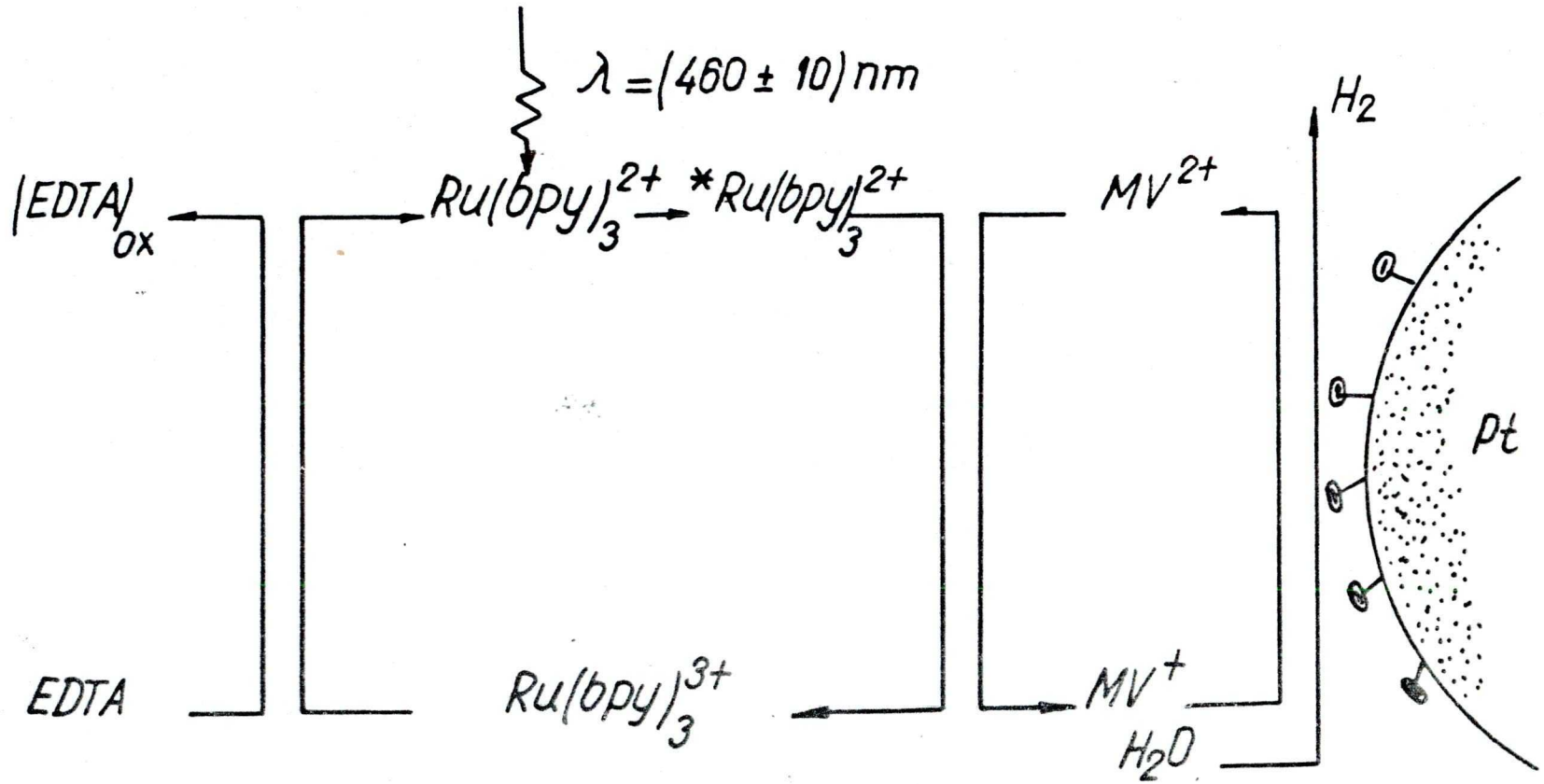

Fig.3.5. Reaction scheme for the four-component system (EDTA/$Ru(bpy.)_3^{2+}$/ MV^{2+}/ Pt) used in the dye-sensitized reduction of water to hydrogen.

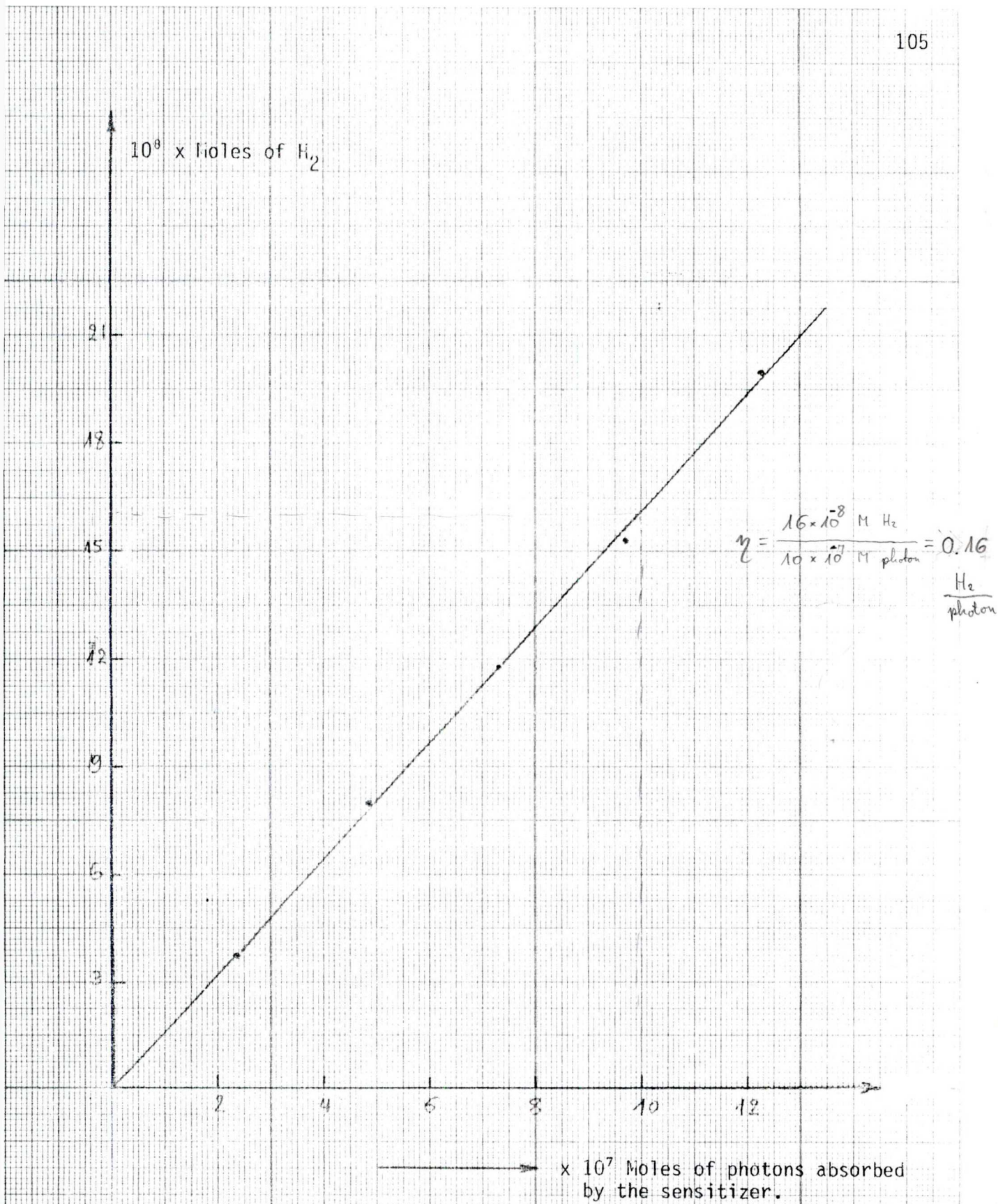

Fig.3.6. Rate of H_2 evolution as a function of the number of moles of photons absorbed by $Ru(bpy)_3^{2+}$ (4×10^{-5} M). The concentrations of other reactants were: EDTA(1.5×10^{-2} M); MV^{2+} (4×10^{-3} M); Colloidal platinum(10^{-5} M). The pH of the mixture was 6.
The sample was irradiated at (460 ± 10)nm.

3.6.2. Photochemical oxidation of a Mn(III)-tetrapyridyl porphyrin derivative by an Zn-tetrapyridyl porphyrin derivative in aqueous micellar solutions of sodium dodecyl sulfate.

In Figures 3.7 and 3.8 the A.C. conductivity of aqueous solutions of sodium dodecyl sulfate (SDS) are presented as a function of the surfactant concentration. If we consider the regions of discontinuity, we find that the critical micelle concentration of SDS is approximately $(0.80 \pm 0.13) \times 10^{-2}$ Moles/litre for SDS dissolved in bidistilled water and $(0.93 \pm 0.24) \times 10^{-2}$ Moles/litre for SDS dissolved in a mixture of bidistilled water and methanol (13:1). The values that we have obtained are in agreement with those indicated by Mukerjee and Mysels /84/ and by Fendler /85/, where other methods have been used.

?

see the figure

Why is it important to determine exactly the c.m.c.?
Can not be used above the c.m.c.?

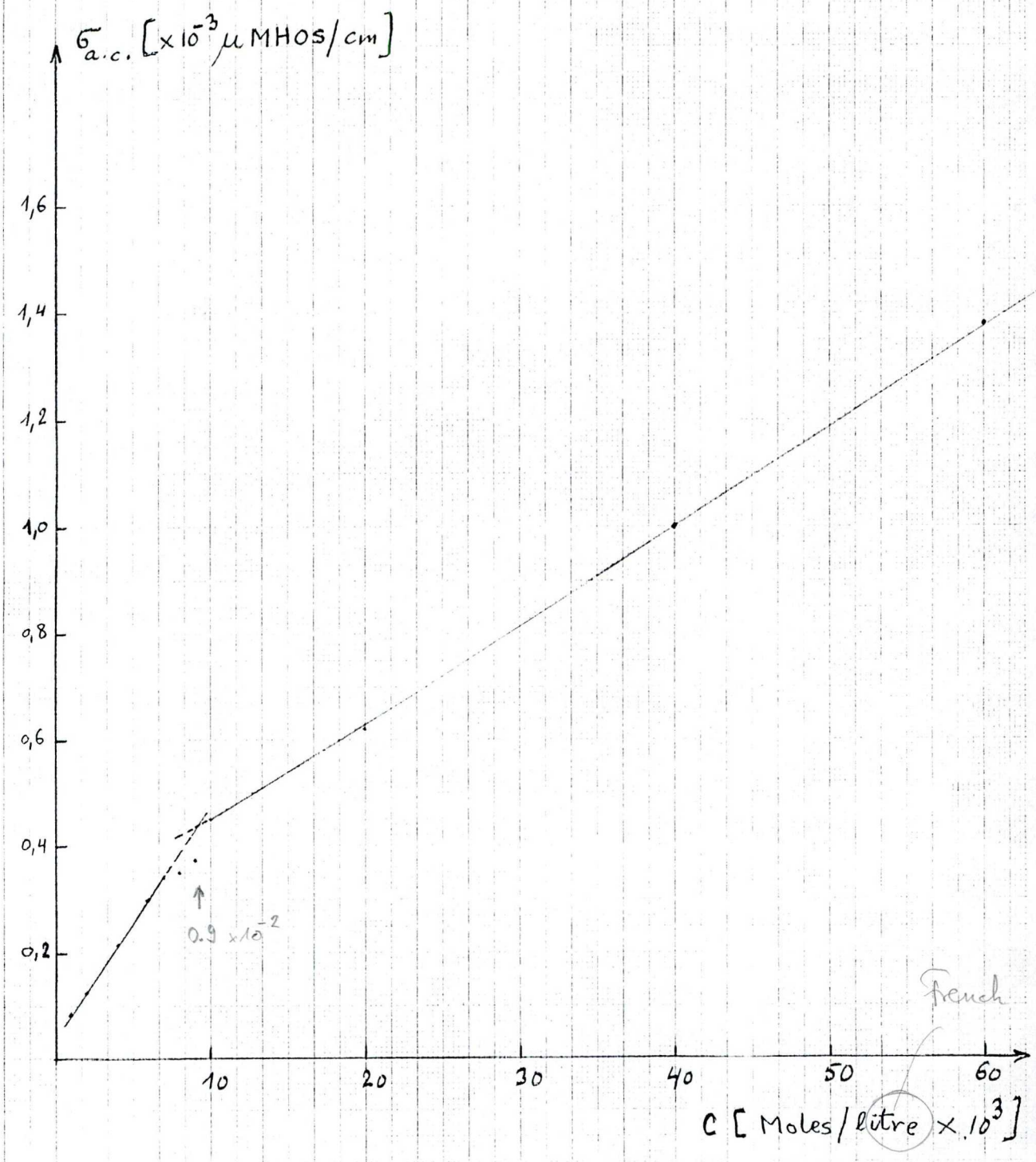

Fig.3.7 . Determination of the critical micelle concentration(CMC) of sodium dodecyl sulfate(SDS). The surfactant was dissolved in bidistilled water. This figure presents the A.C. conductivity as function of the concentration of the surfactant.

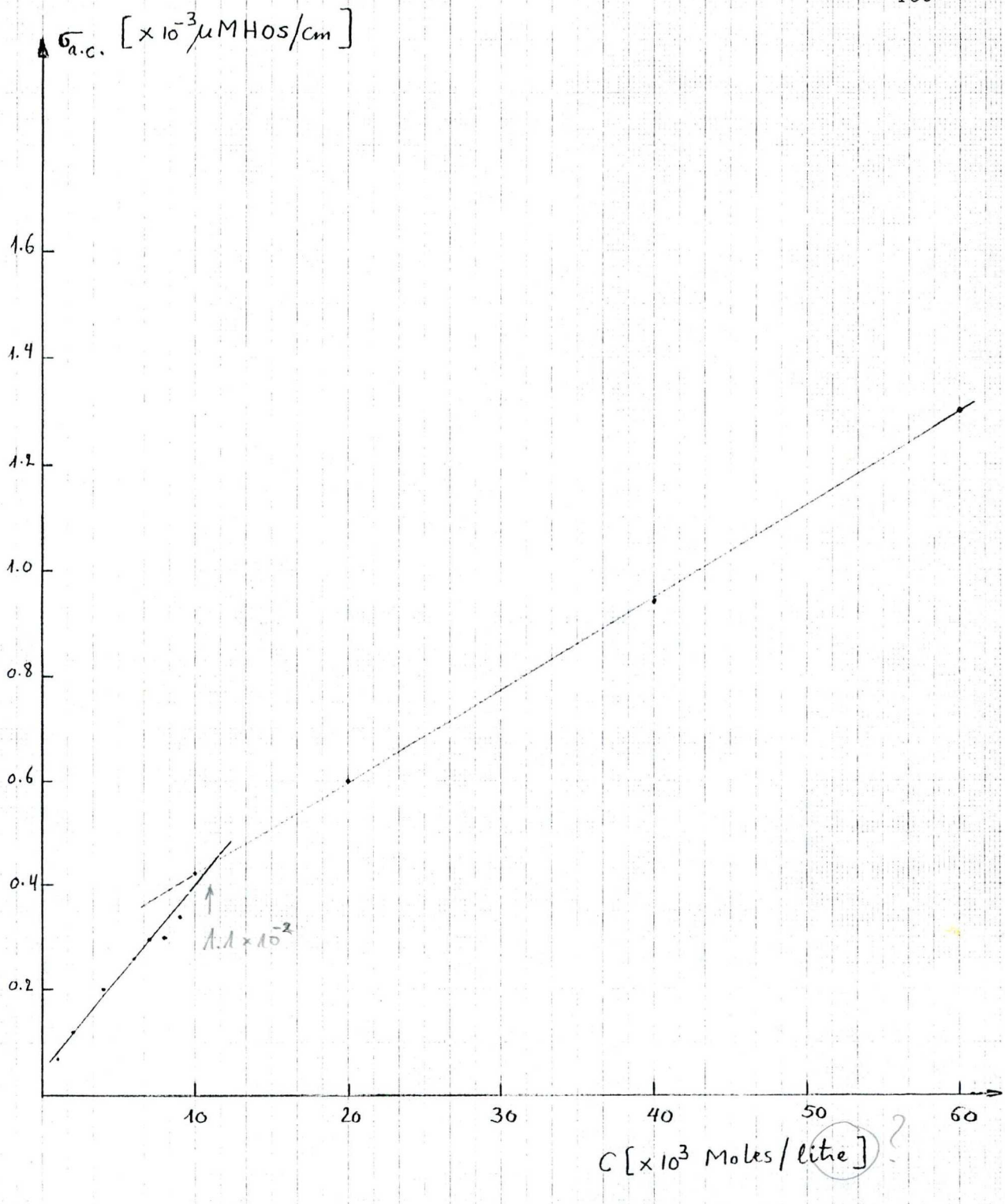

Fig.3.8. Determination of the critical micelle concentration(CMC) of sodium dodecyl sulfate(SDS). The surfactants were dissolved in a mixture of water-methanol (15:1). This figure represents the A.C. conductivity as function of the concentration of the surfactan

In figure 3.9 a schematic representation of the organization of the sensitizer ($ZnTP_yP\text{-}C_{16}$), the electron donor ($MnTP_yP\text{-}C_{16}$) in a micelle of sodium dodecyl sulfate (SDS), is presented. The electron acceptor (PVS°) is in the aqueous phase. When the heterogeneous photochemical system is illuminated at (430 ± 5)nm, the sensitizer ($ZnTP_yP\text{-}C_{16}$) becomes electronically excited to the singlet state, which very quickly transforms to the excited triplet state. The excited triplet state of the sensitizer transfers an electron to propyl viologen sulfonate (PVS°) and goes to $ZnTP_y^+P\text{-}C_{16}$) while PVS° is reduced to PVS^-. Being negatively charged, PVS^- is repelled by the negative interface of the SDS micelle. The oxidized sensitizer, $ZnTP_y^+P\text{-}C_{16}$, is reduced by the electron donor, $Mn^{III}TP_yP\text{-}C_{16}$; then the sensitizer is recycled while $Mn^{III}TP_yP\text{-}C_{16}$ is oxidized to $Mn^{IV}TP_yP\text{-}C_{16}$, a compound which has a characteristic absorption peak at a wavelength λ = 424nm. We have followed the reaction spectrophotometrically by measuring the optical density changes with illumination times.

They are very close. How could you determine the number of photons, absorbed solely by the sensitizer?

Figure 3.10 shows the difference spectra of system I (6.3×10^{-6}M $Mn^{III}TP_yP\text{-}C_{16}$; 4.6×10^{-4}M PVS°; 1.1×10^{-2}M SDS and 5×10^{-6}M $ZnTP_yP\text{-}C_{16}$) vs. system II(6.3×10^{-6}M $Mn^{III}TP_yP\text{-}C_{16}$; 4.6×10^{-4}M PVS° and 1.1×10^{-2}M SDS). The spectrum obtained at zero time should simply be that of $ZnTP_yP\text{-}C_{16}$. The increase of optical absorbance at approximately 430nm with successive irradiation is due to $Mn^{IV}TP_yP\text{-}C_{16}$ photoproduction. However, according to Figure 3.10, the rate of the disappearance of $Mn^{III}TP_yP\text{-}C_{16}$ (negative peak at approximately 460nm) seems to be smaller than the apparent rate of the increase of $Mn^{IV}TP_yP\text{-}C_{16}$. The rate of the disappearance of $Mn^{III}TP_yP\text{-}C_{16}$ should be equal to the rate of the increase of $Mn^{IV}TP_yP\text{-}C_{16}$. The fact that these rates seem to be different according to Figure 3.10 may be explained as follows: although the concentration of the sensitizer ($ZnTP_yP\text{-}C_{16}$) is assumed to remain constant during successive irradiations, when the absorption spectra of the photoproducts (PVS^-, $Mn^{IV}TP_yP\text{-}C_{16}$) vary, the absorption spectrum of the sensitizer "follows" slightly (i.e., the absorption spectrum of the sensitizer does not recover its absorption spectrum at zero time). Then, in Figure 3.10, both $Mn^{IV}TP_yP\text{-}C_{16}$ and $ZnTP_yP\text{-}C_{16}$ are responsible for the increase of absorbance around 430nm. It is obvious that the contribution of $Mn^{IV}TP_yP\text{-}C_{16}$ to the peak around 430nm is much greater than that of $ZnTP_yP\text{-}C_{16}$.

versus wavelength

The donor in the sensitizer?

$\lambda_{exc} = 430$ nm

In Figure 3.13b the rate of propyl viologen radical (PVS^-) formation as a function of the illumination time is presented. This rate was determined by measuring the optical density changes at 602nm (the molar extinction coefficient of PVS^- at this wavelength is equal to $1.41 \times 10^4 M^{-1} \times cm^{-1}$) as a function of the illumination time. The initial slope (i.e., the rate of PVS^- formation) to the curve of Figure 3.10 is equal to 1.1×10^{-8} Moles x min^{-1}.

The model presented in Figure 3.9. agrees quite well with the experiment described above and shows that by illuminating the heterogeneous photochemical system designated "system I", we have dye-sensitized a photo-induced electron transfer along the interface of the SDS micelle from the $MnTP_yP\text{-}C_{16}$ donor to the PVS° electron acceptor through the $ZnTP_yP\text{-}C_{16}$ sensitizer in its excited triplet state, and we have achieved, photochemically, the oxidation of $MnTP_yP\text{-}C_{16}$ from the Mn^{3+} oxidation state to the Mn^{4+} oxidation state and at the same time, the propyl viologen sulfonate (PVS°) was reduced in the aqueous phase.

FIGURE 3.9

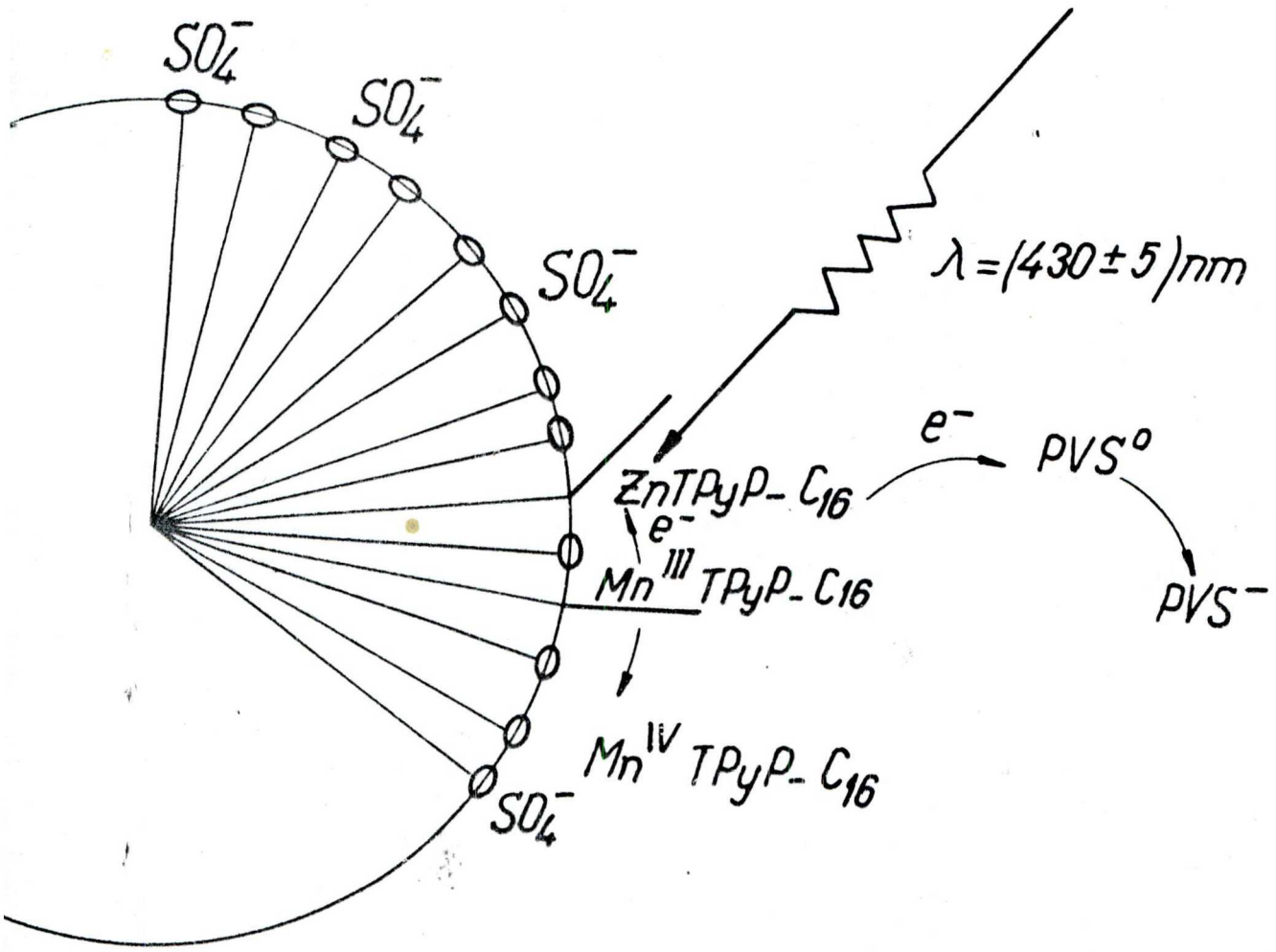

Fig.3.9. Schematic representation of the organization of the sensitizer ($ZnTP_yP\text{-}C_{16}$), the electron donor ($Mn^{III}TP_yP\text{-}C_{16}$) in a micelle of sodium dodecyl sulfate with the electron acceptor(PVS°) in the aqueous phase.

igure 3.10: Rate of formation of PVS^- and $Mn^{IV}TP_yP - C_{16}$ (interval ?
of illumination : 1 minute). We have recorded the difference
absorption spectrum of system I (6.3×10^{-6} M $Mn^{III}TP_yP - C_{16}$;
4.6×10^{-4} M PVS°; 1.1×10^{-2} M SDS and 5×10^{-6} M $ZnTP_yP - C_{16}$)
vs. system II (6.3×10^{-6} M $Mn^{III}TP_yP - C_{16}$;
4.6×10^{-4} M PVS° and 1.1×10^{-2} M SDS).
The pH of system I and system II ~~was~~ were 7.0 buffered?

What are the individual spectra?
More legend required!

$E_h = ?$

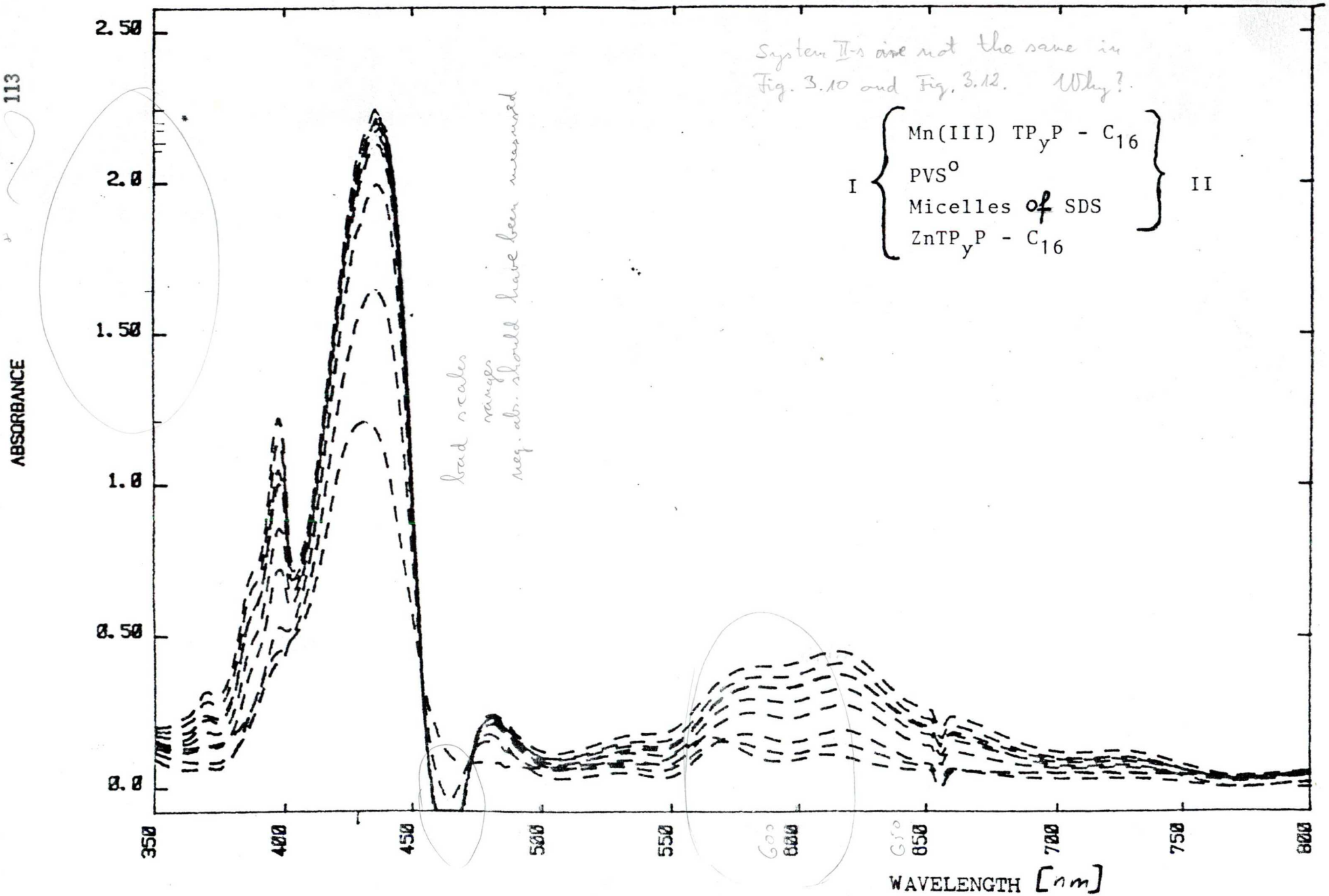

System II-s are not the same in Fig. 3.10 and Fig. 3.12. Why?

Scale ranges req. should have been measured

In a second experiment, we have used an heterogeneous photochemical system consisting of a mixture of the following chemicals: (6.3×10^{-6}M $MnTP_yP\text{-}C_{16}$; 4.6×10^{-4}M PVS°; 1.1×10^{-2}M SDS; 5×10^{-6}M $ZnTP_yP\text{-}C_{16}$ and 2×10^{-4} 5-HA, where 5-HA means 5-hexenoic acid). In Figure 3.11 a schematic representation of the organization of the sensitizer ($ZnTP_yP\text{-}C_{16}$), the electron donors ($MnTP_yP\text{-}C_{16}$ and 5-HA) in a micelle of sodium dodecyl sulfate (SDS), is presented. All these compounds are surfactants and thus they are solubilized in the micelle in such a way that their hydrophobic chains are located in the hydrophobic core of the micelle while their polar head groups are located at the outer periphery of the micelle. As in the previous experiment, the electron acceptor (PVS°) is located in the aqueous phase. Figure 3.12 shows the difference spectra of system I (6.3×10^{-6}M $MnTP_yP\text{-}C_{16}$; 4.6×10^{-4}M PVS°; 1.1×10^{-2}M SDS; 2×10^{-4}M 5-HA and 5×10^{-6}M $ZnTP_yP\text{-}C_{16}$)vs. System II (4.6×10^{-4}M PVS°; 1.1×10^{-2}M SDS; 2×10^{-4}M 5-HA and 5×10^{-6}M $ZnTP_yP\text{-}C_{16}$). The difference spectrum at zero time is that of $Mn^{III}TP_yP\text{-}C_{16}$ (see the characteristic absorption peak at 460nm). Upon successive irradiations the peak around 460nm disappears and a new peak around 440nm appears; the latter is probably associated with the production of $Mn^{II}TP_yP\text{-}C_{16}$. The absorption peaks at about 602nm correspond to the propyl viologen radical ($PVS^{\cdot}$) formation upon successive irradiation.

Figure 3.13a presents the rates of $PVS^{\cdot}$ formation as a function of the illumination time. The initial slope (rate of formation of $PVS^{\cdot}$) to the curve of Figure 3.13a is equal to 6.7×10^{-8}Moles x min^{-1}. The quantum yield for the photoproduction of $PVS^{\cdot}$ is approximately six times that we have obtained in the previous experiment (Fig.3.13b). This result would be explained by the fact that in the second experiment two coupled electron donors ($MnTP_yP\text{-}C_{16}$ and 5-HA) participate in the dye-sensitized photoinduced electron transfer reactions while for the first experiment (Fig.3.13b) only one electron donor ($MnTP_yP\text{-}C_{16}$) is involved.

less! (3-4)

This is not an explanation.

Is this not coupled to PVS reduction?

According to the model presented in Figure 3.11, the experiment described above shows that by illuminating the heterogeneous photochemical system designated "system I", we have achieved the dye-sensitized photoinduced electron transfer across the interface of the SDS micelle from the two coupled electron donors ($MnTP_yP\text{-}C_{16}$ and 5-HA) dissolved in the micelle to the

Who, more definitely? There are very old results!

PVS° outside the micelle using the $ZnTP_yP\text{-}C_{16}$ as a sensitizer.

We have made three complementary experiments in order to check: (i) first, if the $MnTP_yP\text{-}C_{16}$ electron donor was necessary; (ii) second, if the double bond of the 5-HA was necessary and; (iii) third, if the micelles were necessary.

These questions were already answered in the literature.

In order to check the importance of $MnTP_yP\text{-}C_{16}$, we have repeated the experiment schematized in Figure 3.11, but without putting in the aqueous micellar solution of SDS, the $MnTP_yP\text{-}C_{16}$ donor. The quantum yield for the photoproduction of PVS^- was about 12 times lower than that obtained in the second experiment: the initial slope to the curve indicating the rate of formation of PVS^- (Fig.3.13c) is approximately 5.5×10^{-9} Moles x min^{-1}. We conclude that $MnTP_yP\text{-}C_{16}$ was necessary in the dye-sensitized redox reactions described in the second experiment.

← It is not surprising! Donor is required.

The fourth experiment was carried out on an heterogeneous photochemical system containing the same reactant as those mentioned in the second experiment except that the 5-hexenoic acid was replaced by hexanoic acid. The quantum yield for the photoproduction of PVS^- was about (12-15) times lower than that obtained in the second experiment.
In fact, the initial slope to the curve indicating the rate of PVS^- formation (Fig.3.13d) is approximately 4.2×10^{-9} Moles x min^{-1}. Since this rate is very small, we conclude that the double bond of the 5-HA was necessary in the dye-sensitized redox reactions described in the second experiment.

The fifth experiment was carried out on an homogeneous photochemical system containing the same reactants as those mentioned in the second experiment. No PVS^- was observed at all. We conclude that the micelles (or any other interfacial system) were necessary in order to achieve the dye-sensitized photochemical reactions described in the first and second experiment. By organizing the reactants and by keeping spatially separated the oxidized and reduced species of the dye-sensitized redox reactions, micelles favor the photoinduced electron transfer reactions and, at the same time, they retard the thermal back electron transfer between the photoproducts. It is quite reasonable to expect that micelles allow it to achieve some photochemical reactions which otherwise could not happen in homogeneous solutions.

In figure 3.13, one observes that the curves indicating the rate of PVS^- formation deviate from the linearity when the illumination time increases; this deviation could be due to some thermal back reactions between the photoproducts. or exhausted pools

Table 3.1 recapitulates the five forementioned experiments and the results obtained.

Table 3.1. Rate of PVS^- or Mn^{IV} formation in the various photochemical systems

	MnP	ZnP	SDS	MeOH	5-HA	PVS°	Hexa-noic acid	Rate of PVS^- or Mn^{IV} formation
Exp.1 Final solvent (12 : 1)	x	x	x	x		x		PVS^-: 1.7×10^{-8} mol x min^{-1}; Mn^{IV}: 1.7×10^{-8} moles x min^{-1}
Exp.2 Final solvent H_2O : CH_3OH (12 : 2)	x	x	x	x	x	x		PVS^-: 6.7×10^{-8} Moles x min^{-1} Mn^{IV} ?
Exp.3 Final solvent H_2O : CH_3OH (12 : 2)	x	x	x	x		x	x	PVS^-: 5.5×10^{-9} Moles x min^{-1} Mn^{IV} = ?
Exp.5 Final solvent H_2O : CH_3OH	x	x		x	x	x		No mole of PVS^- other detergents?

Exp.4 ?

Abbreviations

MnP : $MnTP_yP$ $(C_{16}H_{33})_4$ $(ClO_4)_4$ $Cl.H_2O$ (electron donor) ;

ZnP : $ZnTP_yP$ $(C_{16}H_{33})_4$ $(ClO_4)_2$ $\frac{1}{2}$ H_2O (sensitizer) ;

SDS : Sodium dodecyl sulfate ($C_{12}H_{25}SO_4^-$ $-Na^+$: interfacial system)

MeOH : Methanol (CH_3OH)

PVS° : Propyl viologen sulfonate (electron acceptor)

5-HA : Hexenoic acid (electron donor)

Discussion ?

- critical evaluation of the measured data (intermicelle transfer of photo-reactants)
- reaction scheme
- thermodynamics
- kinetics
- new suggestions for constituents
- practical realization for energy production (conversion)

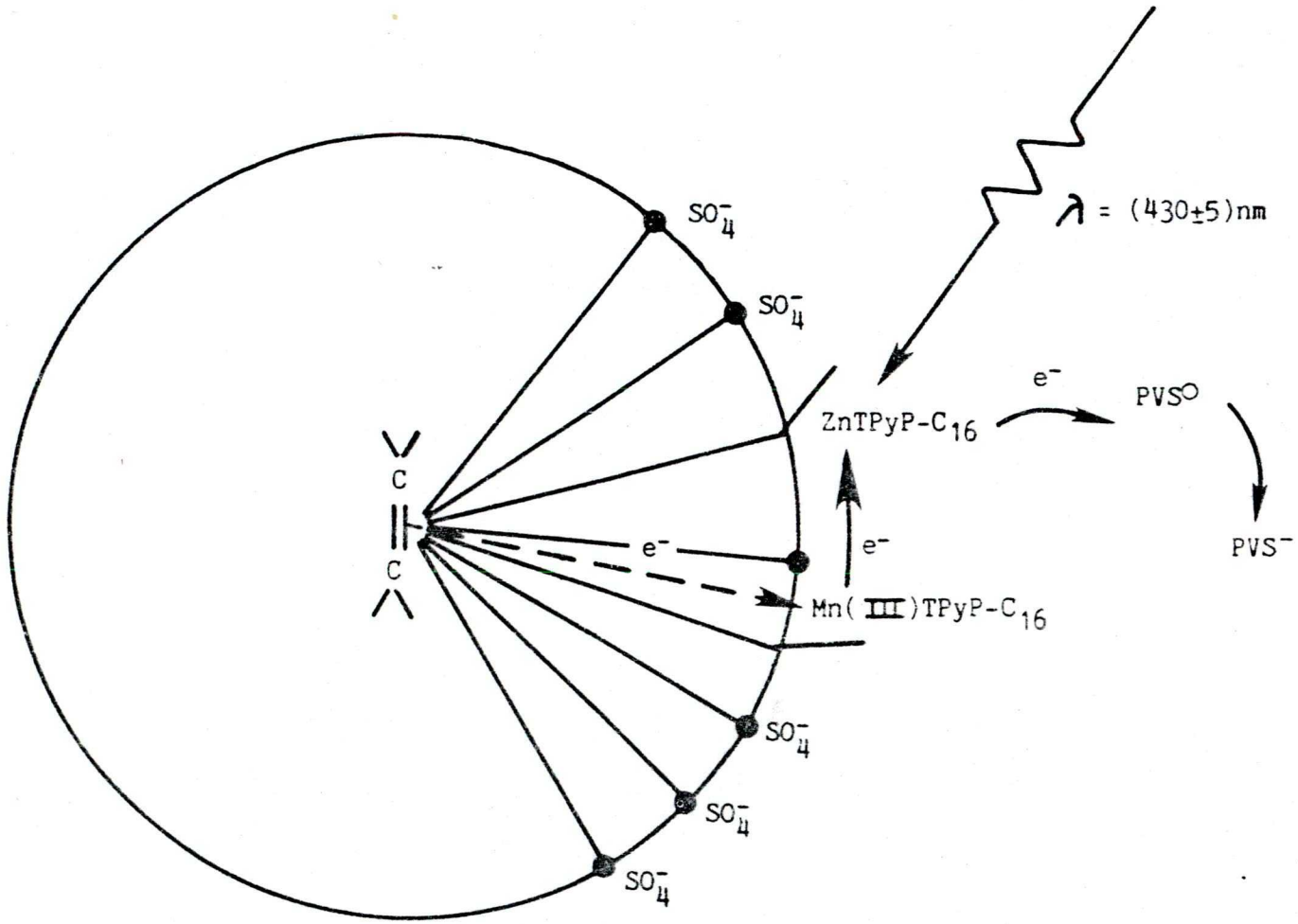

Fig. 3.11. Schematic representation of the organization of the sensitizer ($ZnTP_yP - C_{16}$), the electron donors ($MnTP_yP - C_{16}$ and 5 - HA) in a micelle of sodium dodecyl sulfate with the electron acceptor in the aqueous phase.

Fig.3.12.

Rate of formation of the PVS^- radical as a function of the illumination time (interval of illumination: 1 minute).
We have recorded the difference absorption spectrum of system I (6.3×10^{-6}M $MnTP_yP\text{-}C_{16}$; 4.6×10^{-4}M PVS°; 2×10^{-4}M 5-HA; 1.1×10^{-2}M SDS and 5×10^{-6}M $ZnTP_yP\text{-}C_{16}$) vs.
System II ($4{,}6 \times 10^{-4}$M PVS°; 2×10^{-4}M 5-HA; 1.1×10^{-2}M SDS and 5×10^{-6}M $ZnTP_yP\text{-}C_{16}$).
The pH of system I and system II was 8.5. ?

was
why
Fig. 3.10. pH = 7.0

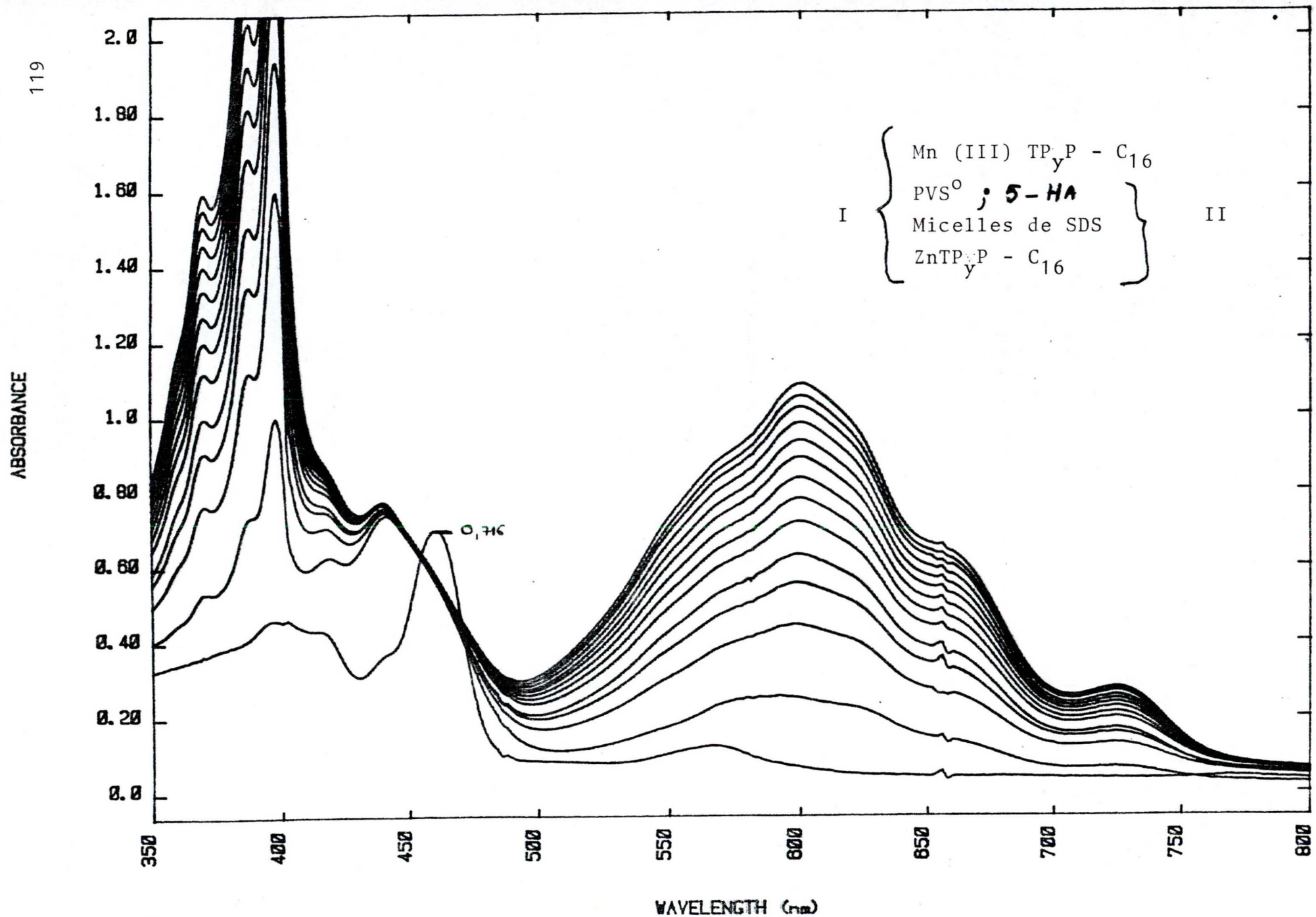
ABSORBANCE
2.0
1.80
1.60
1.40
1.20
1.0
0.80
0.60
0.40
0.20
0.0
350
400
450
500
550
600
650
700
750
800
WAVELENGTH (nm)
0,716
I
Mn (III) TPyP - C16
PVS° ; 5-HA
Micelles de SDS
ZnTPyP - C16
II

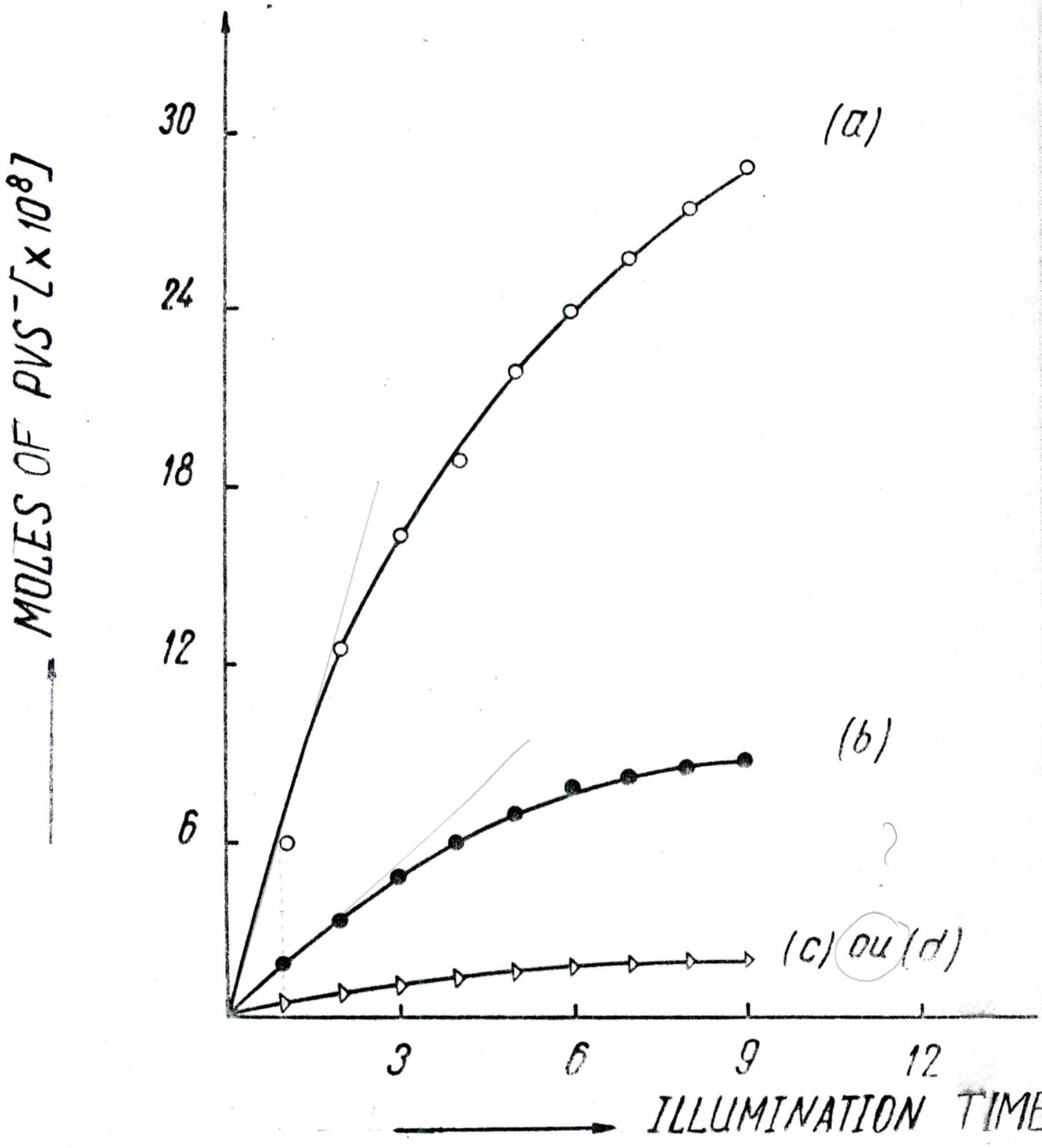

Fig.3.13. Rate of formation of PVS as a function of the illumination time in various heterogeneous photochemical systems:

(a) SDS, PVS°, $ZnTP_yP\text{-}C_{16}$, $MnTP_yP\text{-}C_{16}$, 5-HA;

(b) SDS, PVS°, $ZnTP_yP\text{-}C_{16}$, $MnTP_yP\text{-}C_{16}$;

(c) SDS, PVS°, $ZnTP_yP\text{-}C_{16}$, 5-HA;

(d) SDS, PVS°, $ZnTP_yP\text{-}C_{16}$, $MnTP_yP\text{-}C_{16}$, hexanoic acid.

CONCLUSIONS

We have determined the electric polarizabilities and the relaxation time of the electric polarizability of chloroplast big fragments, for the first time (as far as we know), by using the electric linear dichroism and the electric field light scattering methods. The mean values obtained for the electric polarizability and its relaxation time are, respectively, in the order of 10^{-12} cm^3 and 6×10^{-5} sec. An electric polarisability's relaxation time of that order of magnitude is characteristic of the interfacial charge dynamics, i.e. it is due to the electric field induced movement of counterions on the fragment's surface. Thus, the orientation of chloroplasts and that of chloroplast big fragments in an electric field is due to the deformation of the electric double layer by the electric field. Such an electric double layer may play an important role in the photochemical conversion and storage of sunlight energy by preventing the thermal back electron transfer between the primary products of the photochemical reactions of the natural photosynthesis in a manner similar to the role assumed by the electric double layer of interfacial systems (ionic micelles, vesicles, etc...) used in artificial photosynthetic systems.

The rotational relaxation times of chloroplast big fragments that we have obtained by using the electric field light-scattering method are in agreement with those obtained by GEACINTOV et al. (1972) from the magnetic field induced transient fluorescence intensity changes.

We have achieved, photochemically, the oxidation of a Mn-tetrapyridyl porphyrin derivative ($MnTP_yP\text{-}C_{16}$) from the Mn^{3+} oxidation state to the Mn^{4+} oxidation state in aqueous micellar solutions of sodium dodecyl sulfate (SDS) and at the same time, the propyl viologen sulfonate (PVS^0) was reduced in the aqueous phase. Our experimental observations confirms those obtained by WOHLGEMUTH et al. (1982) using negatively charged vesicles to organize reactants. The photochemical production of the Mn^{4+} oxidation state constitutes an important approach in the characterization of catalysts which may mediate the multi-electron-exchange process of the dye-sensitized oxidation of water to oxygen since suitable polynuclear manganese complexes susceptible to oxidation from the Mn^{3+} state to the Mn^{4+} state have been suggested (CALVIN, 1974, 1983; PORTER, 1978) as probable candidates for the photochemical oxidation of water to oxygen without the production of free hydroxyl radicals or other intermediates.

We have demonstrated a dye-sensitized photoinduced electron transfer along and across the organic-water interface of an SDS micelle upon illumination of a suitable heterogeneous photochemical system containing $ZnTP_yP\text{-}C_{16}$ (a compound which resembles the chlorophyll molecules) as a sensitizer. Thus, we have simulated the main feature of the natural photosynthesis photochemical reaction, i.e. an irreversible photoinduced electron transfer across a membrane or a water-to-organic phase boundary.

REFERENCES

1. MURERAMANZI, S. and TIEN, H.T.; "Photoelectrochemical methods for the utilization of solar energy, International Journal of Ambient Energy, Vol. 7 n° 1 (January 1986), pp. 3-30.

2. BOLTON, J.R. and HALL, D.O.; "Photochemical conversion and storage of Solar Energy", Ann. Rev. Energy, Vol. 4 (1979), pp. 353-401.

3. Revue de l'AGCD, Dimension 3, N° 2, Mai-Juin 1981.

4. PORTER, G. and ARCHER, M.D.; "In Vitro Photosynthesis", Interdisci. Sci. Rev., Vol. 1 n° 2 (1976), pp. 119-143.

5. BOLTON, J.R., "Solar Fuels. Prospects for the reduction of Carbon dioxide using solar energy", Proceedings of the Second Int. Gas Research Confernece, 1981 (Publ. 1982), pp. 603-612.

6. DANIELS, F., "Direct Use of the Sun's Energy", Yale University Press, New Haven, U.S.A., p. 374 (1964).

7. CALVIN, M., "Photosynthesis as Resource for Energy and Materials", Kemia-Kemi, Vol. 2 (1975), pp. 46-57; see also, Photochem. Photobiol., Vol. 64 (1976), pp. 425-444.

8. (a) PORTER, G., "In Vitro Models for Photosynthesis". (The Backerian Lecture), Proc. Roy. Soc. Lond., Vol. 362A (1978), pp. 281-303.

   (b) PORTER, G., "Pure and Applied Photochemistry", Pure and Appl. Chem., Vol. 50 (1978), pp. 263-271.

9. CANNOLLY, J.S., "Photochemical conversion and storage of Solar Energy", Academic Press, N.Y., p. 444 (1981).

10. (a) CALVIN, M., "Simulating Photosynthetic Quantum Conversion", See Ref. 9, pp. 1-26; see also Acc. Chem. Res., Vol. 11 (1978), pp. 369-374.

    (b) CALVIN, M., "Synthetic Chloroplasts", Energy Research, Vol. 3 (1979), pp. 73-87.

11. BOLTON, J.R., "Solar Electricity : Lessons Gained from Photosynthesis, Am. Chem. Soc. Symposium Series, Vol. 211 (1983), pp. 3-19.

12. VEZIROGLOU, T.M., VAN VORST, W.D. and KELLEY, J.H. (eds), "Hydrogen Energy Progress-IV. Proceedings of the fourth World Hydrogen Energy Conference (Vol. 2), California, U.S.A., June 1982". Pergamon Press, N.Y., pp. 451-929 (1982).

13. (a) GREENBAUM, E., "Biosolar Hydrogen and Oxygen Production". See Ref. 12, pp. 763-769.

(b) GREENBAUM, E., "Simultaneous photoproduction of hydrogen and oxygen by photosynthesis", Biotech. Bioeng. Symp., Vol. 10 (1980), pp. 1-13.

(c) GREENBAUM, E., "Photosynthetic hydrogen and oxygen production: kinetic studies, Science, Vol. 215 (1982), pp. 291-293.

14. HALL, D.O., et RAO, K.K., "Photosynthèse". Traduit de l'anglais par Philippe Brenier. Adapté par Paul MAZLIAK. Librairie Vuilbert, Paris, 1978.

15. GERISCHER, H., and KATZ, J.J. (eds.), "Light-Induced Charge Separation in Biology and Chemistry" (Berlin, Dahlem Conferences), Life Sciences Research Reports, Vol. 12 (1979).

16. WITT, H.T., "Charge separation in photosynthesis", See Ref. 15, pp. 303-330.

17. BARBER, J., (ed.), "Photosynthesis in Relation to Model Systems (Topics in Photosynthesis, Vol. 3)", Elsevier, Amesterdam, Hollande, p. 434 (1970).

18. HARRIMAN, A. and BARBER, J., "Photosynthetic water-splitting process and artificial chemical systems". See Ref. 17, pp. 243-280.

19. SHOWELL, M.S. and FONG, F.K., "Photoelectrochemical properties of chlorophyll dihydrate on metal as a catalyst for water photolysis". See Ref. 12, pp. 725-738.

20. HAUTALA, R.R., KING, R.B., and KUTAL, C., (eds.), "Solar Energy: Chemical Conversion and Storage", Humana Press, Clifton, New Jersey (USA), p. 419 (1979).

21. BOLTON, J.R., "Solar Energy Conversion in Photosynthesis-Features relevant to artificial systems for the photochemical conversion of solar energy". See Ref. 20, pp. 31-50.

22. AKOYUNOGLOU,G., (ed.), "Photosynthesis I. Photophysical Processes-Membrane Energization", Balaban International Science Services, Philadelphia, 1981.

23. CALVIN, M., "Solar Energy by Photosynthesis", Science, Vol. 184 (1974) pp. 375-381.

24. (a) BECKER, J.F., BRETON, J., GEACINTOV, N.E., and TRENTACOSTI, F., "Anisotropy of Photosynthetic Membranes and the Degree of Fluorescence Polarization", Biophys. Biochim. Acta, Vol. 440 (1976), pp. 531-544.

(b) GARAB, G.I., KISS, J.G., and MUSTARDY, L.A., "Orientation and Energy Transfer in Thylakoids", Biophys. J. Biophysical Society, Vol. 34 (1981), pp. 423-437.

25. (a) O'KONSKI, C.T., (ed.), "Molecular Electro-Optics. Part I. Theory and Methods", Marcel Dekker, N.Y., 1976.

(b) O'KONSKI, C.T., "Molecular Electro-Optics. Part II. Applications to Biopolymers", Marcel Dekker, N.Y., 1978.

26. TIEN, H.T., "Energy Conversion via Pigmented Bilayer Lipid Membranes", Separation Science Technology, Vol. 15, n° 4 (1980), pp. 1035-1058.

27. BRUGGER, P.A., CUENDET, P., and GRATZEL, M., "Ultrathin and Specific Catalysts affording efficient hydrogen evolution from water under visible light illumination", J. Am.Chem.Soc., Vol. 103 (1981), pp. 2923-2927.

28. FENDLER, J.H., "Aspects of artificial photosynthesis in surfactant vesicles", J. Photochem., Vol. 17 (1981), pp. 303-310.

29. HARRIMAN, A., PORTER, G., and RICHOUX, M.-C., "Photosensitized reduction of water to hydrogen using water-soluble zinc porphyrins", J. Chem. Soc., Faraday Trans. 2, Vol. 77 (1981), pp. 833-844.

30. CALVIN, M., WILLNER, I., LAANE, C., and OTVOS, J.W., "Photosensitized electron transfer reactions in organized interfacial systems", J. Photochem., Vol. 17 (1981), pp. 195-206.

31. CALVIN, M., "Artificial photosynthesis: Quantum capture and energy storage", Photochem. Photobiol., Vol. 37 (1983), pp. 349-360.

32. WEGNER, E.E., and ADMSON, A.W., "Photochemistry of Complex Ions. Absolute quantum yields for the photolysis of some aqueous chromium (III) complexes. Chemical actinometry in the long wavelength visible region", J. Am. Chem. Soc., Vol. 88 (1966), pp. 394-404.

33. GAFFRON, H. and RUBIN, J., "Fermentative and photochemical production of hydrogen in algae", J. Gen. Physiol., Vol. 26 (1942), pp. 219-240.

34. ARNON, D.I., MITSUI, A., and PANECQUE, A., "Photoproduction of hydrogen gas coupled with photosynthetic phosphorylation", Sciences, Vol. 134 (1961), p. 1425.

35. BENEMAN, J.R., BERENSON, J.A., KAPLAN, N.O., and KAMEN, M.D., "Hydrogen evolution by a chloroplast - Ferredoxin - hydrogenase system", Proc. Natl. Acad. Sci., U.S.A., Vol. 70 (1973), pp. 2317-2320.

36. KALYANASUNDARAM, K., and GRATZEL, M., in: "Photovoltaic and Photoelectrochemical Solar Energy Conversion", CARDON, F., GOMES, W.P., and DEKEYSER, W., (eds.), Plenum Press, N.Y. (1981), pp. 349-409.

37. GRATZEL, M., "Photoinduced water splitting in heterogeneous solutions". See Ref. 9, pp. 131-160.

38. HENGLEIN, A., "Reactions of organic free radicals of colloidal silver in aqueous solution. Electron pool effect in water decomposition", J. Phys. Chem., Vol. 83 (1979), pp. 2209-2216.

39. MEISEL, D., "Catalysis of hydrogen production in irradiated aqueous solutions by gold sols", J. Am. Chem. Soc., Vol. 101 (1979), pp. 6133-6135.

40. PORTER, G., "Recent progress in the photolysis of water", J. Photochem., Vol. 17 (1981), pp. 1-2.

41. LEHN, J.-M., Sauvage, J.-P. and ZIESSEL, R., "Thermal and photoinduced oxidation of water. Continuous generation of oxygen by visible light irradiation of aqueous solutions of metal complexes", Nouveau Journal de Chimie, Vol. 3 (1979), pp. 423-442.

42. KIWI, J., and GRATZEL, M., "Oxygen evolution from water via redox catalysis", Angew. Chem. Int. Ed. Engl., vol. 17, n° 11 (1978), pp. 860-861.

43. COOPER, S.R. and CALVIN, M., "Mixed valence interactions in dioxo bridged manganese complexes", J. Am. Chem. Soc., Vol. 99, n° 20 (1977), pp. 6623-6630.

44. BARBER, J., Biochim. Biophys. Acta, vol. 594 (1981), 253.

45. GAGLIANO, A.G., Geacintov, N.E. and BRETON, J., "Orientation and linear dichroism of chloroplasts and sub-chloroplast fragments oriented in an electric field", Biochim. Biophys. Acta, vol. 461 (1977), pp. 460-474.

46. FREDERICQ, E., and HOUSSIER, C., "Electric Dichroism and Electric Birefrengence", Clarendon Press, Oxford, U.K. (1973).

47. STOYLOV, S.P., "Colloid Electro-optics. Electrically induced optical Phenomena in dispersed systems", Advances Colloid Interface Sci., Vol. 3 (1971), pp. 45-110.

48. PAULSON, C.M., "Electric Dichroism of Macromolecules". See Ref. 23a, pp. 243-273.

49. LORRAIN, P., and CORSON, D.R., "Electromagnetic Fields and Waves", W.H. FREEMAN and Company, San Francisco, 1970.

50. TODOROV, G., SOKEROV, S., and STOYLOV, S.P. "Interfacial electric polarizability of purple membranes in solution", Biophys. J. Biophysical Society, Vol. 40 (1982), pp. 1-5.

51. ZHIVKOV, A. and STOYLOV, S.P., Abstracts of International School-Colloquium on "Membrane Structure and Functions", Varna, Bulgaria, 1981.

52. O'KONSKI, C.T., YASHIOKA, K. and ORTTUNG, W.H., J. Phys. Chem., Vol. 63 (1959), pp. 1558-1568.

53. KRAUSE, S., (ed.), "Molecular Electro-Optics (Electro-optic properties of macromolecules and colloid in solutions)", Plenum Publ. Corp. N.Y. (1981), p. 520.

54. O'KONSKI, C.T., "Theory of the kerr constant", see Ref. 53, pp. 119-146.

55. HOUSSIER, C. and O'KONSKI, C.T., "Electro-optical instrumentations systems with their data acquisition and treatment". See Ref. 53, pp. 309-339.

56. YAVORSKI, B. et DETLAF, A., "Aide-Mémoire de Physique", Editions Mir, Moscou, 1975.

57. WEILL, G., CH. IV, "Diffusion de la Lumière", dans: Initiation à la Chimie et à la Physico-chimie des Polymères. Vol. 1. Edité par le Groupe Français d'Etudes et d'Applications des Polymères, Strasbourg, 1980.

58. JENNINGS, B.R., Electric Field Light Scattering". See Ref. 25a, pp. 275-319.

59. ANDERSON, J.M. and BOARDMAN, N.K., BBA, Vol. 112 (1966), 403

60. (a) ROBINSON, H.H., SHARP, R.R. and YOCUM, C.F., Biochem. Biophys. Res. Commun., Vol. 93 (1980), pp. 755-781.

(b) ROBINSON, H.H., and YOCUM, C.F., BBA, Vol. 590 (1980), 98.

61. HOFF, A.J., and VAN DER WAALS, J.H., BRA., Vol. 590 (1980), 75.

62. (a) Compte rendu de l'Académie Bulgare des Sciences, Tome 27, n° 11 (1974), pp. 1593-1596.

(b) Comptes rendus de l'Académie Bulgare des Sciences, Tome 29, n° 3 (1976), pp. 415-421.

63. ELLENSON, J.L., Ph.D. Thesis, University of California, Berkeley (1973).

64. DZHENEV, I., Diploma work, Sofia, 1981.

65. BOTCHEVA, N., Diploma work, Sofia, 1979.

66. TOMASELI, J., Diploma work, Sofia, 1980.

67. ZHIVKOV, A., STOYLOV, S.P. and GOLZEV, V., FIZIOL., RAST., Vol. 6 (1982), 543.

68. MURERAMANZI, S., GOLTZEV, V., TODOROV, G., ZHIVKOV, A., and STOYLOV, S.P., "Electro-optic study of the dimensions and electric polarizability of chloroplasts and sub-chloroplast fragments", "Bioelectrochemistry and Bioenergetics", Vol. 13 (1984), pp. 453-457.

69. FUJISHIMA, A., and HONDA, K., "Electrochemical photolysis of water at a semiconductor electrode", Nature (London), Vol. 238 (1972), pp. 37-38.

70. (a) KRASNA, A.I., "Proflavin catalyzed photoproduction of hydrogen from organic compounds", Photochem. Photobiol., Vol. 29 (1979), pp. 267-276.

(b) KRASNA, A.I., "Acridines, deazaflavins and Tris (2, 2' - bipyridine) ruthenium as catalysts for photoproduction of hydrogen from organic compounds", Photochem. Photobiol., Vol. 31 (1980), pp. 75-82.

71. HENGLEIN, A., "Photoinduced electron transfer in micelles". See Ref. 15, pp. 205-221.

72. XIAO, X.-R., WANG, C.B., and TIEN, H.T., "Photoreduction of alkyl viologens by zinc tetraphenyl porphyrin in organic solvent-water systems", Journal of Molecular Catalysis, Vol. 23 (1984), pp. 9-16.

73. WILLNER, I., FORD, W.E., OTVOS, J.W., and CALVIN, M., "Photoinduced electron transfer across a water-oil boundary as a model for redox reaction separation", Nature (London), Vol. 280 (1979), pp. 823-824.

74. FORD, W.E., OTVOS, J.W. and CALVIN, M., "Photosensitized electron transfer across phospholipid vesicle walls", Nature, Vol. 274 (1978), pp. 507-508; see also, Proc. Natl. Acad. Sci., U.S.A., Vol. 76, n° 8 (1979), pp. 3590-3593.

75. INFELTA, P.P., Gratzel, M., and FENDLER, J.H., "Aspects of artificial photosynthesis. Photosensitized electron transfer and charge separation in cationic surfactant vesicles", J. Am. Chem. Soc., Vol. 102 (1980), pp. 1479-1483.

76. WILLNER, I., YANG, J.-M., LAANE, C., OTVOS, J.W., and CALVIN, M., "The function of SiO_2 colloids in photoinduced reactions. Interfacial effects on quenching, charge separation and quantum yields", J. Phys. Chem., Vol. 85 (1981), pp. 3277-3282.

77. YANG, J.-M., "Photoinduced electron transfer in heterogeneous media", Ph.D. Thesis, University of California, Berkeley, 1981.

78. KIWI, J., and GRATZEL, M., "Protection, size factors and reactions dynamics of colloidal redox catalysts mediating light-induced hydrogen evolution from water", J. Am. Chem. Soc., Vol. 101 (1979) pp. 7214-7217.

79. LEMAIRE, J., Une introduction élémentaire à la photochimie, pp. 11-46, dans "Photochimie", édité par COURTOT, P., Dunod, Paris, 1972.

80. BOLTON, J.R., "Solar Fuels. The production of energy - rich compound by the photochemical conversion and storage of solar energy", Science, Vol. 202 (1978), pp. 705-711.

81. (a) NOZIK, A.J., "p - n photoelectrolysis cells", Appl. Phys. Letters, Vol. 29 (1976), pp. 150-153.

(b) NOZIK, A.J., "Photochemical diodes", Appl. Phys. Letters, Vol. 30 (1977), pp. 567-569.

82. WRIGHTON, M.S., GINLEY, D.S., WOLEZANSKI, P.T., ELLIS, A.B., MORSE, D.L., and LINZ, A., "Photoassisted electrolysis of water by irradiation of a titanium dioxide electrode", Proc. Natl. Acad. Sci., U.S.A., Vol. 72 n° 4 (1975), pp. 518-522.

83. (a) BORGARELLO, E., and GRATZEL, M., "Visible light induced generation of H_2 from water and H_2S in colloidal semiconductor dispersion". See Ref. 12, pp. 739-747.

(b) BORGARELLO, E., GRATZEL, M., KALYANASUNDARAM, K., and PELEZZETTI, E., "Photochemical water splitting", Chem. Tech. Vol. 13 (1983), pp. 118-119.

84. MUKERJEE, P., and MYSELS, K.J., " Critical Micelle Concentration of Aqueous Surfactant Systems". Natl. Stand. Ref. Data Ser. Natl. Bur. Stand. 36, Washington, 1971.

85. FENDLER, J.H. and FENDLER, E.J., "Catalysis in Micellar and Macromolecular Systems", Academic Press, N.Y. (1975).

86. OKUNO, Y., FORD, W.E., and CALVIN, M., "An improved synthesis of surfactant Porphyrins", synthesis, Vol. 7 (1980), pp. 537-539.

87. WOHLGEMUTH, R., OTVOS, J.W. and CALVIN, M., "Environmental Influences on the photooxidation of manganese by a Zn - porphyrins sensitizer", Proc. Natl. Acad. Sci., U.S.A., Vol. 79, n° 16 (1982), pp. 5111-5114.

88. TURKEVICH, J., AIKA, K., BAN, L.L., OKURA, I., and NAMBA, S., J. Res. Inst. Catalysis, Hokkaido Univ., Vol. 24 (1976), 54.

89. KANDEL, R.J. (ed), Proceedings of the Third Solar Photochemistry Research Confernece, Asimolar Conference Grounds, Pacific Grove, California, June 1979.

90. SYSBESMA, C., (ed.), "Advances in Photosynthesis Research". Proceedings of the VIth International Congress on Photosynthesis, August 1-6, 1983, Brussels, Belgium, (publ. 1984, 3480 pp. in 4 volumes ISBN 90-247-2946-7).

91. BISHOP, N.I., "Further assessment through mutational analysis of chloroplast membrane polypeptide required in water photolysis". See Ref. 90, pp. 1.3.321-1.3.328.

92. RENGER Gernot and WEISS Wolfgang, "Studies on the functional mechanism and structural organization of water cleavage by system I". See Ref. 90, pp. 1.3.253-1.3.260.

93. AMESZ, J., "The role of manganese in photosynthetic oxygen evolution". Biochim. Biophys. Acta Vol. 726 (1983), pp. 1-12.

94. GOVINDJEE, "Photosystem II : the oxygen evolving system of photosynthesis". See Ref. 90, pp. 1.3.227-1.3.238.

95. PETER, L.M., "Photochemical aspects of solar energy conversion". Photochemistry, Vol. 13 (1982), pp. 567-599.

96. BI, Z.-C., and TIEN, H.T., "Photoproduction of hydrogen by dye-sensitized systems", Int. J. Hydrogen Energy, Vol. 9, n° 9 (1984), pp. 717-722.

97. DUNNE, L.J., BRANDAS, E.J., and CLARK, A.D., "On the possibility of an anomalous static electric polarizability on bacteriorhodopsin assemblies in a coherent electronic state", Chem. Phys. Letters, Vol. 104, n° 5 (1984), pp. 431-434.

98. GEACINTOV, N.E., VAN NOSTRAND, F., BECKER, J.F. and TINKEL, J.B., "Magnetic field induced orientation of photosynthetic systems", Biochim. Biophys. Acta, Vol. 567 (1972), pp. 65-79.